Astro/Phys 224 Spring 2014

Origin and Evolution of the Universe

Week 7

Galaxy Formation

Joel Primack

University of California, Santa Cruz

Dependence of Halo Concentration on Mass and Redshift

Profiles of dark haloes: evolution, scatter, and environment

J. S. Bullock[1,2], T. S. Kolatt[1,3], Y. Sigad[3], R.S. Somerville[3,4], A. V. Kravtsov[2,5⋆], A. A. Klypin[5], J. R. Primack[1], and A. Dekel[3] 2001 MNRAS 321, 559

ABSTRACT

We study dark-matter halo density profiles in a high-resolution N-body simulation of a ΛCDM cosmology. Our statistical sample contains ∼5000 haloes in the range $10^{11} - 10^{14} h^{-1} M_{\odot}$ and the resolution allows a study of subhaloes inside host haloes. The profiles are parameterized by an NFW form with two parameters, an inner radius r_s and a virial radius R_{vir}, and we define the halo concentration $c_{vir} \equiv R_{vir}/r_s$. We find that, for a given halo mass, the redshift dependence of the median concentration is $c_{vir} \propto (1+z)^{-1}$. This corresponds to $r_s(z) \sim$ constant, and is contrary to earlier suspicions that c_{vir} does not vary much with redshift. The implications are that high-redshift galaxies are predicted to be more extended and dimmer than expected before. Second, we find that the scatter in halo profiles is large, with a 1σ $\Delta(\log c_{vir}) = 0.18$ at a given mass, corresponding to a scatter in maximum rotation velocities of $\Delta V_{max}/V_{max} = 0.12$. We discuss implications for modelling the Tully-Fisher relation, which has a smaller reported intrinsic scatter. Third, subhaloes and haloes in dense environments tend to be more concentrated than isolated haloes, and show a larger scatter. These results suggest that c_{vir} is an essential parameter for the theory of galaxy modelling, and we briefly discuss implications for the universality of the Tully-Fisher relation, the formation of low surface brightness galaxies, and the origin of the Hubble sequence. We present an improved analytic treatment of halo formation that fits the measured relations between halo parameters and their redshift dependence, and can thus serve semi-analytic studies of galaxy formation.

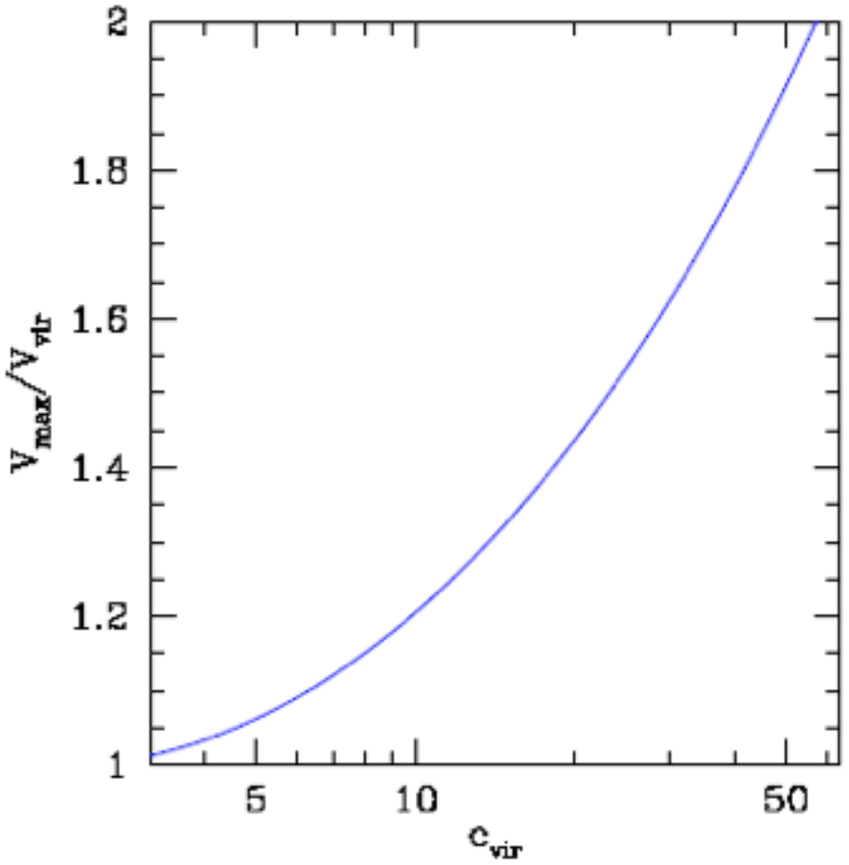

Figure 1. Maximum velocity versus concentration. The maximum rotation velocity for an NFW halo in units of the rotation velocity at its virial radius as a function of halo concentration.

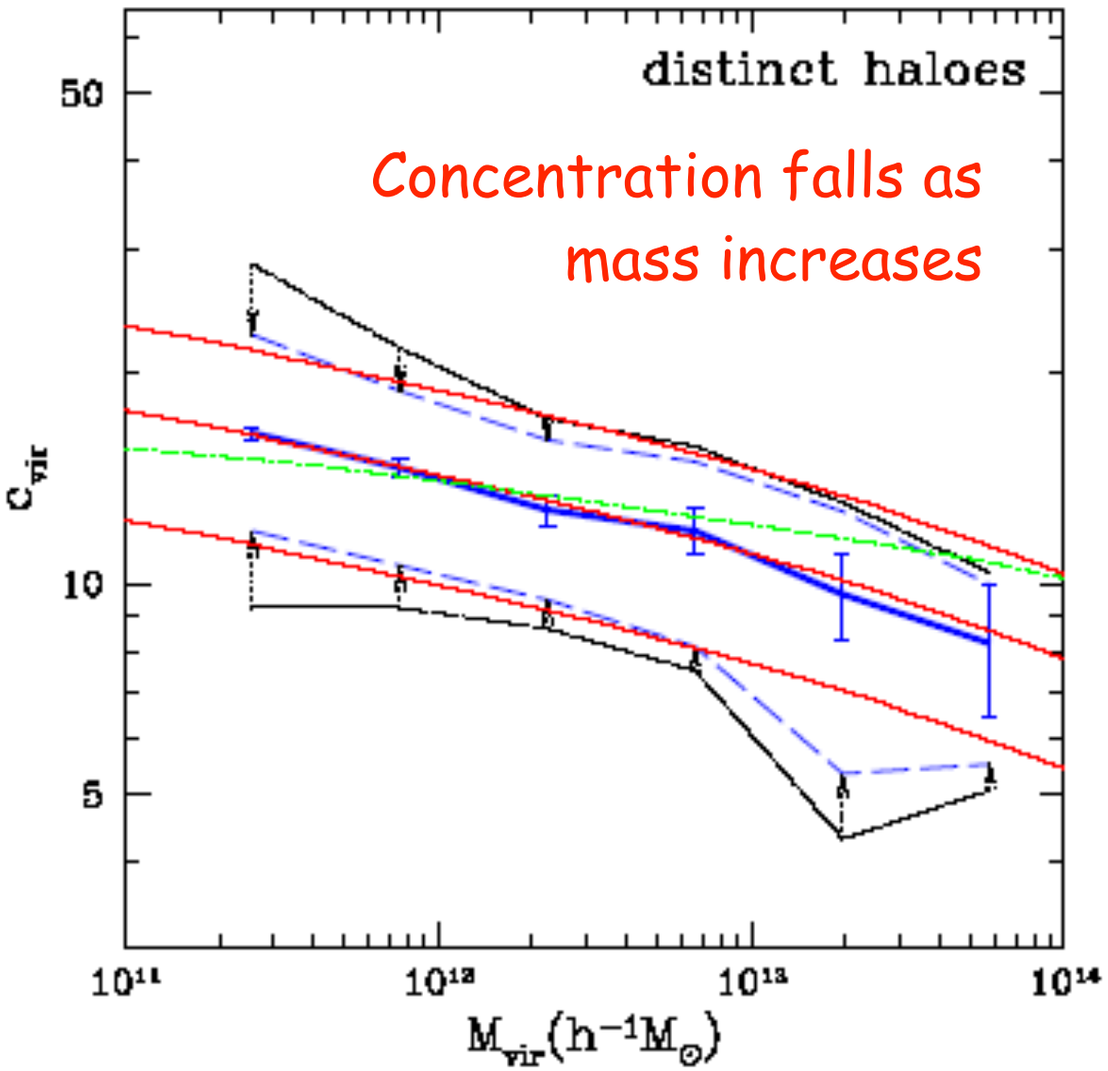

Figure 4. Concentration versus mass for distinct haloes at $z = 0$. The thick solid curve is the median at a given $M_{\rm vir}$. The error bars represent Poisson errors of the mean due to the sampling of a finite number of haloes per mass bin. The outer dot-dashed curves encompass 68% of the $c_{\rm vir}$ values as measured in the simulations. The inner dashed curves represent only the true, intrinsic scatter in $c_{\rm vir}$, after eliminating both the Poisson scatter and the scatter due to errors in the individual profile fits due, for example, to the finite number of particles per halo. The central and outer thin solid curves are the predictions for the median and 68% values by the toy model outlined in the text, for $F = 0.01$ and three different values of K. The thin dot-dashed line shows the prediction of the toy model of NFW97 for $f = 0.01$ and $k = 3.4 \times 10^3$.

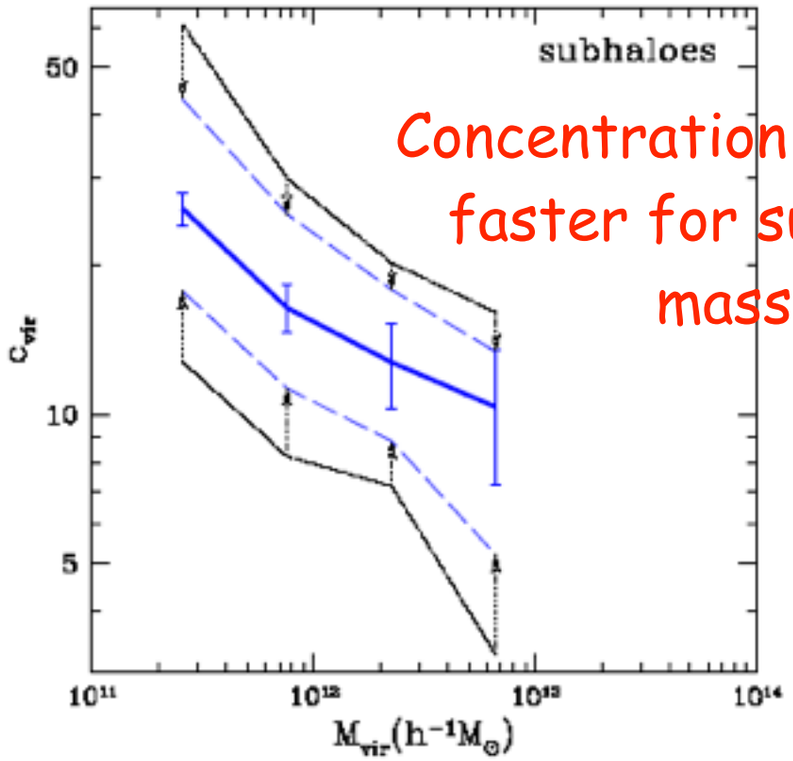

Figure 5. Concentration versus mass for subhaloes at $z = 0$. The curves and errors are the same as in Figure 4.

Bullock et al. 2001

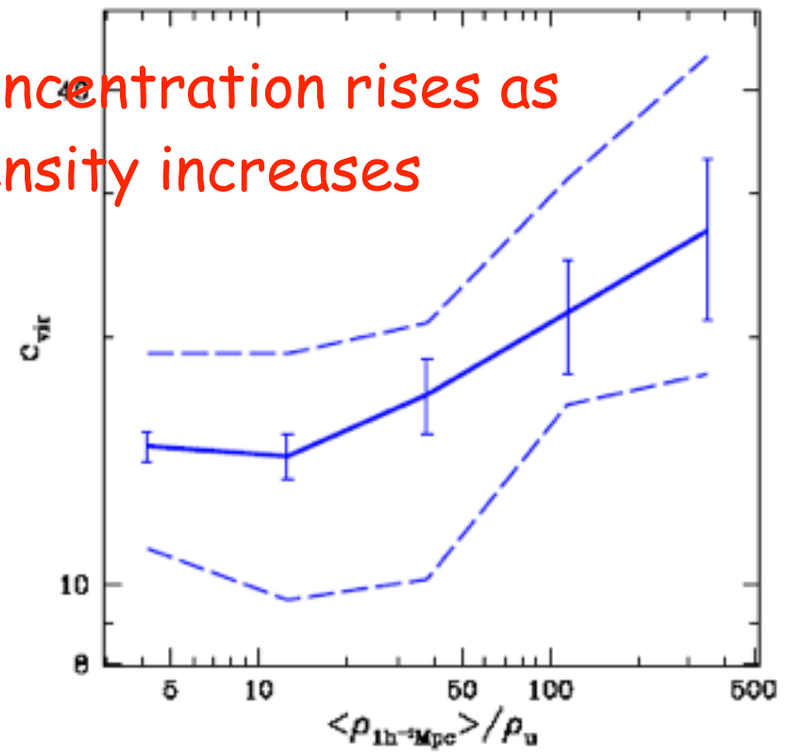

Figure 6. Concentrations versus environment. The concentration at $z = 0$ of all haloes in the mass range $0.5 - 1.0 \times 10^{12} h^{-1} M_\odot$ as a function of local density in units of the average density of the universe. The local density was determined within spheres of radius $1h^{-1}$Mpc. The solid line represents the median $c_{\rm vir}$ value, the error bars are Poisson based on the number of haloes, and the dashed line indicates our best estimate of the intrinsic scatter.

Spread of Halo Concentrations

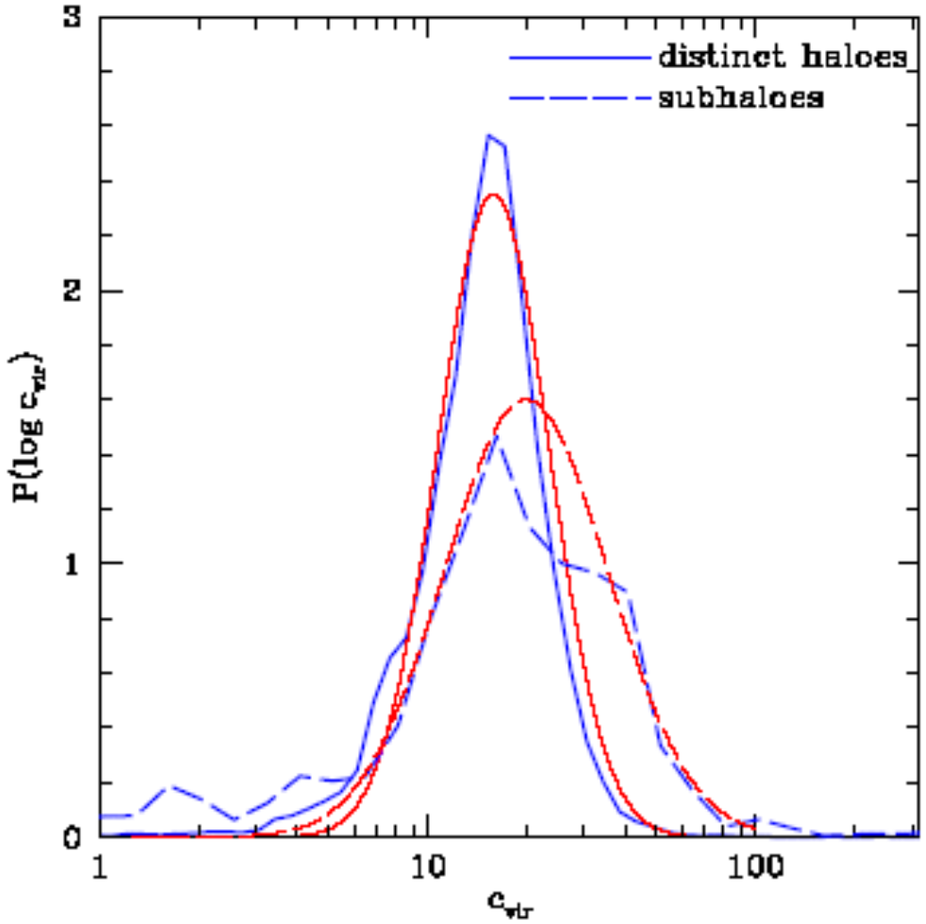

Figure 7. The probability distributions of distinct haloes (solid line) and subhaloes (dashed line) at $z = 0$ within the mass range $(0.5 - 1.0) \times 10^{12} h^{-1} M_{\odot}$. The simulated distributions (thick lines) include, the $\sim 2,000$ distinct haloes and ~ 200 subhaloes within this mass range. Log-normal distributions with the same median and standard deviation as the measured distributions are shown (thin lines). Subhaloes are, on average, more concentrated than distinct haloes and they show a larger spread.

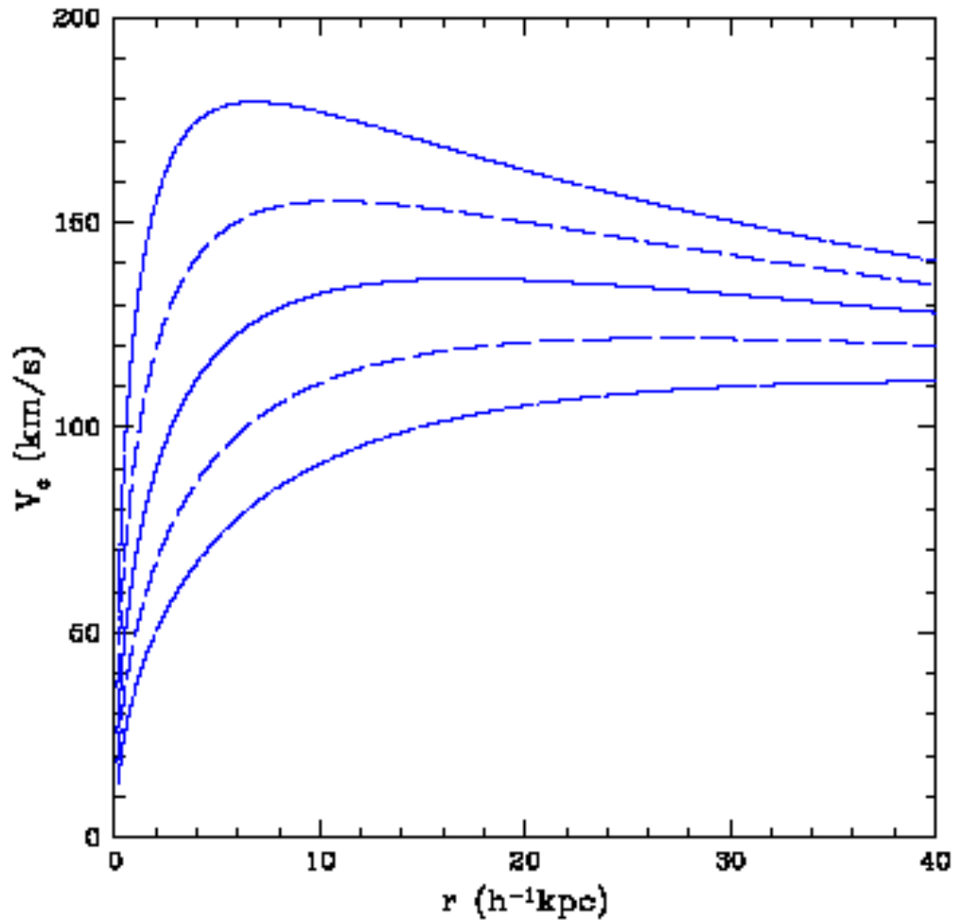

Figure 8. The spread in NFW rotation curves corresponding to the spread in concentration parameters for distinct haloes of $3 \times 10^{11} h^{-1} M_{\odot}$ at $z = 0$. Shown are the median (solid), $\pm 1\sigma$ (long dashed), and $\pm 2\sigma$ (dot-dashed) curves. The corresponding median rotation curve for subhaloes is comparable to the upper 1σ curve of distinct haloes.

Bullock et al. 2001

Evolution of Halo Concentration with Redshift

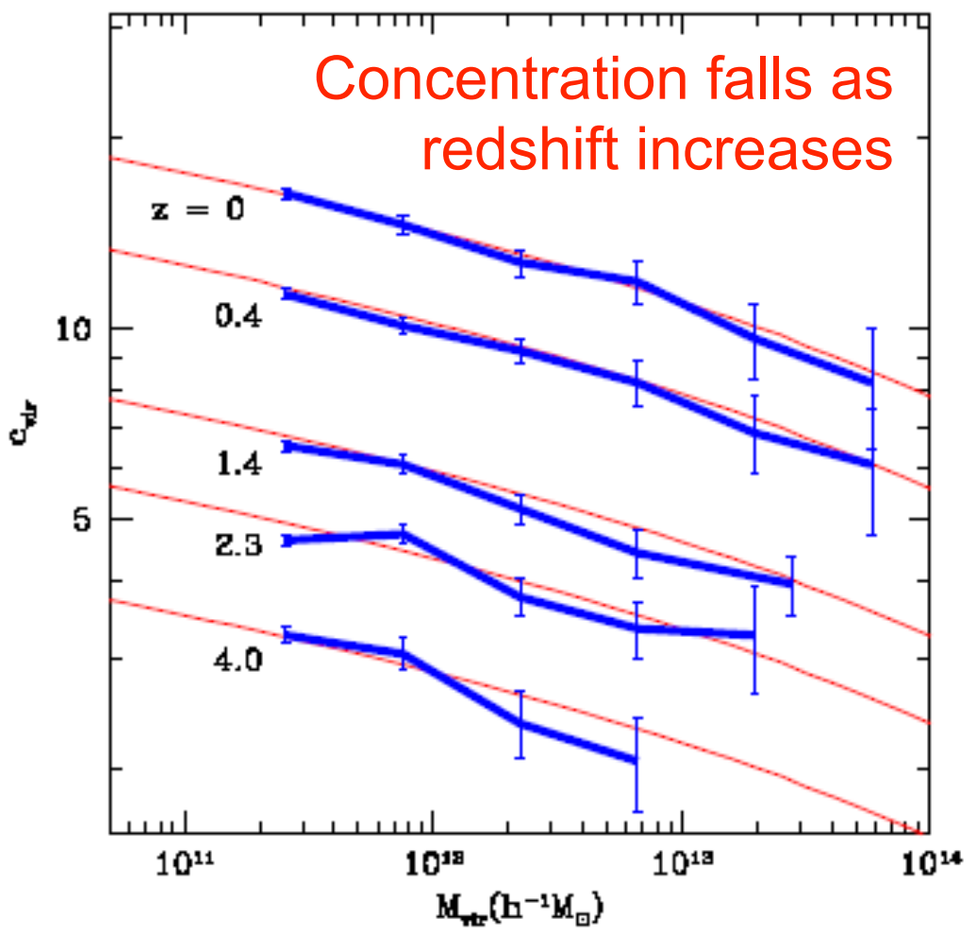

Figure 10. Median $c_{\rm vir}$ values as a function of $M_{\rm vir}$ for distinct haloes at various redshifts. The error bars are the Poisson errors due to the finite number of haloes in each mass bin. The thin solid lines show our toy model predictions.

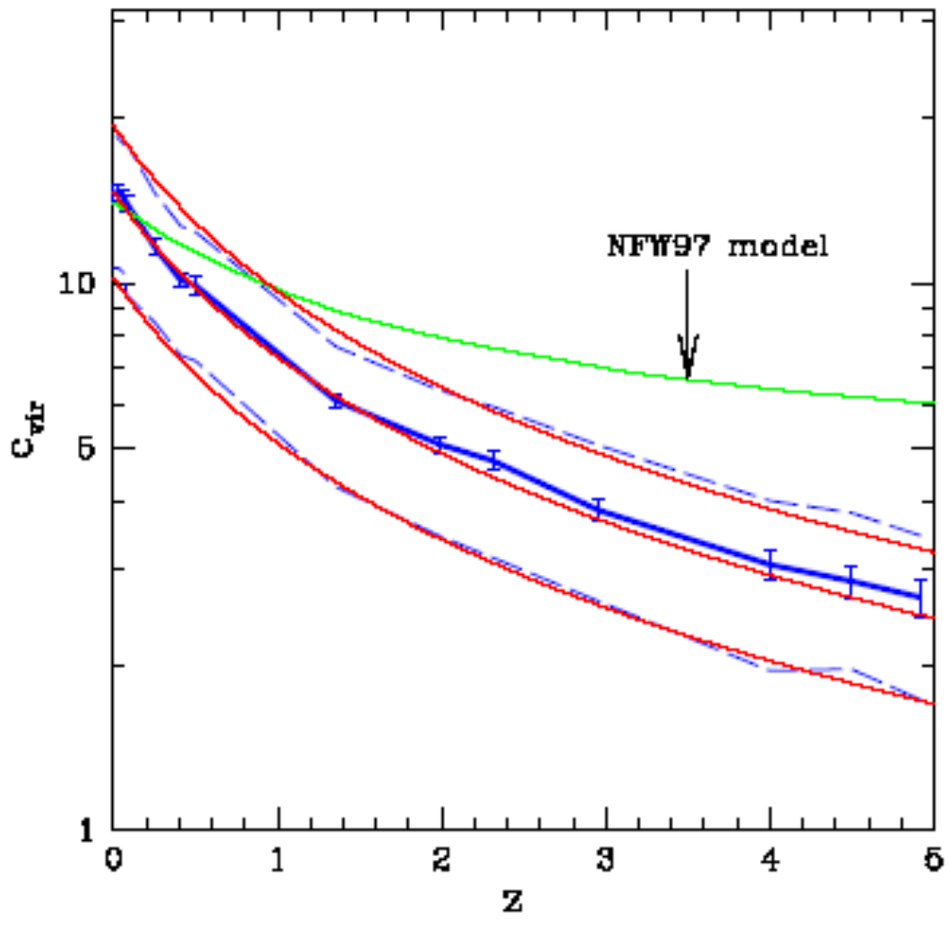

Figure 11. Concentration as a function of redshift for distinct haloes of a fixed mass, $M_{\rm vir} = 0.5 - 1.0 \times 10^{12} h^{-1} M_\odot$. The median (heavy solid line) and intrinsic 68% spread (dashed line) are shown. The behavior predicted by the NFW97 toy model is marked. Our revised toy model for the median and spread for $8 \times 10^{11} h^{-1} M_\odot$ haloes (thin solid lines) reproduces the observed behavior rather well.

$C_{vir} \propto 1/(1+z)$
at fixed mass

Bullock et al. 2001

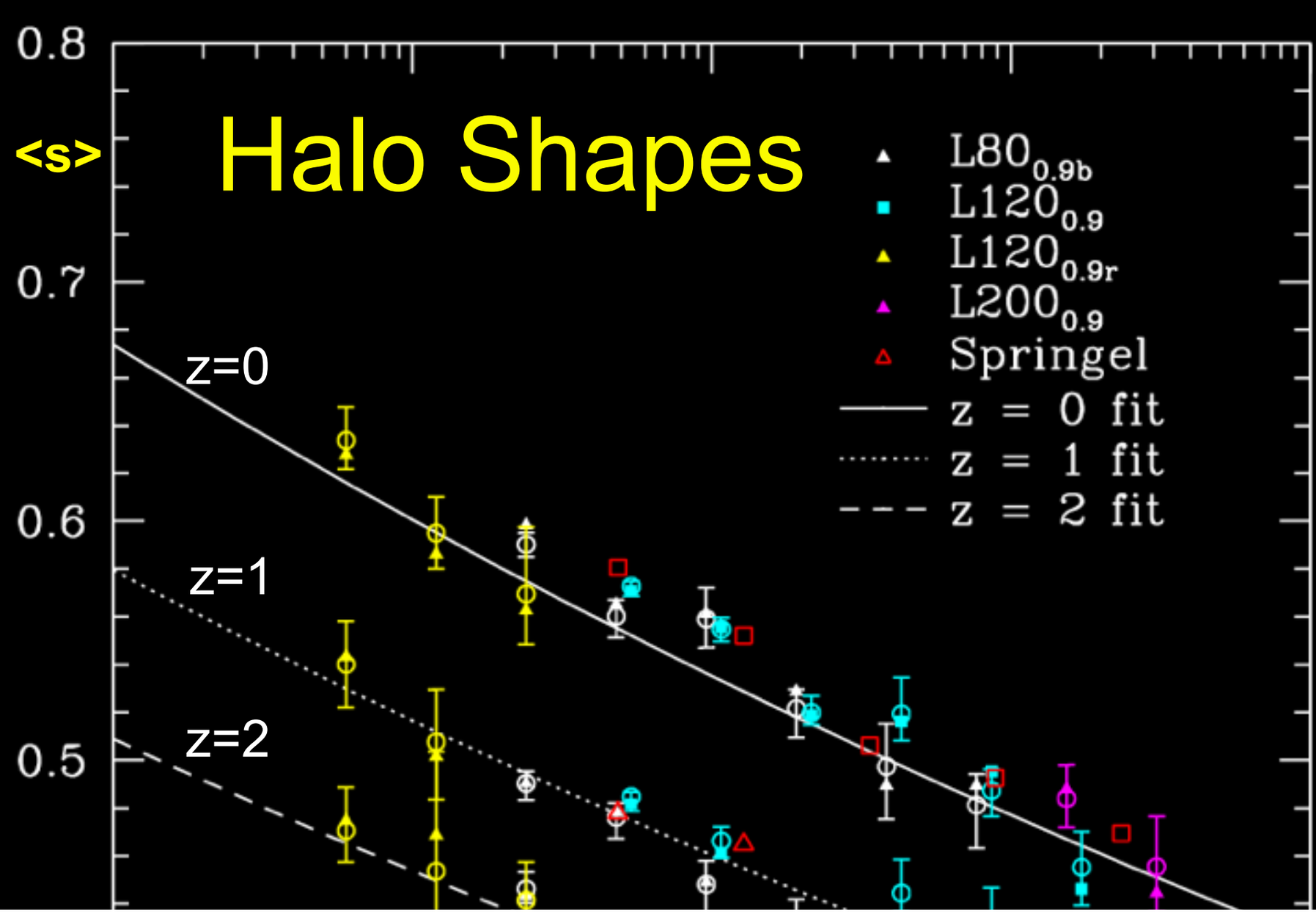

A simple formula describes these results, as well dependence on epoch and cosmological parameter σ_8 :

$$\langle s \rangle (M_{\rm vir}, z = 0) = \alpha \left(\frac{M_{\rm vir}}{M_*} \right)^{\beta}$$

with best fit values

$$\alpha = 0.54 \pm 0.03, \ \beta = -0.050 \pm 0.003.$$

<s> = short / long axis of dark halos vs. mass and redshift. Dark halos are more elongated the more massive they are and the earlier they form. We found that the halo <s> scales as a power-law in Mhalo/M*. Halo shape is also related to the Wechsler halo formation scale factor a_c.

Allgood+2006

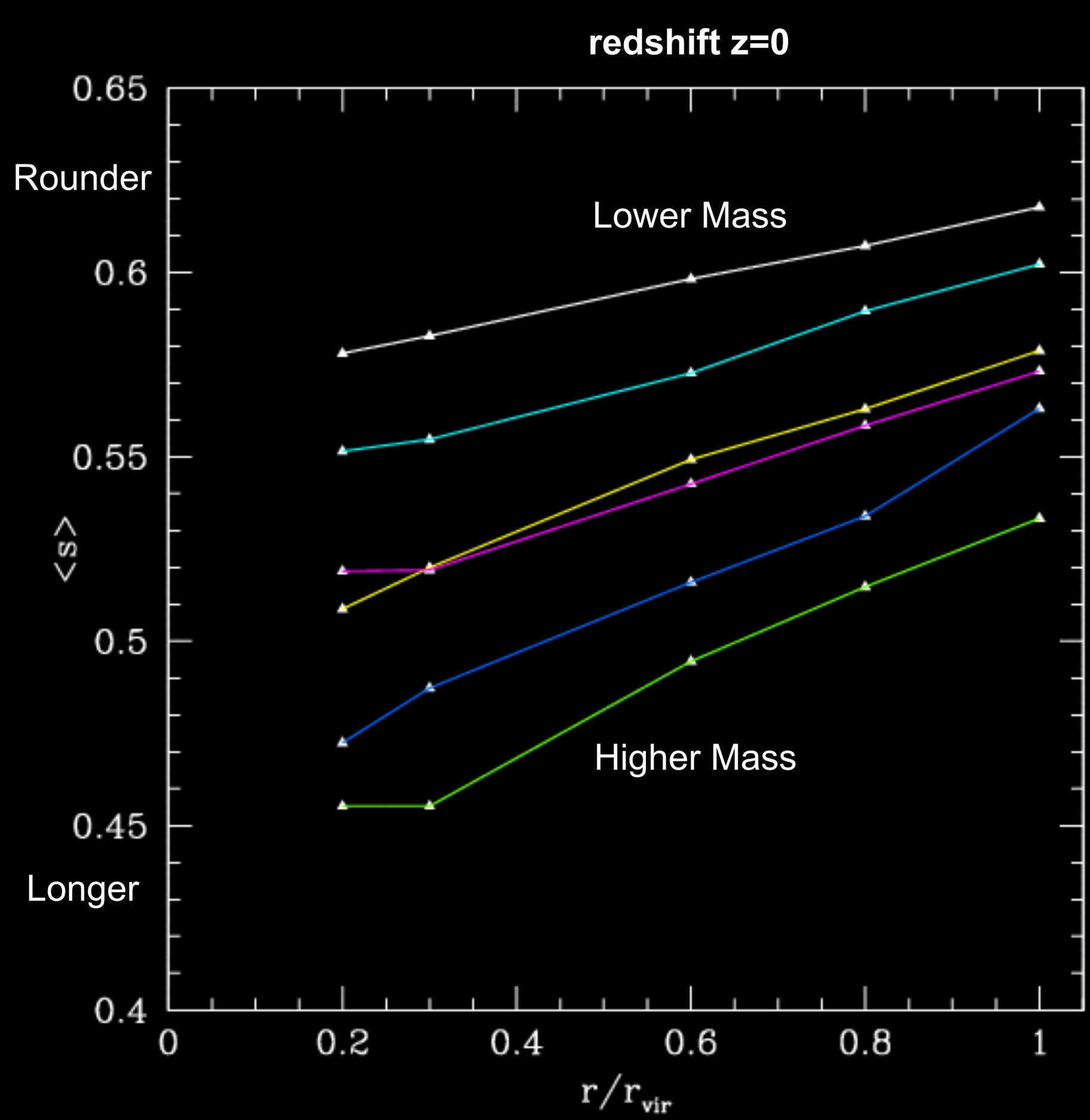

Halos become more spherical at larger radius and smaller mass. As before,

$$s = \frac{\text{short axis}}{\text{long axis}}$$

These predictions can be tested against cluster X-ray data and galaxy weak lensing data.

Allgood+2006

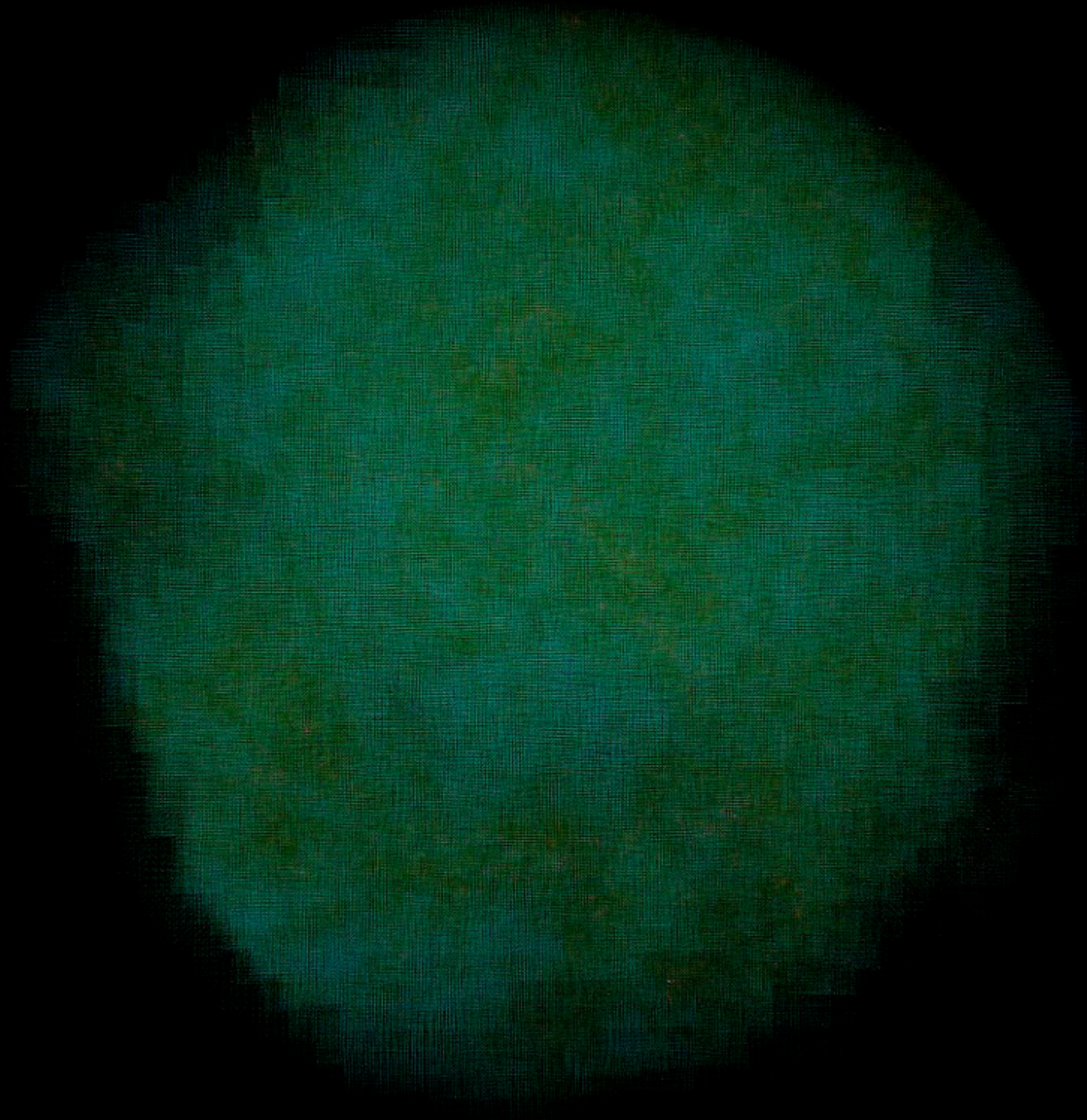

Columbia
Supercomputer
NASA Ames
2005

Simulation:
Brandon
Allgood &
Joel Primack

Visualization:
Chris Henze

(rotation to
show 3D)

Halo Abundance Matching

To investigate the statistics of galaxies and their relation to host DM halos as predicted by the LCDM model, we predicted the properties of our model galaxies using the following Halo Abundance Matching (HAM) procedure:

1. Using the merger tree of each DM halo and subhalo, obtain V_{acc} = the peak value of the circular velocity over the history of the halo (this is typically the maximum circular velocity of the halo when the halo is first accreted). Perform abundance matching of the velocity function of the halos to the LF of galaxies to obtain the luminosity of each model galaxy.

2. Perform abundance matching of the velocity function to the stellar mass function of galaxies to obtain the stellar mass of each model galaxy.

3. Use the observed gas-to-stellar mass ratio as a function of stellar mass to assign cold gas masses to our model galaxies. The stellar mass added to the cold gas mass becomes the total baryonic mass.

4. Using the density profiles of the DM halos, obtain the circular velocity at 10 kpc (V_{10}) from the center of each halo. Multiply the DM mass, as it comes from simulations, by the factor $(1 - f_{bar})$, where f_{bar} is the cosmological fraction of baryons. This is the dark-matter-only contribution. Add the contribution to V_{10} of the baryon mass from step 3 assuming it is enclosed within a radius of 10 kpc.

5. Optionally implement the BFFP86 correction to V_{10} due to the adiabatic contraction of the DM halos from the infall of the baryon component to the center.

Elliptical galaxies follow the Faber-Jackson relation $M \propto \sigma^4$ between their mass or luminosity and their velocity dispersion σ

Disk galaxies follow the Tully-Fisher relation $M \propto V^4$ between and their mass or luminosity and their rotation speed V








When we fill dark matter halos with galaxies using Halo Abundance Matching with the Bolshoi simulation, we can test these relations

Bolshoi Sub-Halo Abundance Matching

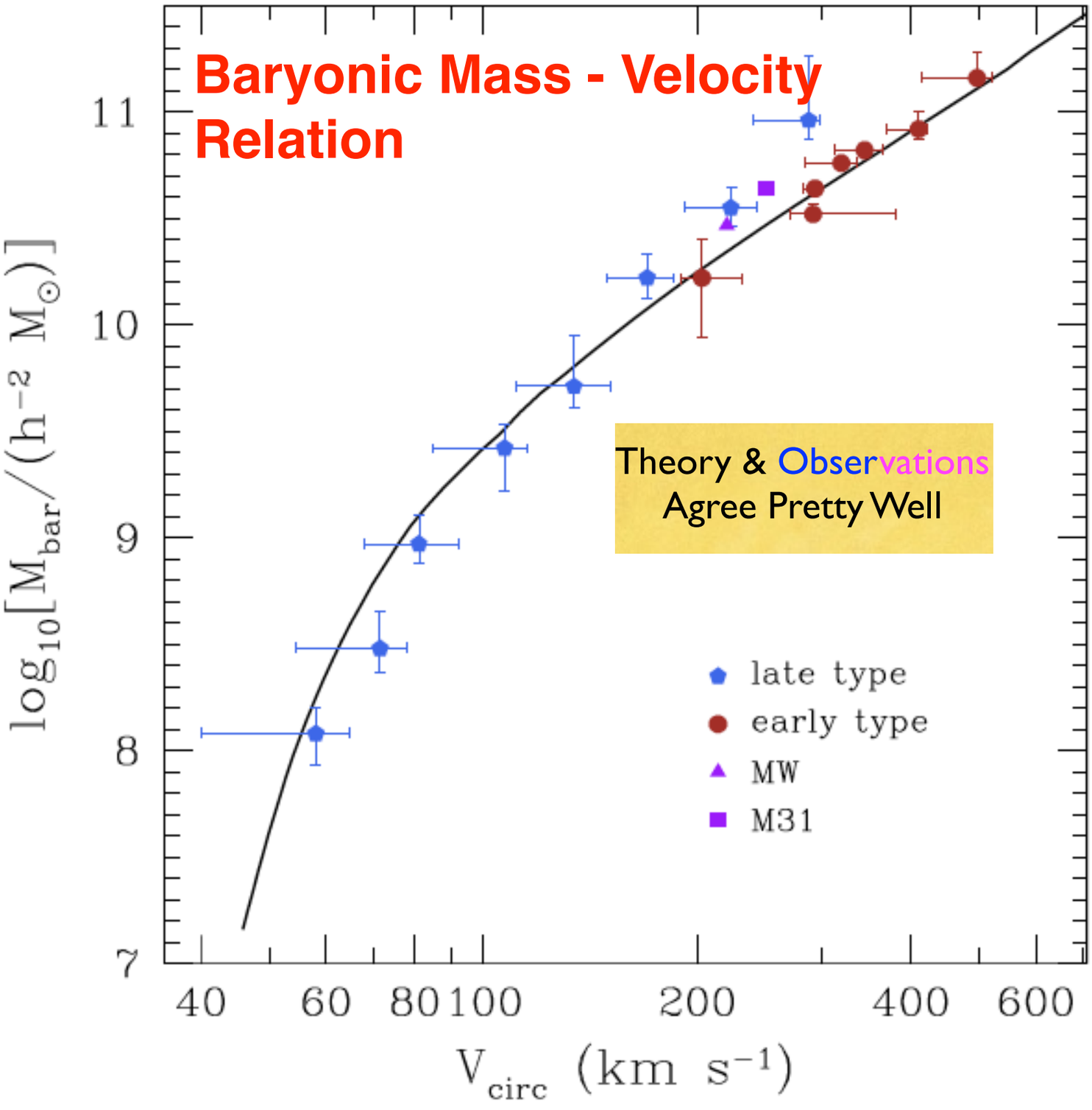

Trujillo-Gomez, Klypin, Primack, & Romanowsky ApJ 2011

Fig. 10.— Mass in cold baryons as a function of circular velocity. The solid curve shows the median values for the ΛCDM model using halo abundance matching. The cold baryonic mass includes stars and cold gas and the circular velocity is measured at 10 kpc from the center while including the effect of adiabatic contraction. For comparison we show the individual galaxies of several galaxy samples. Intermediate mass galaxies such as the Milky Way and M31 lie very close to our model results.

Bolshoi Sub-Halo Abundance Matching

Luminosity-Velocity Relation

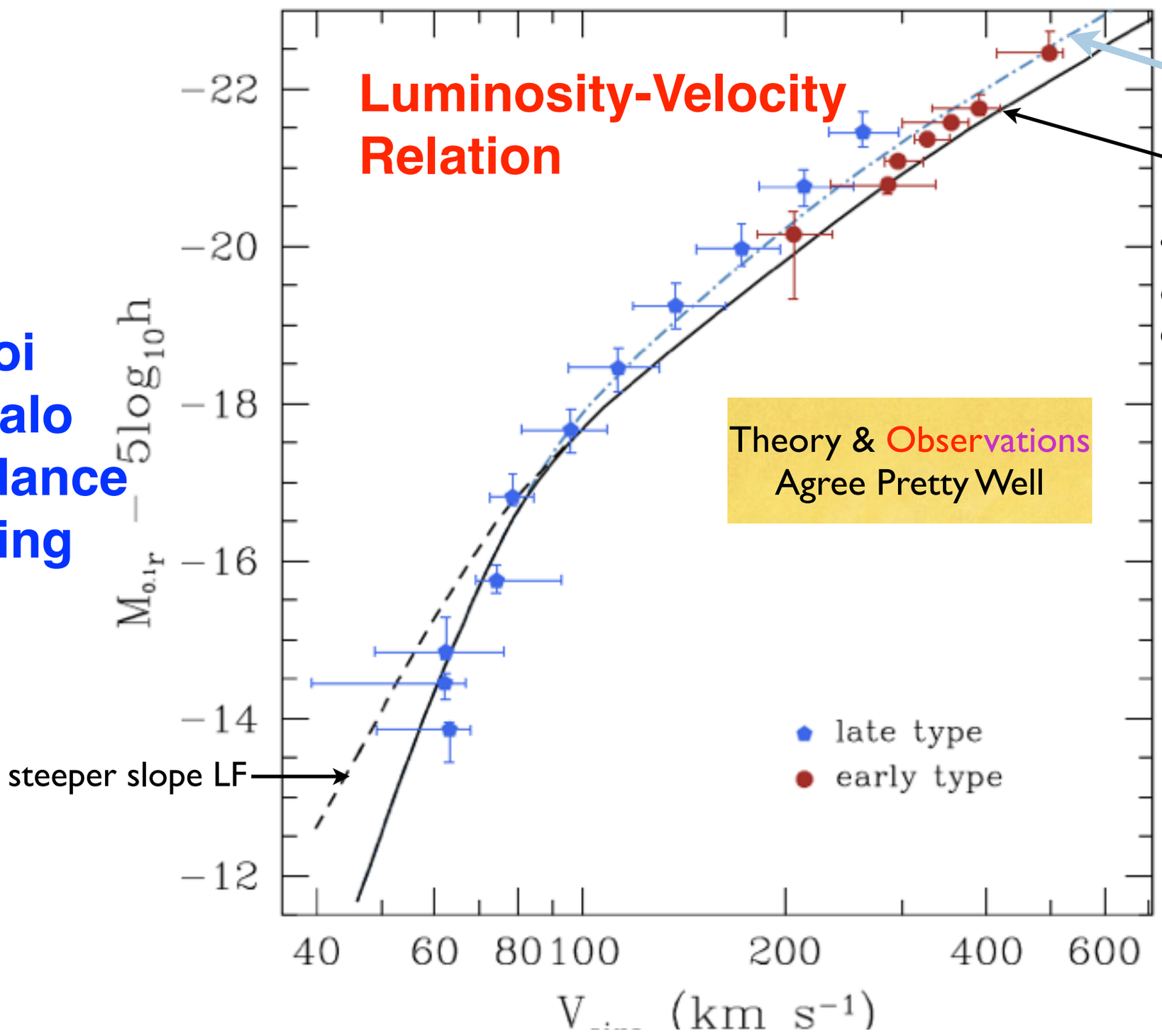

median Vcirc without AC

median Vcirc with AC

"AC" = Adiabatic Contraction of dark matter halos when baryons cool & condense to halo centers, following Blumenthal, Faber, Flores, & Primack 1986

Theory & Observations Agree Pretty Well

Trujillo-Gomez, Klypin, Primack, & Romanowsky ApJ 2011

Fig. 4.— Comparison of the observed LuminosityVelocity relation with the predictions of the ΛCDM model. The solid curve shows the median values of $^{0.1}r$-band luminosity vs. circular velocity for the model galaxy sample. The circular velocity for each model galaxy is based on the peak circular velocity of its host halo over its entire history, measured at a distance of 10 kpc from the center including the cold baryonic mass and the standard correction due to adiabatic halo contraction. The dashed curve show results for a steeper ($\alpha = -1.34$) slope of the LF. The dot-dashed curve shows predictions after adding the baryon mass but without adiabatic contraction. Points show representative observational samples.

Bolshoi Sub-Halo Abundance Matching

Discrepancy due to incomplete observations or ΛCDM failure?

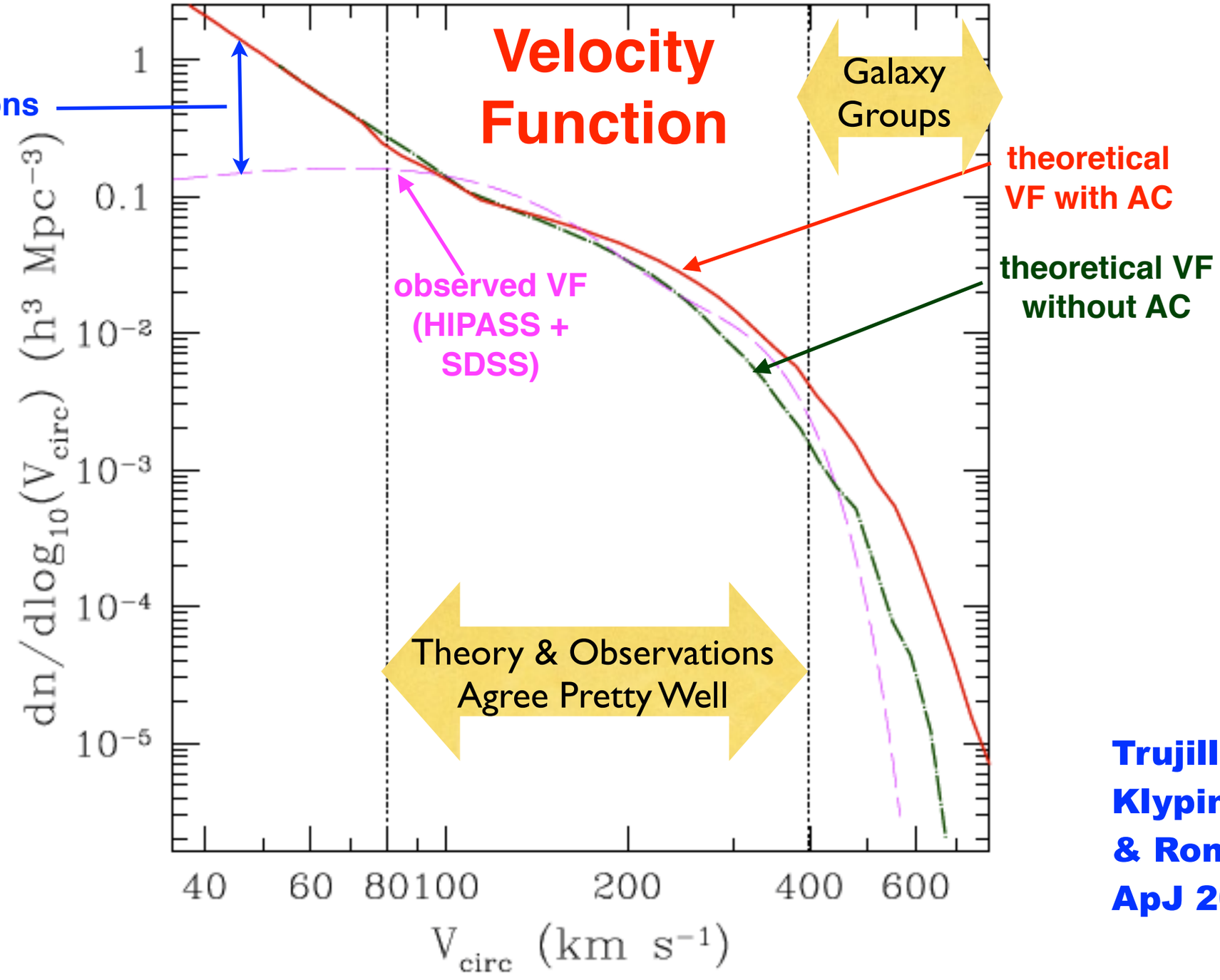

Trujillo-Gomez, Klypin, Primack, & Romanowsky ApJ 2011

Fig. 11.— Comparison of theoretical (dot-dashed and thick solid curves) and observational (dashed curve) circular velocity functions. The dot-dashed line shows the effect of adding the baryons (stellar and cold gas components) to the central region of each DM halo and measuring the circular velocity at 10 kpc. The thick solid line is the distribution obtained when the adiabatic contraction of the DM halos is considered. Because of uncertainties in the AC models, realistic theoretical predictions should lie between the dot-dashed and solid curves. Both the theory and observations are highly uncertain for rare galaxies with $V_{\rm circ} > 400$ km s^{-1}. Two vertical dotted lines divide the VF into three domains: $V_{\rm circ} > 400$ km s^{-1} with large observational and theoretical uncertainties; < 80 km s^{-1} $< V_{\rm circ} <$ 400 km s^{-1} with a reasonable agreement, and $V_{\rm circ} < 80$ km s^{-1}, where the theory significantly overpredicts the number of dwarfs.

Klypin, Karachentsev, Nasonova 2012

Deeper Local Survey -- better agreement with ΛCDM but still more halos than galaxies below 50 km/s

Local Volume: D <10 Mpc

Total sample: 813 galaxies
Within 10 Mpc: 686
M_B<-13 N=304
M_B<-10 N=611

80-90% are spirals or dIrr (T>0)

Errors of distances are 8-10%

80% with D<10Mpc have HI linewidth

Vrot =
150x10^(-(20.5+M_B)/8.5)km/s

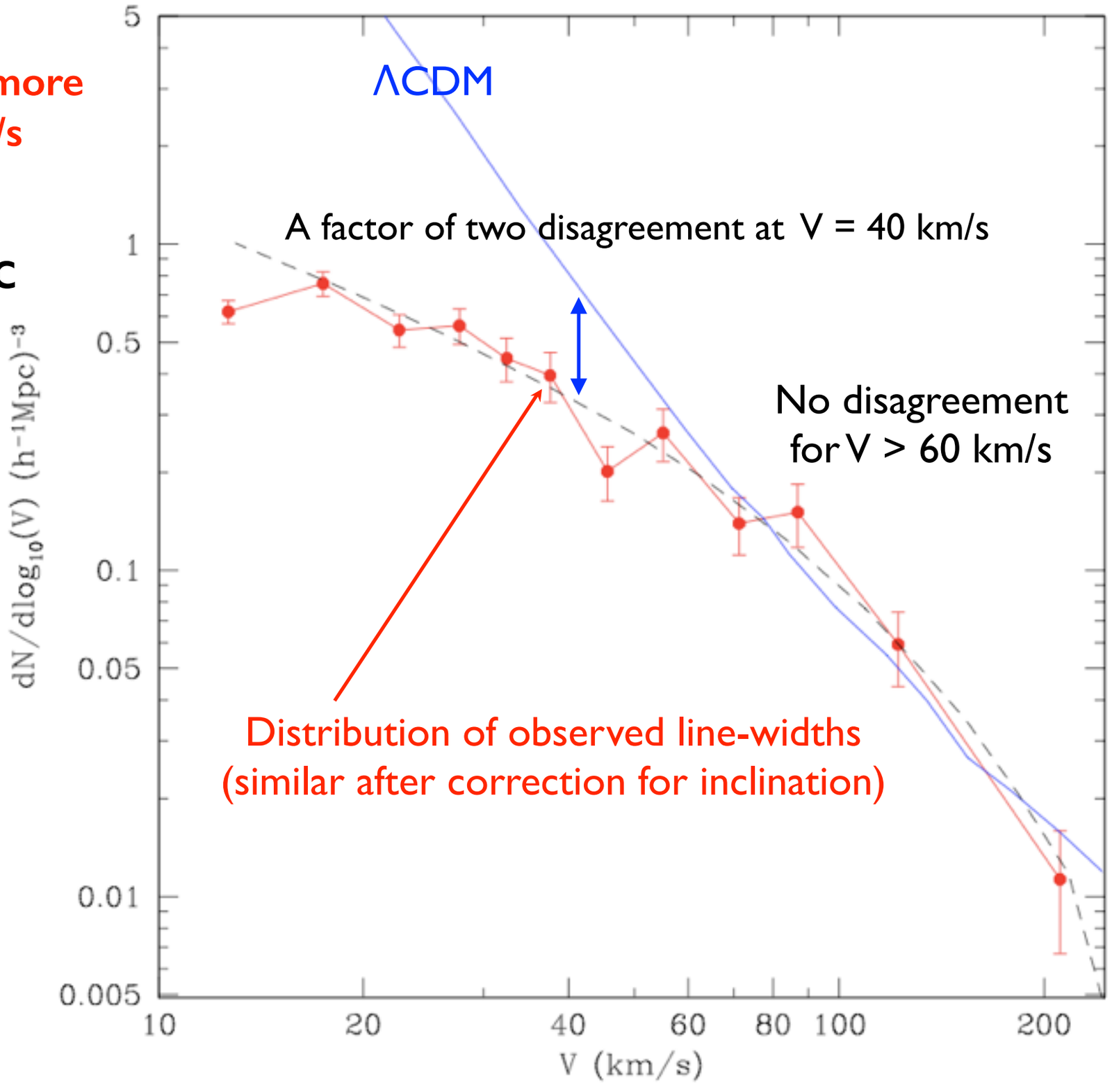

Determination of σ_8 and Ω_M from CMB+

WMAP+SN+Clusters Planck+WP+HighL+BAO

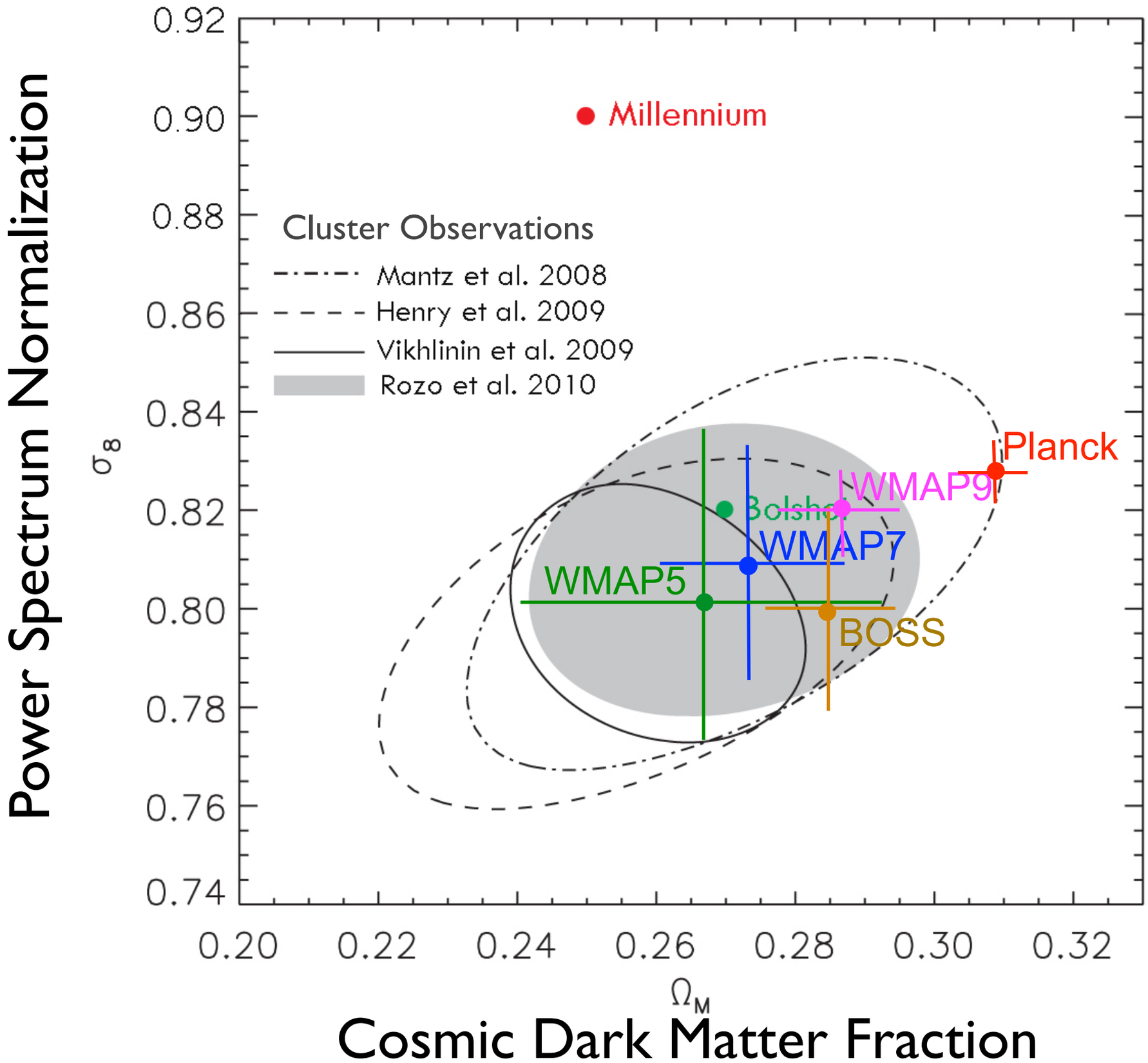

Bolshoi-Planck Cosmological Simulation

Anatoly Klypin & Joel Primack

Finished 6 Aug 2013 on Pleiades computer

at NASA Ames Research Center

8.6×10^9 particles 1 kpc resolution

1 Billion Light Years

New Simulations: Multi Dark and Bolshoi

Box	σ_8	h	Np	m_p	Ω_m	resolution
2500	0.82	0.70	57G	2.07×10^{10}	0.27	10kpch
2500	0.82	0.70	57G	2.22×10^{10}	0.29	10kpch
2500	0.82	0.70	57G	2.36×10^{10}	0.31	10kpch
2500	0.82	0.68	57G	2.35×10^{10}	0.31	10kpch
1000	0.82	0.68	57G	1.5×10^{9}	0.31	5kpc
400	0.82	0.68	57G	0.96×10^{8}	0.31	1kpc
250	0.82	0.68	8G	1.5×10^{8}	0.31	1kpc

A. Klypin (NMSU), F. Prada (Madrid), G. Yepes (Madrid),
S.Gottlober (Potsdam), J.Primack(UCSC)

New Simulations: Multi Dark and Bolshoi

20 M cpu hrs 3e11 particles 5 PTb of stored data

Gadget and ART codes

5 trillion halos at different redshifts z=0-10
with properties such as :
mass, concentration, circular velocity shape, rotation
Spherical Overdensity (BDM and RockStar) and FoF

Halos and some snapshots are publicly available

Bolshoi-Planck has a lot more massive halos at high redshifts than Bolshoi!

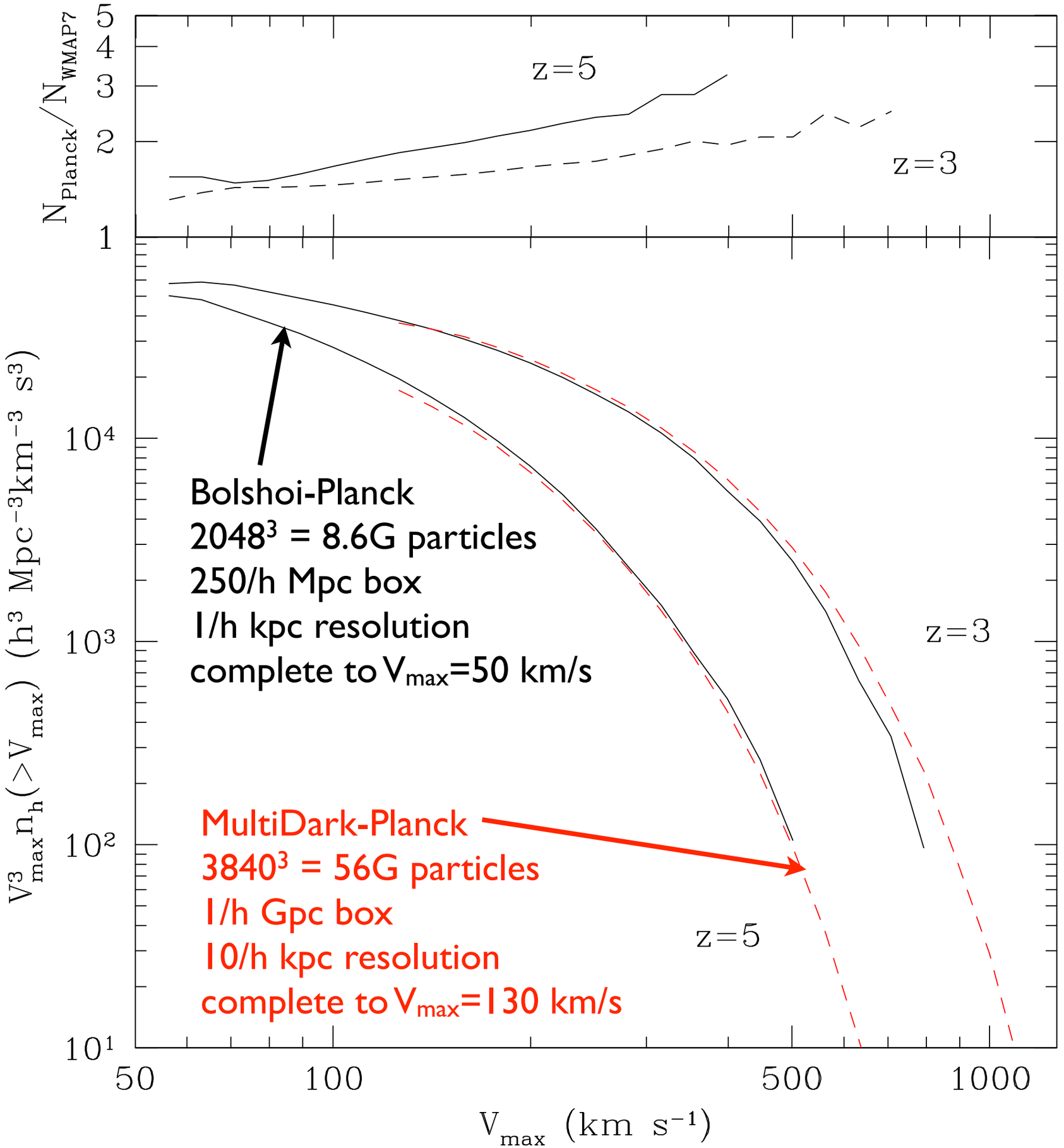

STELLAR MASS – HALO MASS RELATION

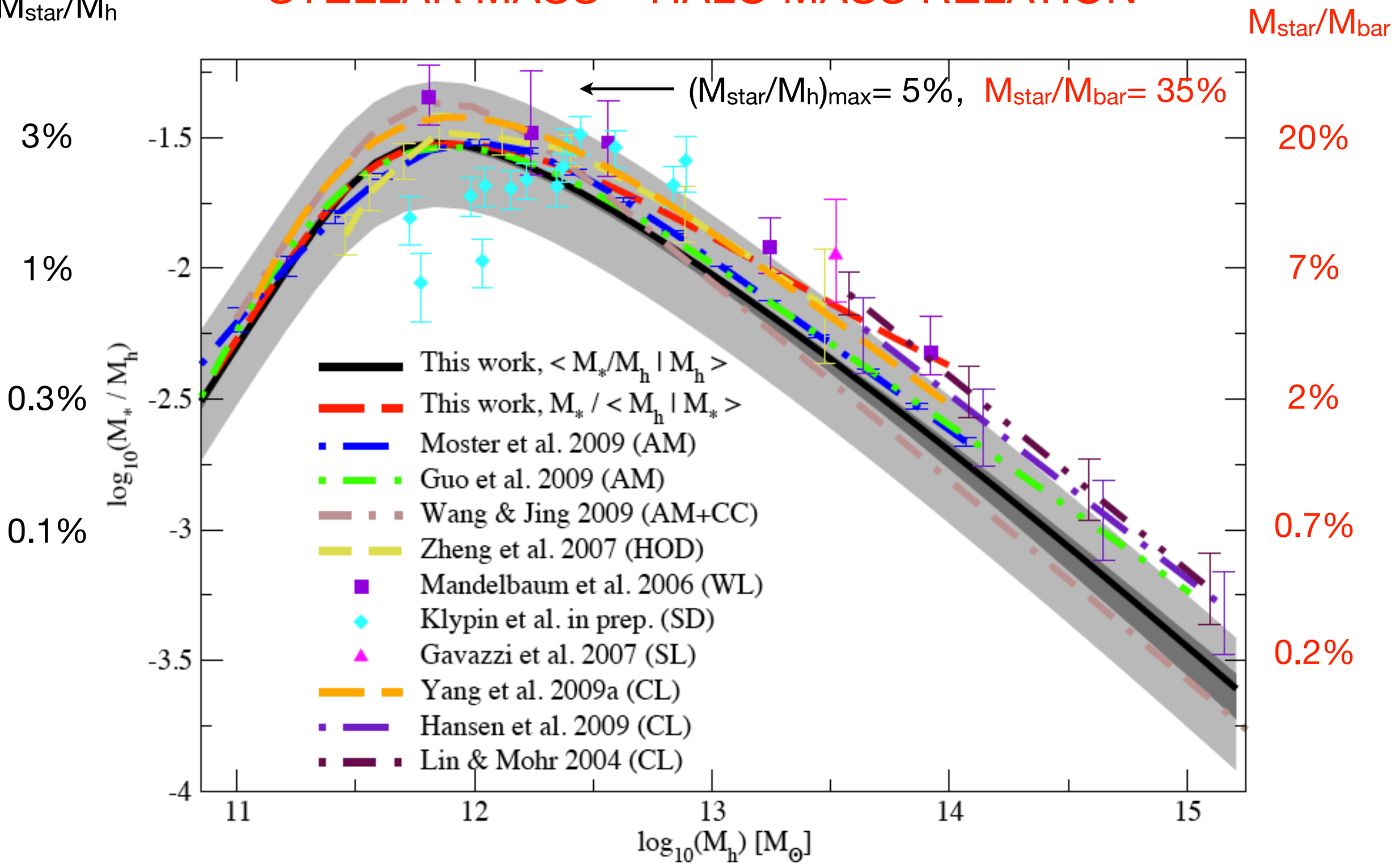

Comparison of best-fit model of Behroozi, Conroy, Wechsler (2010) at $z = 0.1$ to previously published results.

STELLAR MASS – HALO MASS RELATION

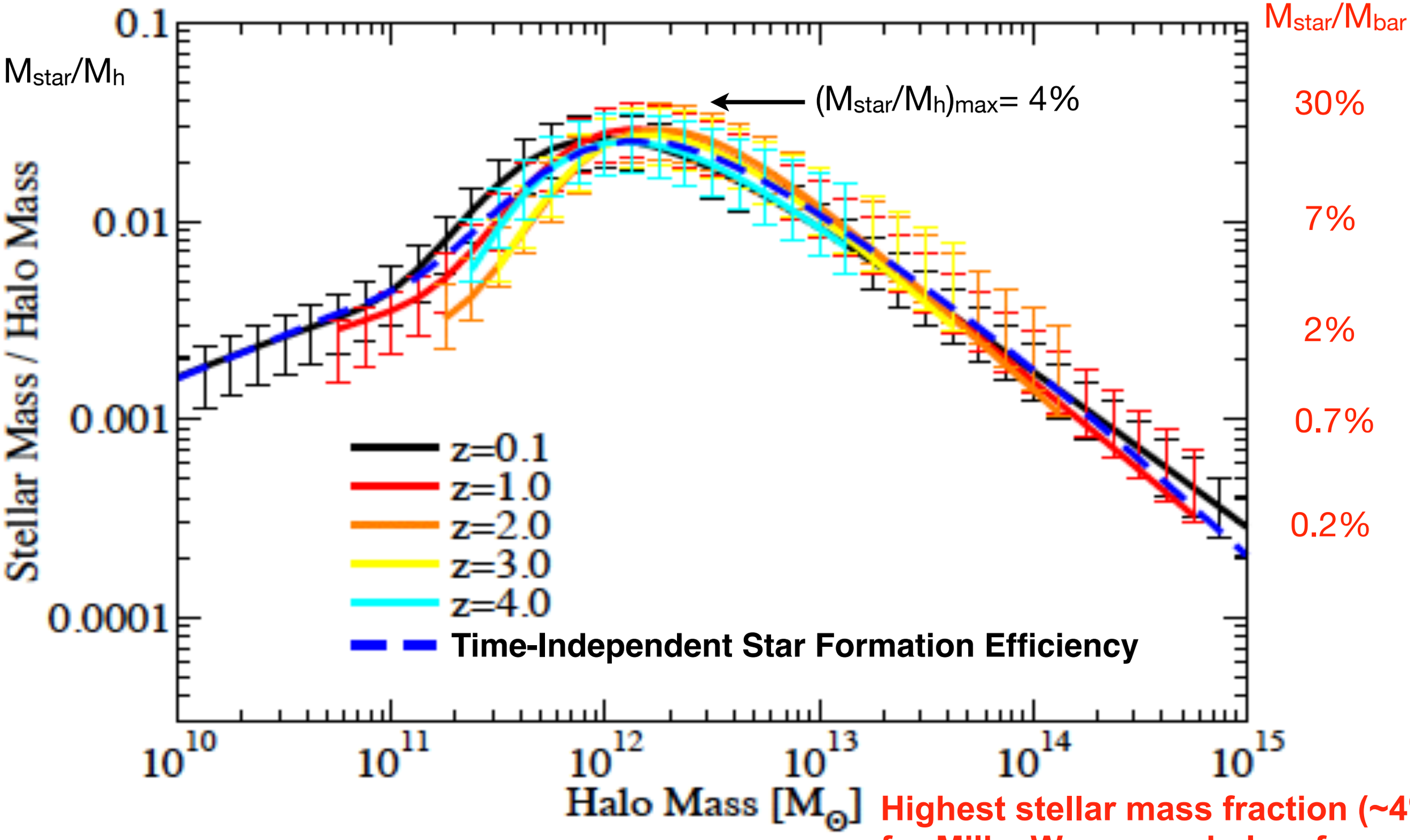

Cosmic baryon fraction = 0.045/0.31 = 14%
Milky Way M^*/M_{halo} = 0.3 x 14% = 4%

Highest stellar mass fraction (~4%) for Milky Way mass halos, for which stars are ≲30% of baryons.

Behroozi, Wechsler, Conroy ApJL, 762, L31 (2013)

Inefficient Star-Formation

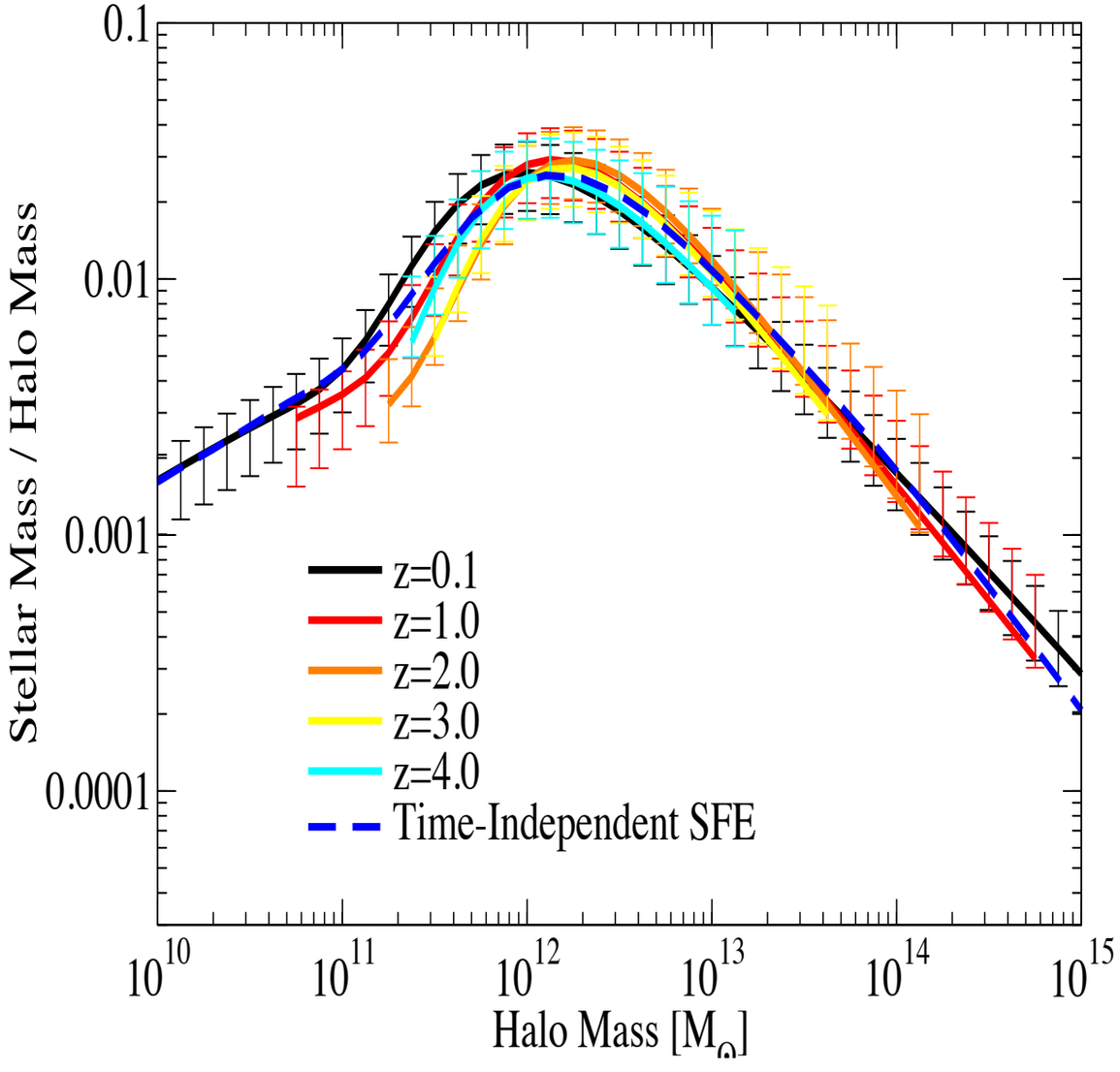

Highest stellar mass fraction (~3%) for Milky Way mass halos, for which stars are ~ 20% of baryons.

Cosmic baryon fraction = 0.045/0.31 = 14%

Milky Way M^*/M_{halo} = 0.2 x 14% = 3%

Star-Formation History

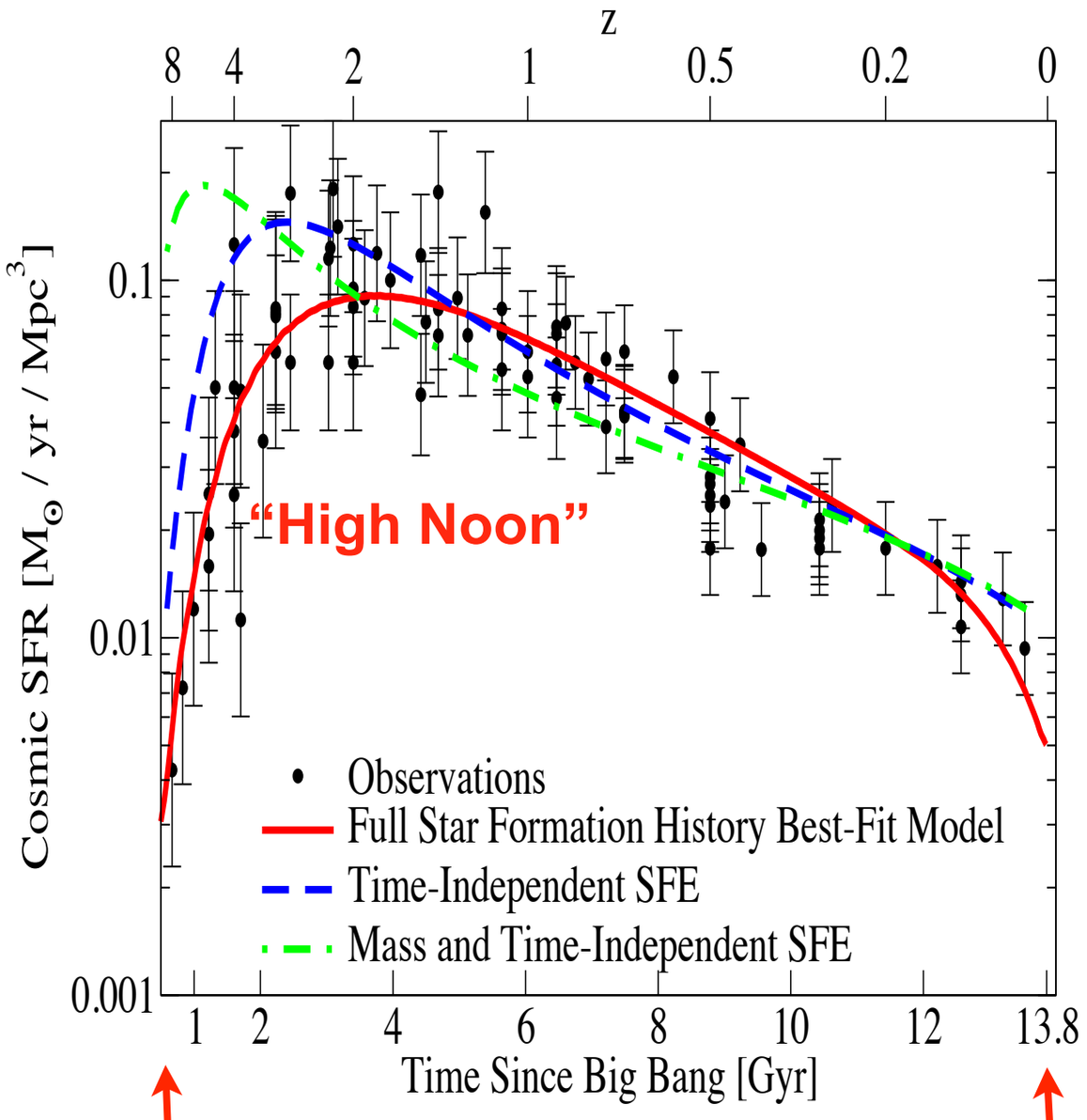

"Cosmic Dawn"

Today

Based on Bolshoi simulation and HAM:

Behroozi, Wechsler, Conroy ApJL, 762, L31 (2013)

Galaxy Formation - Introduction

ΛCDM vs. Downsizing

ΛCDM:

hierarchical formation
(small things form first)

"Downsizing":

massive galaxies are old, star formation moves to smaller galaxies

small structures

large structures

early

late

large galaxies

small galaxies

Galaxy Formation - Introduction

ΛCDM vs. Downsizing

ΛCDM:

hierarchical formation
(small things form first)

"Downsizing":

massive galaxies are old, star formation moves to smaller galaxies

mass assembly

DM simulations

present-day structure

How are these processes related?

star formation history

semi-analytic models

current stellar population

Galaxy Formation - Introduction

An old criticism of ΛCDM has been that the order of cosmogony is wrong: halos grow from small to large by accretion in a hierarchical formation theory like ΛCDM But the oldest stellar populations are found in the most massive galaxies -- suggesting that these massive galaxies form earliest, a phenomenon known as "downsizing." The key to explaining the downsizing phenomenon is the realization that **star formation is most efficient in dark matter halos with masses about 10^{11} - $10^{12.5}$ $M_\odot$**. This goes back at least as far as the original Cold Dark Matter paper (BFPR84), from which the following figure is reproduced.

Formation of galaxies and large-scale structure with cold dark matter

Blumenthal, Faber, Primack, & Rees -- Nature 311, 517 (1984)

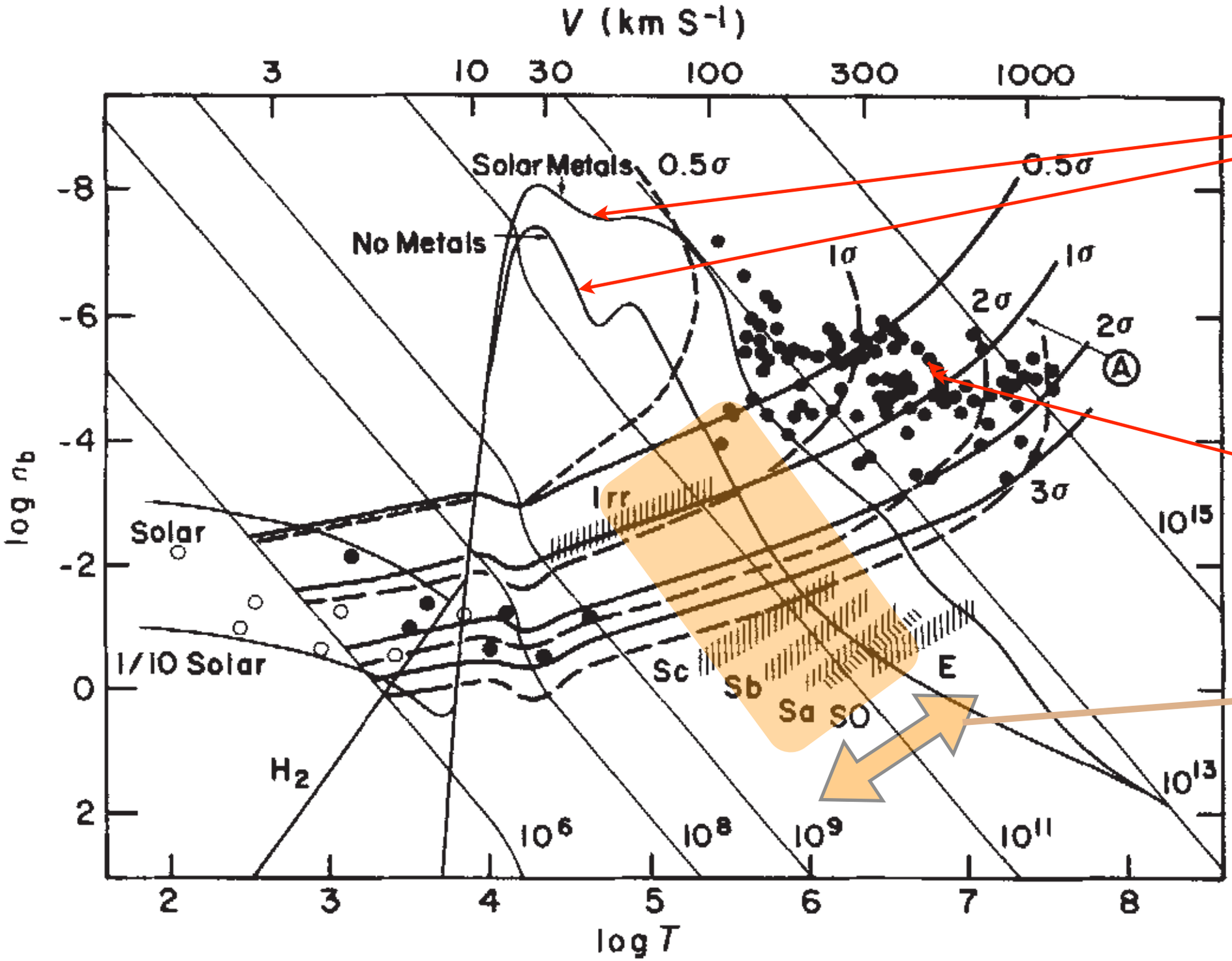

Galaxies form beneath the cooling curves

Galaxy groups and clusters form above the cooling curves

Star Forming Band: 10^{10} - 10^{12} Msun

Fig. 3 Baryon density n_b versus three-dimensional, r.m.s. velocity dispersion V and virial temperature T for structures of various size in the Universe. The quantity T is $\mu V^2/3k$, where μ is mean molecular weight ($\approx$0.6 for ionized, primordial H+He) and k is Boltzmann's constant.

redshift z

8 4 2 1 0.5 0.2 0

No Halos

Star Formation Efficiency
(star formation rate divided by
baryonic mass accretion rate)

Star-Forming Band

$\log_{10}$(SFR/MA)

-0.3

-2.6

-5.0

Halo Mass [$M_\odot$]

10^{15} 10^{14} 10^{13} 10^{12} 10^{11} 10^{10} 10^{9}

1 2 4 6 8 10 12 13.8

Time Since Big Bang [Gyr]

From Figure 1 of Behroozi, Wechsler, Conroy ApJL, 762, L31 (2013)

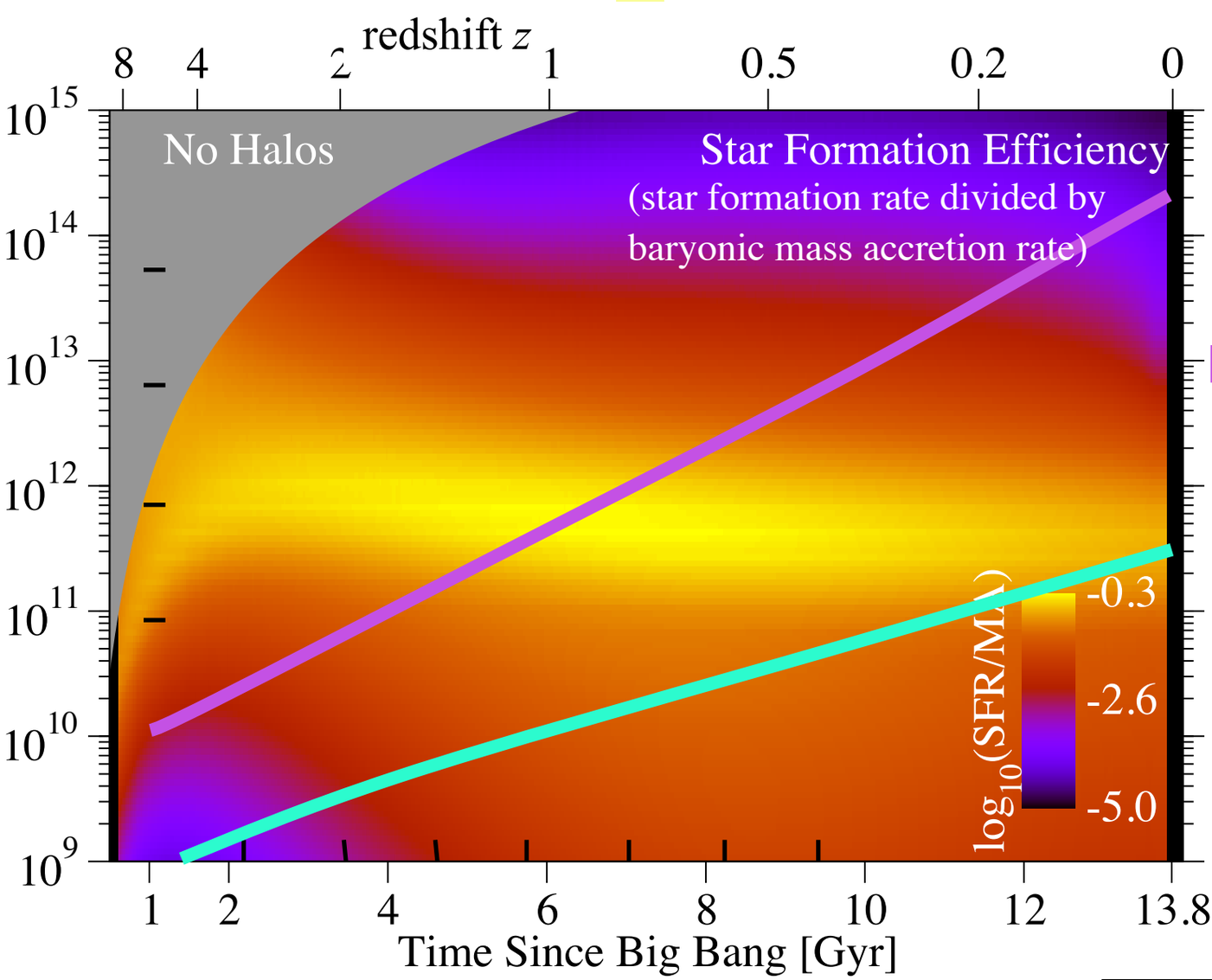

Implications of the Star-Forming Band Model

Massive galaxies:

- Started forming stars early.
- Shut down early.
- Are red today.
- Populate dark halos that are much more massive than their stellar mass.

Small galaxies:

- Started forming stars late.
- Are still making stars today.
- Are blue today.
- Populate dark halos that scale with their stellar mass.

"Downsizing"

Star formation is a wave that started in the largest galaxies and swept down to smaller masses later (Cowie et al. 1996).

From Figure 1 of Behroozi, Wechsler, Conroy ApJL, 762, L31 (2013)

Galaxy Formation via SemiAnalytic Models

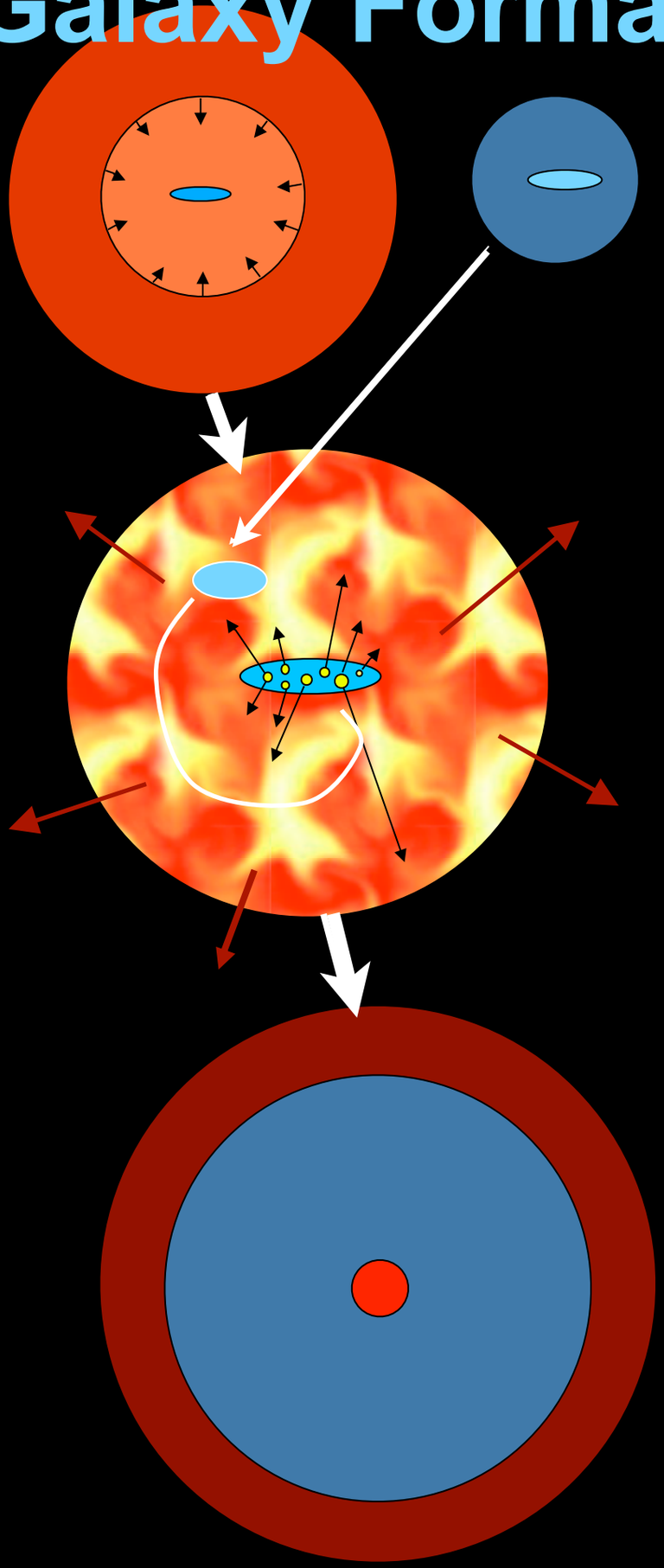

- gas is collisionally heated when perturbations ‘turn around’ and collapse to form gravitationally bound structures
- gas in halos cools via atomic line transitions (depends on density, temperature, and metallicity)
- cooled gas collapses to form a rotationally supported disk
- cold gas forms stars, with efficiency a function of gas density (e.g. Schmidt-Kennicutt Law, metallicity effects?)
- massive stars and SNe reheat (and in small halos expel) cold gas and some metals
- galaxy mergers trigger bursts of star formation; ‘major’ mergers transform disks into spheroids and fuel AGN
- AGN feedback cuts off star formation
- **including effects of dissipation in gas-rich galaxy mergers leads to observed elliptical size-mass relation**
- **including spheroid formation by disk instability is essential to reproduce the observed elliptical luminosity function**

White & Frenk 91; Kauffmann+93; Cole+94; Somerville & Primack 99; Cole+00; Somerville, Primack, & Faber 01; Croton et al. 2006; Somerville +08; Fanidakis+09; Covington et al. 10, 11; Somerville, Gilmore, Primack, & Dominguez 11; Porter et al.14ab

SemiAnalytic Model Low-Redshift Galaxies

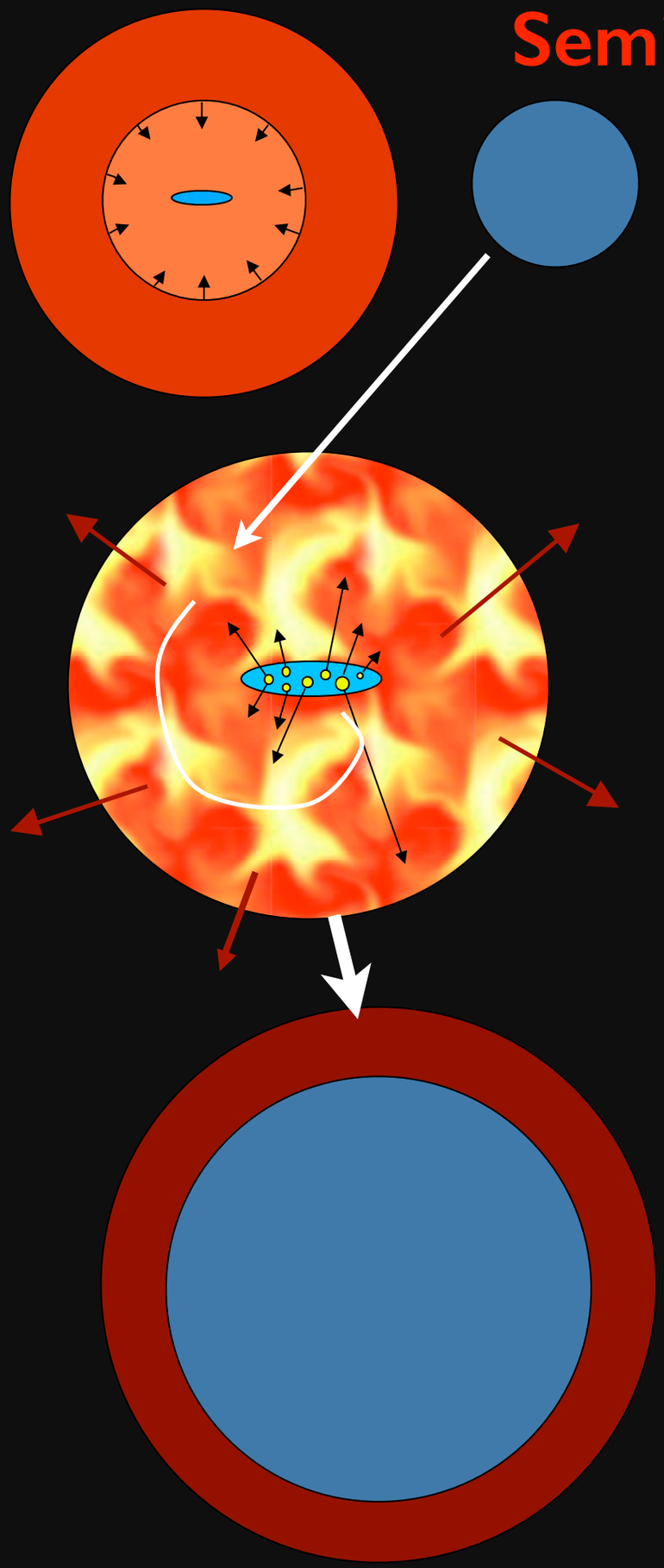

- Elliptical galaxies follow a size-mass relation. Does the theory correctly predict this? What about the other relations of elliptical galaxies?

- Does the theory correctly predict the numbers of Disk Galaxies and Elliptical Galaxies of all masses?

- Elliptical galaxies follow a size-mass relation. The Bolshoi semi-analytic model correctly predicts this and the other relations of elliptical galaxies.

- Disk galaxies follow the TF relation between the speed they spin and their luminosity or mass. The model also correctly predicts this.

- Our semi-analytic model also correctly predicts the numbers of Disk galaxies and Elliptical galaxies of all masses.

SemiAnalytic Model Low-Redshift Galaxies

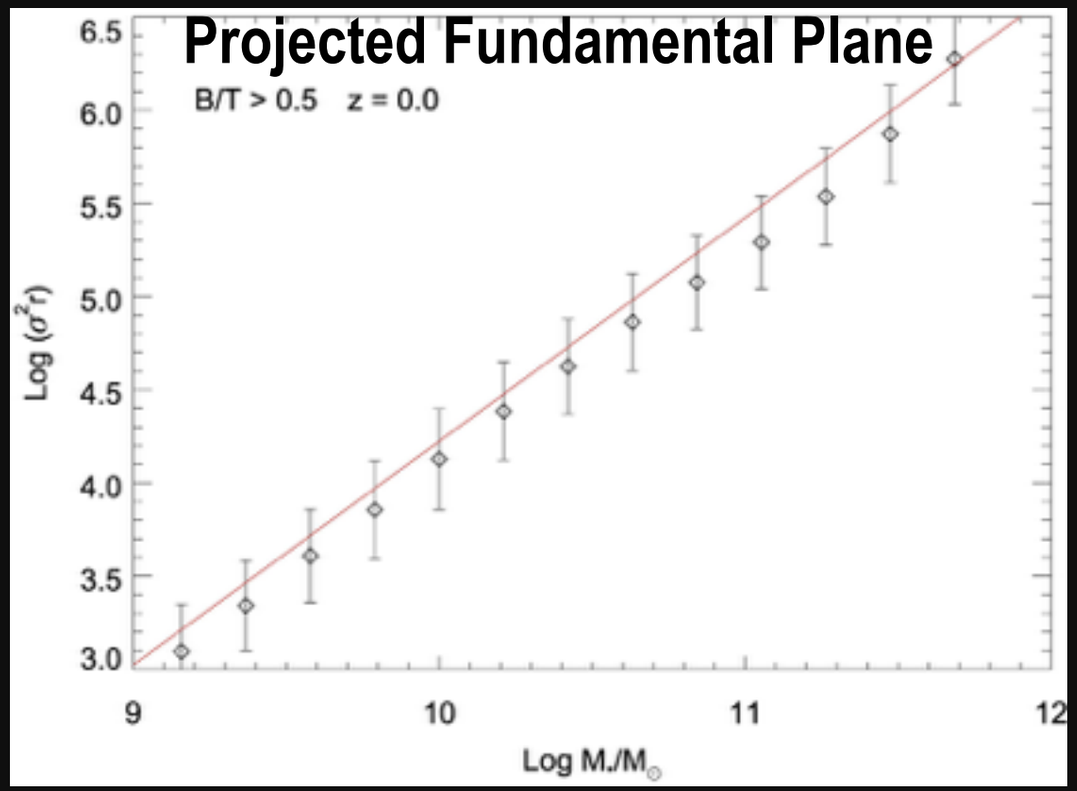

- Correctly reproduces the z=0 size-mass, Faber-Jackson, and Fundamental Plane relations
- Forming spheroids with major mergers + disk instabilities reproduces the morphology-selected z=0 mass function

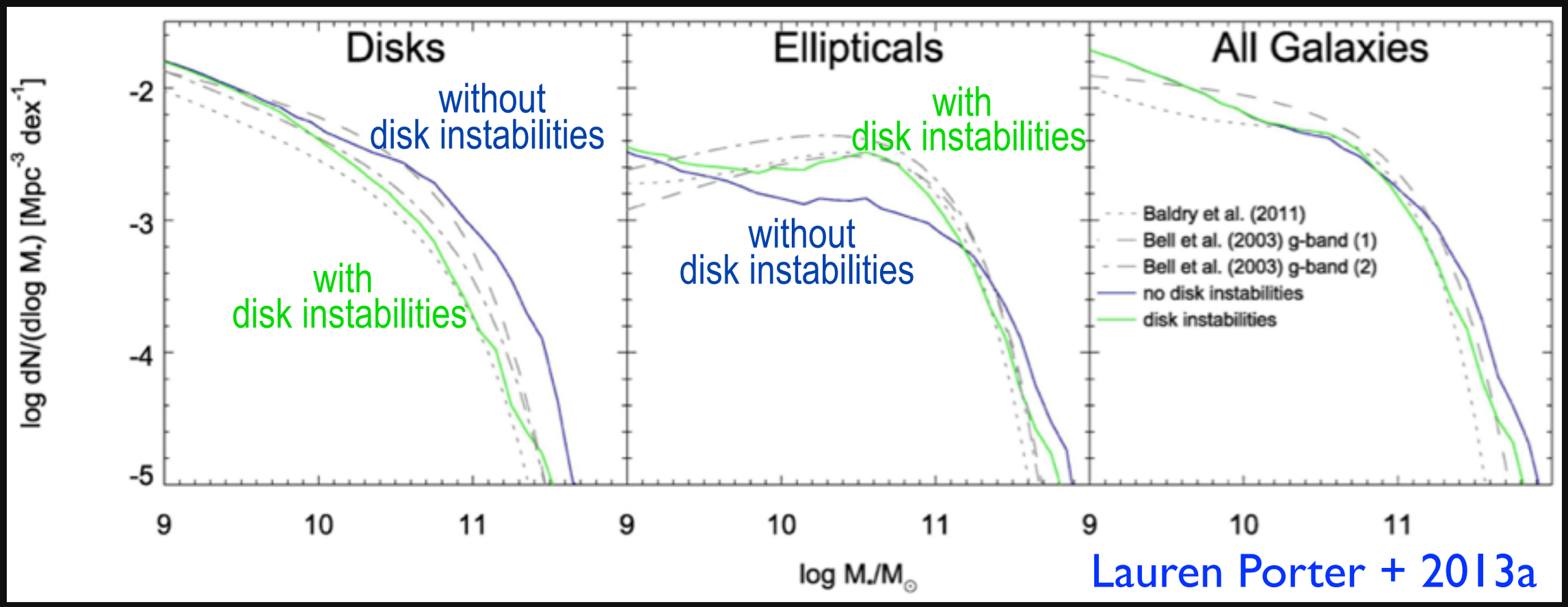

Lauren Porter + 2013a

SAM Predictions vs. SDSS Observations

Galaxy Age

Galaxy Metallicity

SAM
Predictions

Lauren Porter et al. 2013

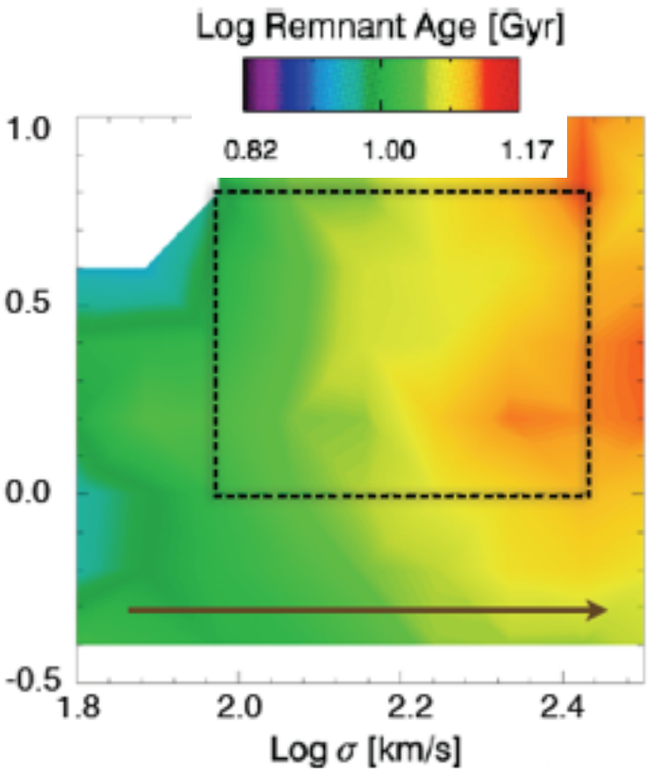

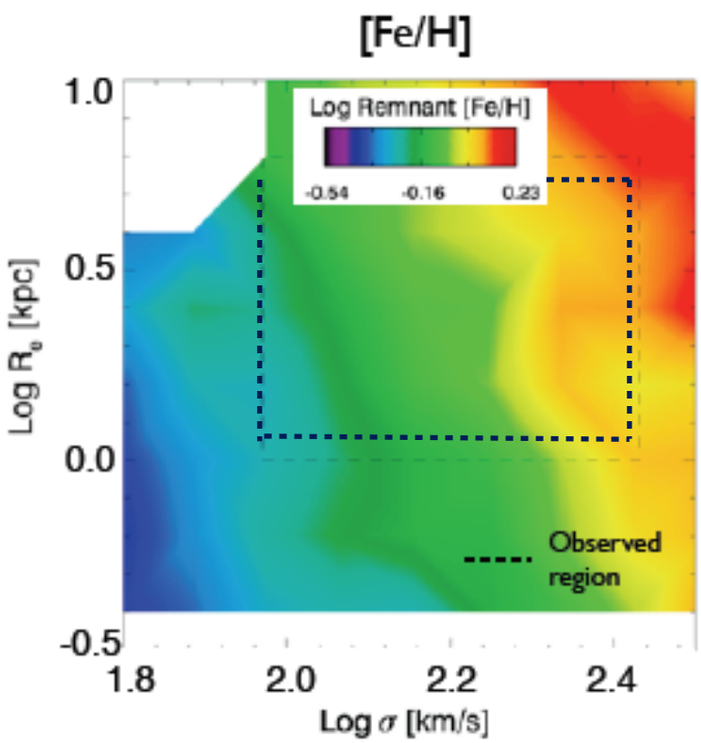

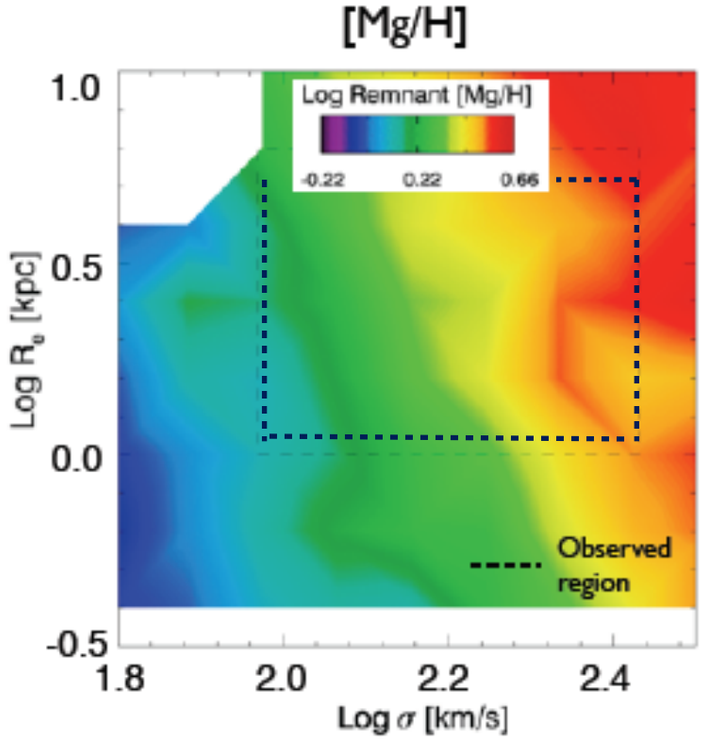

SDSS
Observations

Jenny Graves et al. 2009

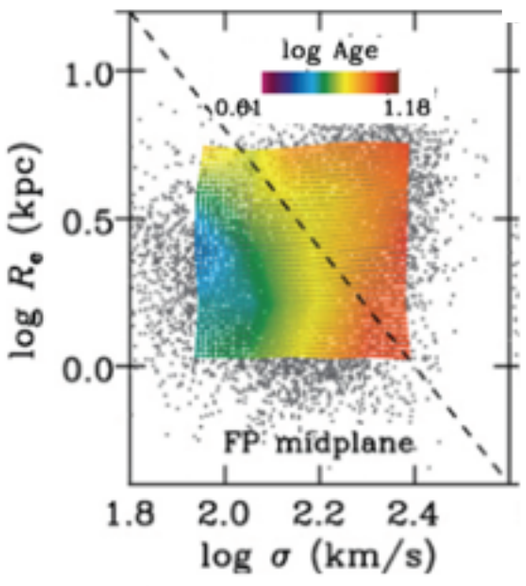

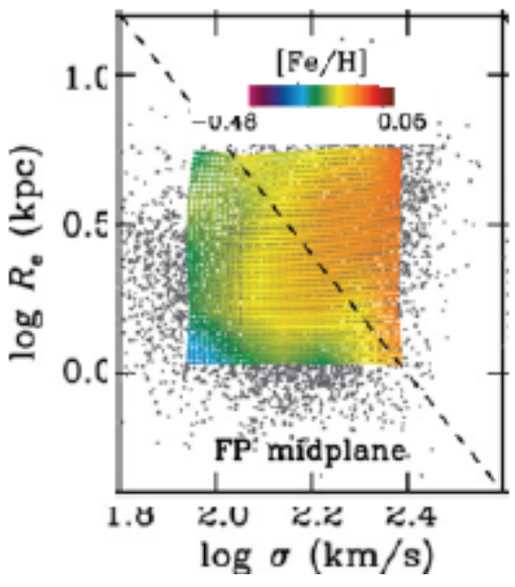

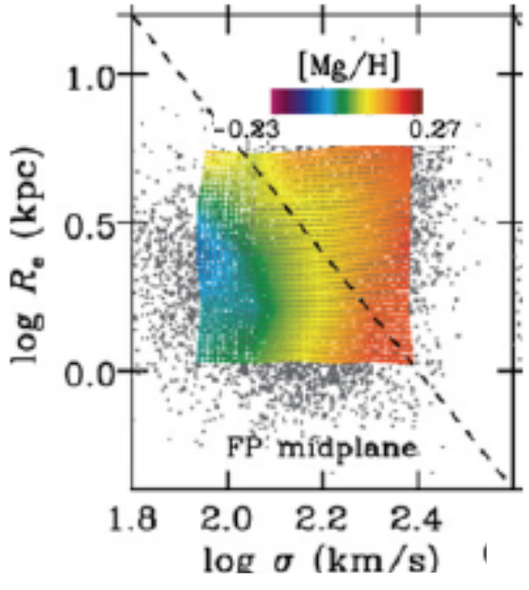

Lauren Porter + 2013b

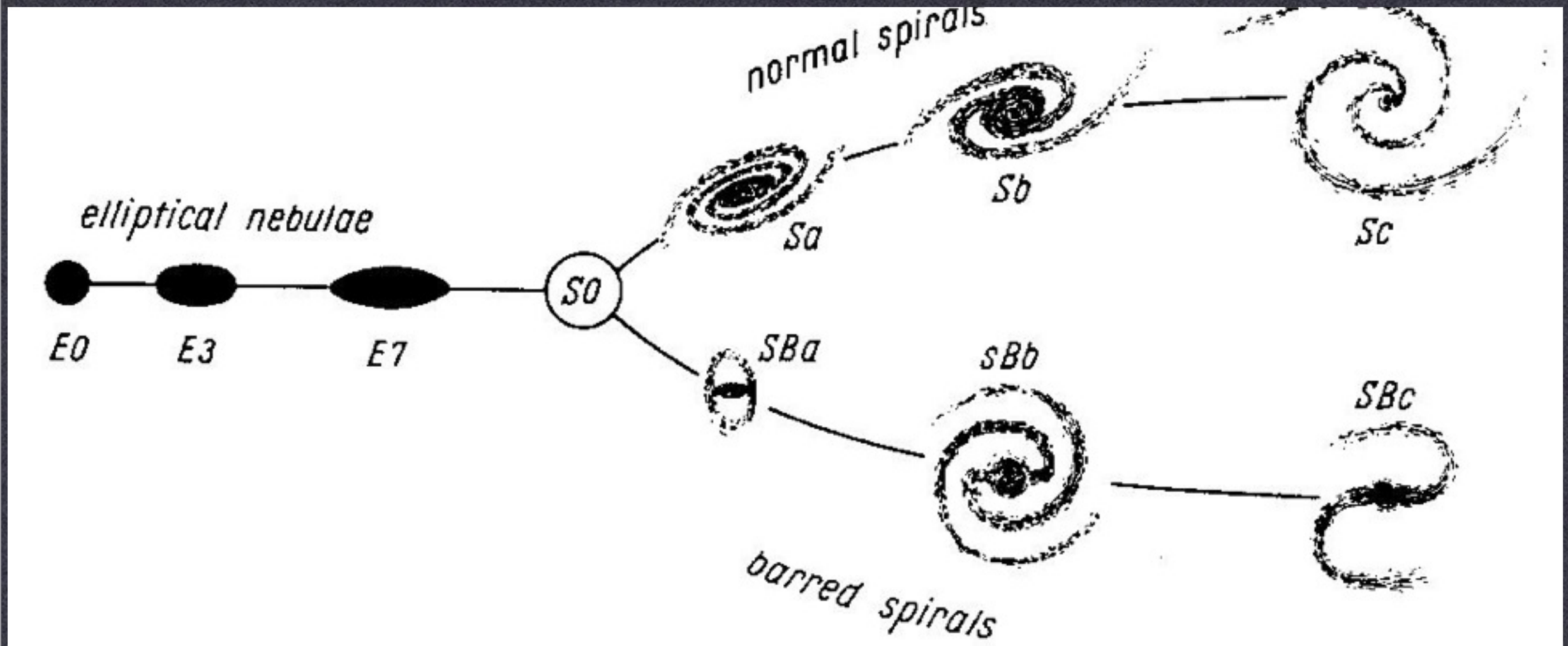

ORIGIN OF HUBBLE SEQUENCE

CIRCA 1930

New Simulations: Multi Dark and Bolshoi

20 M cpu hrs 3e11 particles 5 PTb of stored data

Gadget and ART codes

5 trillion halos at different redshifts z=0-10

with properties such as :
mass, concentration, circular velocity shape, rotation
Spherical Overdensity (BDM and RockStar) and FoF

Halos and some snapshots are publicly available

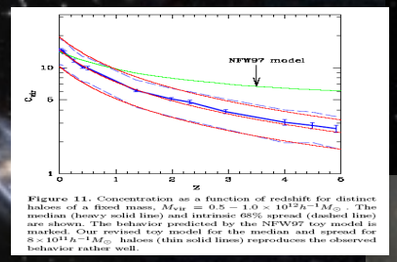

Figure 11. Concentration as a function of redshift for distinct haloes of a fixed mass, $M_{vir} = 0.5 - 1.0 \times 10^{12} h^{-1} M_\odot$. The median (heavy solid line) and intrinsic 68% spread (dashed line) are shown. The behavior predicted by the NFW97 toy model is marked. Our revised toy model for the median and spread for $8 \times 10^{11} h^{-1} M_\odot$ haloes (thin solid lines) reproduces the observed behavior rather well.

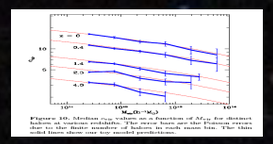

Figure 10. Median c_{vir} values as a function of M_{vir} for distinct haloes at various redshifts. The error bars are the Poisson error due to the finite number of haloes in each mass bin. The thin solid lines show our toy model predictions.

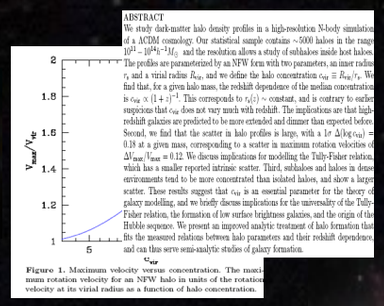

ABSTRACT

We study dark-matter halo density profiles in a high-resolution N-body simulation of a ΛCDM cosmology. Our statistical sample contains ∼5000 haloes in the range $10^{12} - 10^{15} h^{-1} M_\odot$ and the resolution allows a study of subhaloes inside host haloes. The profiles are parameterized by an NFW form with two parameters, an inner radius r_s and a virial radius R_{vir}, and we define the halo concentration $c_{vir} \equiv R_{vir}/r_s$. We find that, for a given halo mass, the redshift dependence of the median concentration is $c_{vir} \propto (1+z)^{-1}$. This corresponds to $r_s(z) \sim$ constant, and is contrary to earlier suspicions that c_{vir} does not vary much with redshift. The implications are that high-redshift galaxies are predicted to be more extended and dimmer than expected before. Second, we find that the scatter in halo profiles is large, with a 1σ $\Delta(\log c_{vir}) = 0.18$ at a given mass, corresponding to a scatter in maximum rotation velocities of $\Delta V_{max}/V_{max} = 0.12$. We discuss implications for modelling the Tully-Fisher relation, which has a smaller reported intrinsic scatter. Third, subhaloes and haloes in dense environments tend to be more concentrated than isolated haloes, and show a larger scatter. These results suggest that c_{vir} is an essential parameter for the theory of galaxy modelling, and we briefly discuss implications for the universality of the Tully-Fisher relation, the formation of low surface brightness galaxies, and the origin of the Hubble sequence. We present an improved analytic treatment of halo formation that fits the measured relations between halo parameters and their redshift dependences, and can thus serve semi-analytic studies of galaxy formation.

Figure 1. Maximum velocity versus concentration. The maximum rotation velocity for an NFW halo in units of the rotation velocity at its virial radius as a function of halo concentration.

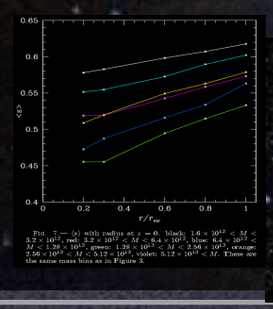

FIG. 7.— $\langle s \rangle$ with radius at $z = 0$. black: $1.6 \times 10^{12} < M < 3.2 \times 10^{12}$, red: $3.2 \times 10^{12} < M < 6.4 \times 10^{12}$, blue: $6.4 \times 10^{12} < M < 1.28 \times 10^{13}$, green: $1.28 \times 10^{13} < M < 2.56 \times 10^{13}$, orange: $2.56 \times 10^{13} < M < 5.12 \times 10^{13}$, violet: $5.12 \times 10^{13} < M$. These are the same mass bins as in Figure 3.

ORIGIN OF HUBBLE SEQUENCE

CIRCA 1930

New Simulations: Multi Dark and Bolshoi

20 M cpu hrs 3e11 particles 5 PTb of stored data

Gadget and ART codes

5 trillion halos at different redshifts z=0-10

with properties such as :
mass, concentration, circular velocity shape, rotation
Spherical Overdensity (BDM and RockStar) and FoF

Halos and some snapshots are publicly available

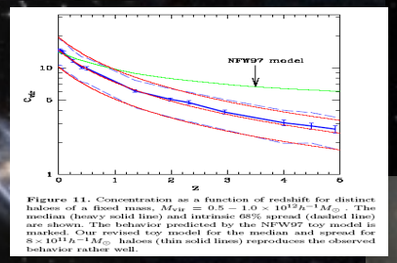

Figure 11. Concentration as a function of redshift for distinct halos of a fixed mass, $M_{vir} = 0.5 - 1.0 \times 10^{12} h^{-1} M_\odot$. The median (heavy solid line) and intrinsic 68% spread (dashed line) are shown. The behavior predicted by the NFW97 toy model is marked. Our revised toy model for the median and spread for $8 \times 10^{11} h^{-1} M_\odot$ halos (thin solid lines) reproduces the observed behavior rather well.

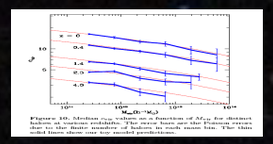

Figure 10. Median c_{vir} values as a function of M_{vir} for distinct halos at various redshifts. The error bars are the Poisson error due to the finite number of halos in each mass bin. The thin solid lines show our toy model predictions.

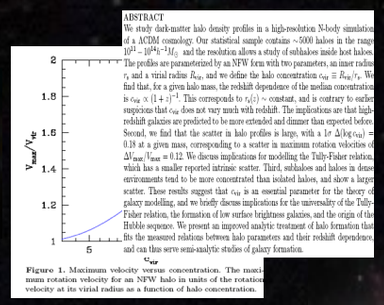

ABSTRACT

We study dark-matter halo density profiles in a high-resolution N-body simulation of a ΛCDM cosmology. Our statistical sample contains ∼5000 halos in the range $10^{12} - 10^{15} h^{-1} M_\odot$ and the resolution allows a study of subhalos inside host halos. The profiles are parameterized by an NFW form with two parameters, an inner radius r_s and a virial radius R_{vir}, and we define the halo concentration $c_{vir} \equiv R_{vir}/r_s$. We find that, for a given halo mass, the redshift dependence of the median concentration is $c_{vir} \propto (1+z)^{-1}$. This corresponds to $r_s(z) \sim$ constant, and is contrary to earlier suspicions that c_{vir} does not vary much with redshift. The implications are that high-redshift galaxies are predicted to be more extended and dimmer than expected before. Second, we find that the scatter in halo profiles is large, with a 1σ $\Delta(\log c_{vir}) = 0.18$ at a given mass, corresponding to a scatter in maximum rotation velocities of $\Delta V_{max}/V_{max} = 0.12$. We discuss implications for modelling the Tully-Fisher relation, which has a smaller reported intrinsic scatter. Third, subhalos and halos in dense environments tend to be more concentrated than isolated halos, and show a larger scatter. These results suggest that c_{vir} is an essential parameter for the theory of galaxy modelling, and we briefly discuss implications for the universality of the Tully-Fisher relation, the formation of low surface brightness galaxies, and the origin of the Hubble sequence. We present an improved analytic treatment of halo formation that fits the measured relations between halo parameters and their redshift dependences, and can thus serve semi-analytic studies of galaxy formation.

Figure 1. Maximum velocity versus concentration. The maximum rotation velocity for an NFW halo in units of the rotation velocity at its virial radius as a function of halo concentration.

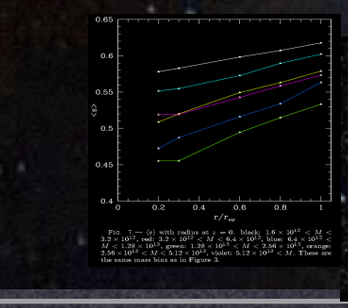

FIG. 7.— $\langle s \rangle$ with radius at $z = 0$. black: $1.6 \times 10^{12} < M < 3.2 \times 10^{12}$, red: $3.2 \times 10^{12} < M < 6.4 \times 10^{12}$, blue: $6.4 \times 10^{12} < M < 1.28 \times 10^{13}$, green: $1.28 \times 10^{13} < M < 2.56 \times 10^{13}$, orange: $2.56 \times 10^{13} < M < 5.12 \times 10^{13}$, violet: $5.12 \times 10^{13} < M$. These are the same mass bins as in Figure 3.

ORIGIN OF HUBBLE SEQUENCE

CIRCA 1930

New Simulations: Multi Dark and Bolshoi

20 M cpu hrs 3e11 particles 5 PTb of stored data

Gadget and ART codes

5 trillion halos at different redshifts z=0-10
with properties such as :
mass, concentration, circular velocity shape, rotation
Spherical Overdensity (BDM and RockStar) and FoF

Halos and some snapshots are publicly available

ABSTRACT

We study dark-matter halo density profiles in a high-resolution N-body simulation of a ΛCDM cosmology. Our statistical sample contains ~5000 halos in the range $10^{11} - 10^{14}h^{-1}M_\odot$ and the resolution allows a study of subhalos inside host halos. The profiles are parameterized by an NFW form with two parameters, an inner radius r_s and a virial radius R_{vir}, and we define the halo concentration $c_{vir} \equiv R_{vir}/r_s$. We find that, for a given halo mass, the redshift dependence of the median concentration is $c_{vir} \propto (1+z)^{-1}$. This corresponds to $c_s(z) \sim$ constant, and is contrary to earlier suspicions that c_{vir} does not vary much with redshift. The implications are that high-redshift galaxies are predicted to be more extended and dimmer than expected before. Second, we find that the scatter in halo profiles is large, with a 1σ $\Delta(\log c_{vir}) = 0.18$ at a given mass, corresponding to a scatter in maximum rotation velocities of $\Delta V_{max}/V_{max} = 0.12$. We discuss implications for modelling the Tully-Fisher relation, which has a smaller reported intrinsic scatter. Third, subhalos and halos in dense environments tend to be more concentrated than isolated halos, and show a larger scatter. Those results suggest that [illegible] is an essential parameter for the theory of galaxy modelling, and [illegible] plications for the universality of the Tully-Fisher relation, t[illegible] ichtless galaxies, and the origin of the Hubble sequen[illegible] treatment of halo formation that fits the new [illegible] their redshift dependence and can[illegible]

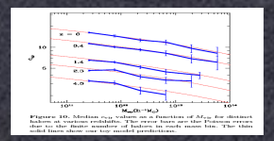

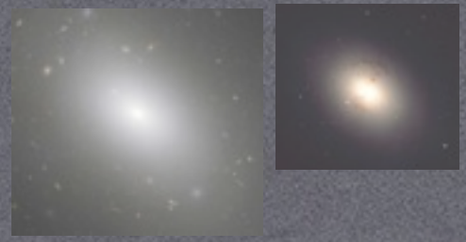

normal spirals

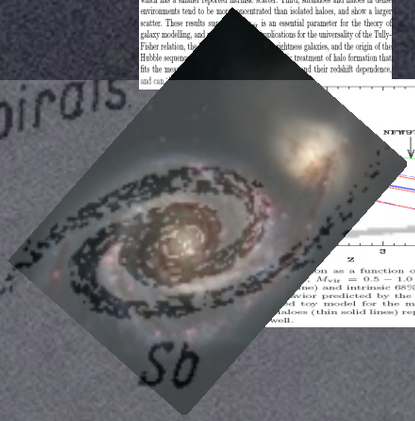

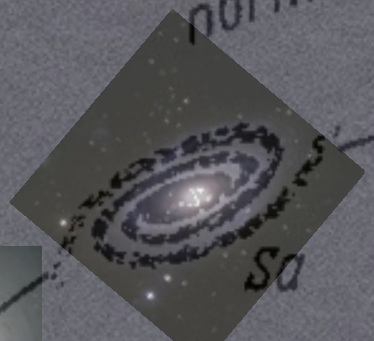

elliptical nebulae

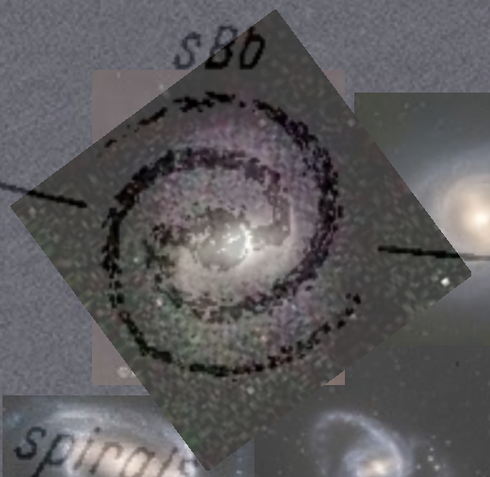

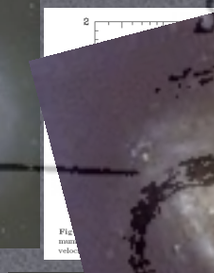

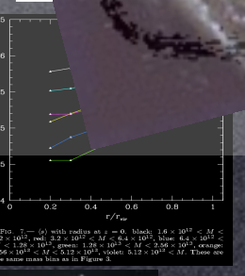

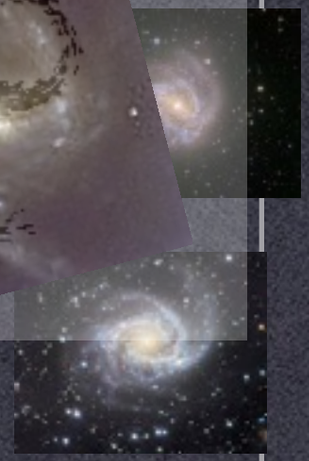

ORIGIN OF HUBBLE SEQUENCE

CIRCA 1930

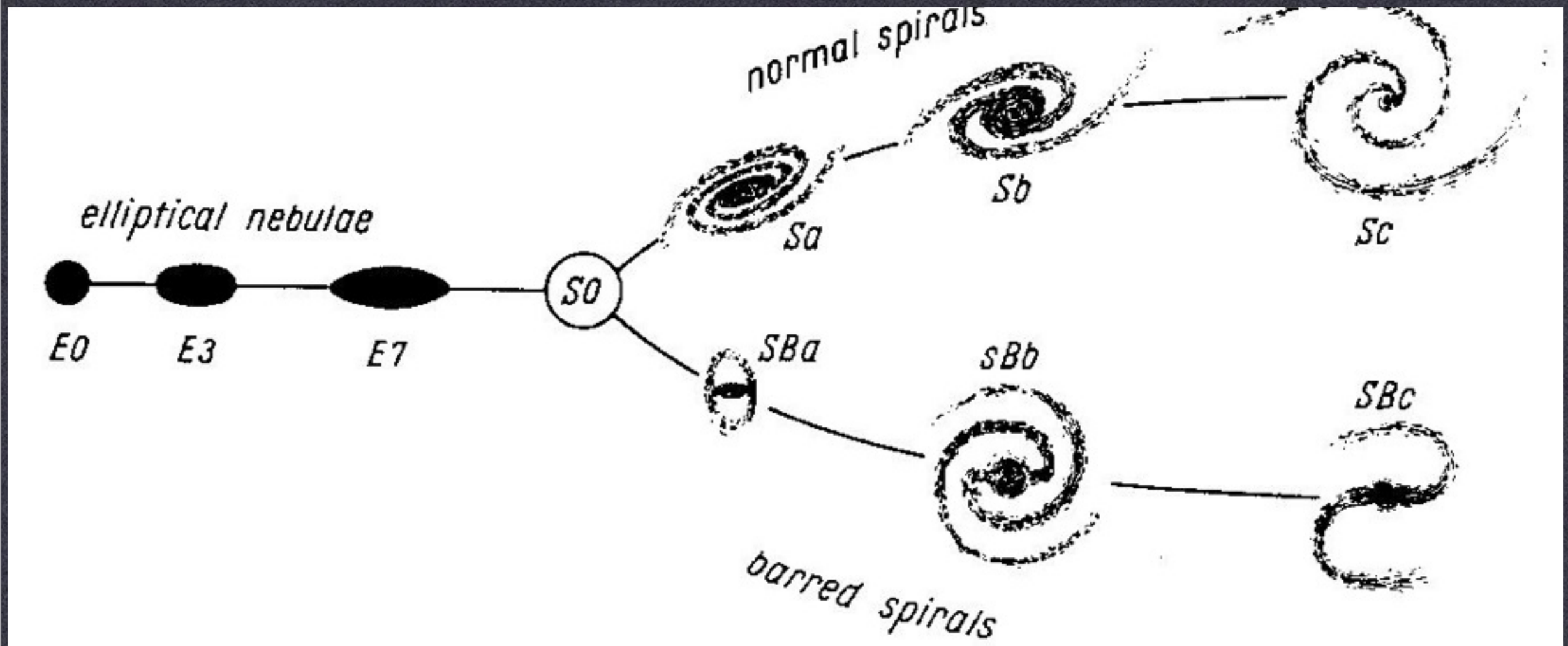

ORIGIN OF HUBBLE SEQUENCE

CIRCA 1930

Galaxy Formation via SemiAnalytic Models

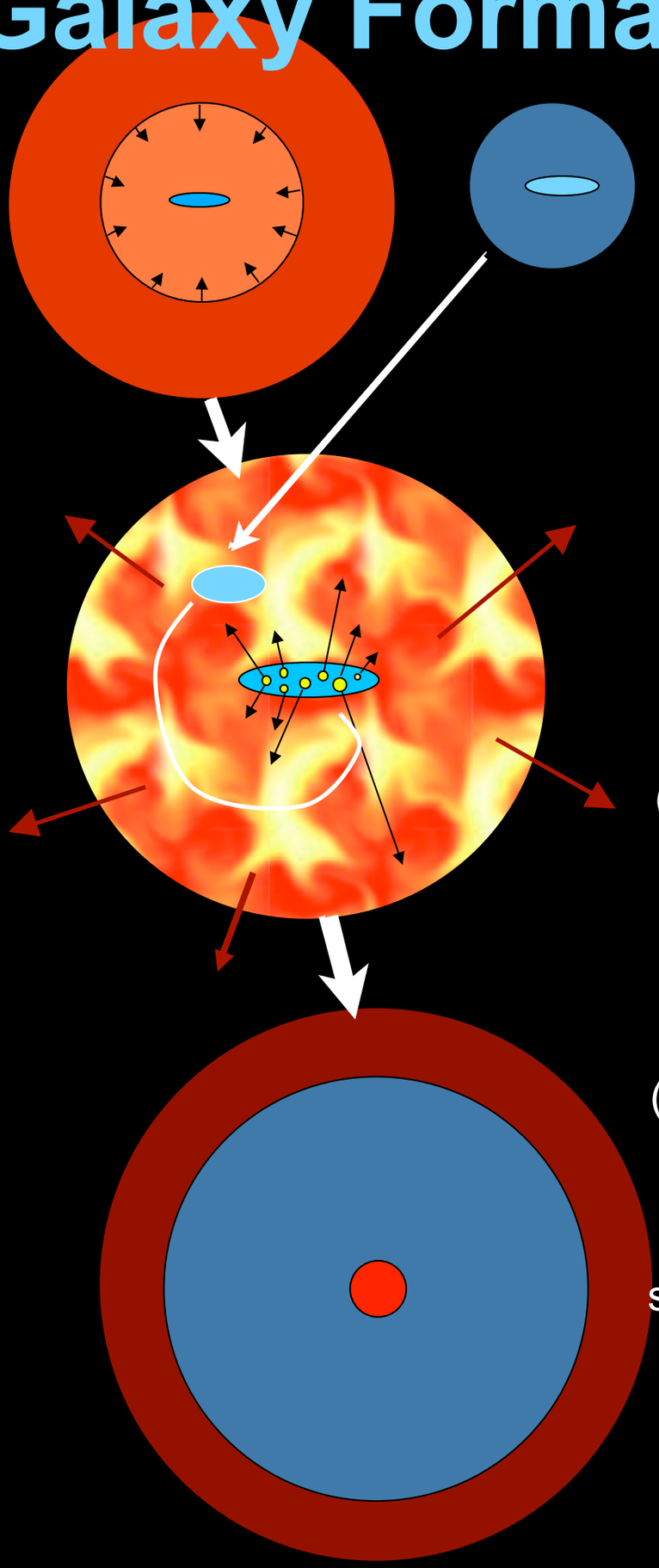

- gas is collisionally heated when perturbations ‘turn around’ and collapse to form gravitationally bound structures
- gas in halos cools via atomic line transitions (depends on density, temperature, and metallicity)
- cooled gas collapses to form a rotationally supported disk
- cold gas forms stars, with efficiency a function of gas density (e.g. Schmidt-Kennicutt Law, metallicity effects?)

Schmidt-Kennicutt laws on nearby (including Local Group galaxies as shaded regions) and distant galaxies, as well as Milky Way Giant Molecular Clouds (Krumholz et al. 2012): Rate of change of stellar surface density is proportional to gas surface density divided by free-fall time $t_{ff}=(G\rho)^{-1/2}$

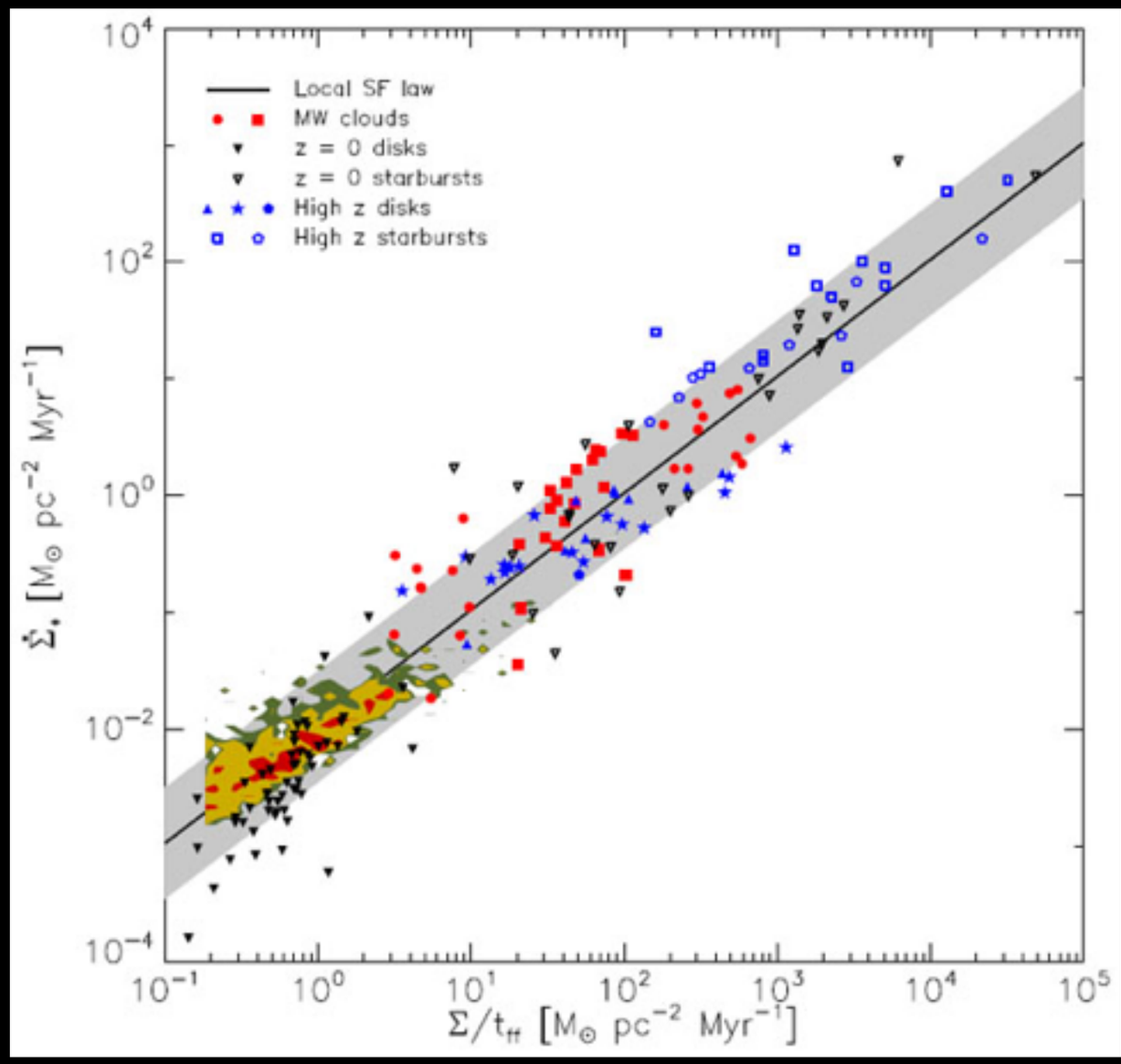

Galaxy Formation via SemiAnalytic Models

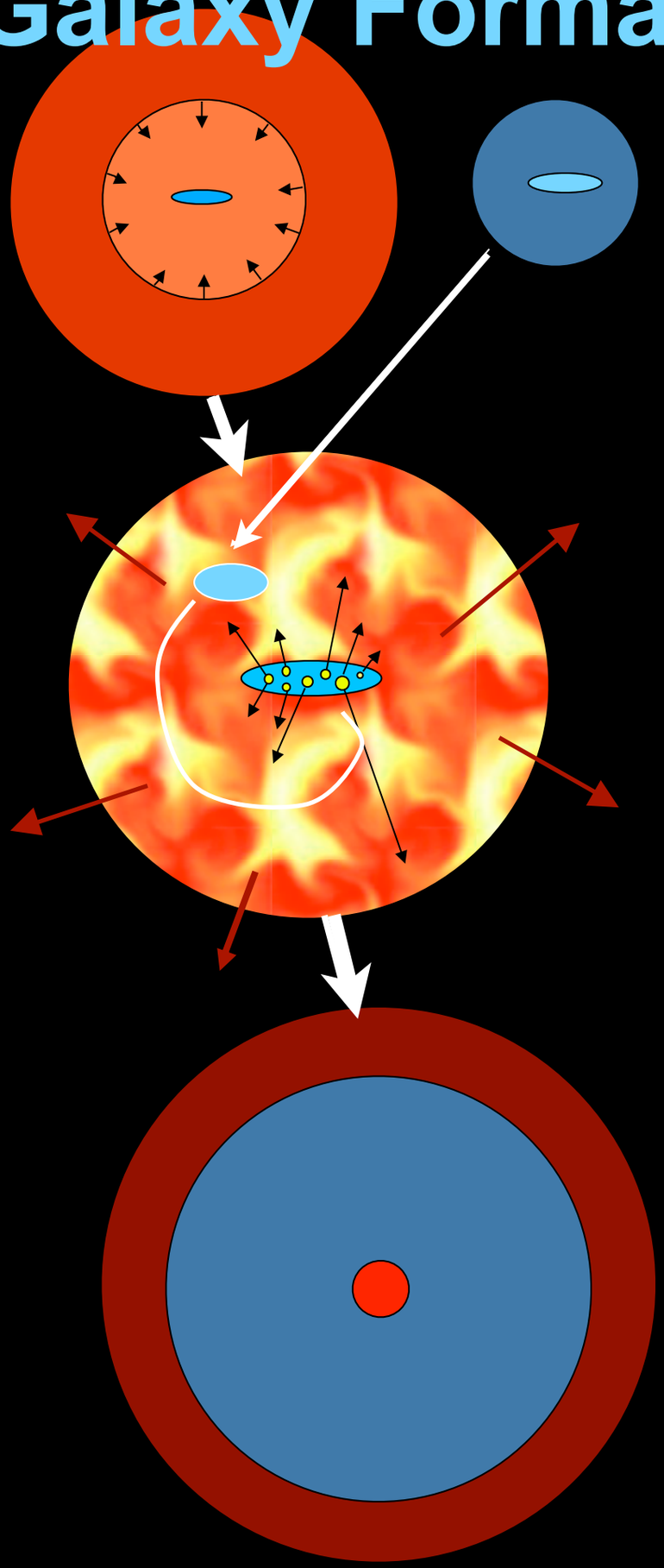

- cooled gas collapses to form a rotationally supported disk
- cold gas forms stars, with efficiency a function of gas density (e.g. Schmidt-Kennicutt Law, metallicity effects?)
- massive stars and SNe reheat (and in small halos expel) cold gas and some metals
- galaxy mergers trigger bursts of star formation; ‘major’ mergers transform disks into spheroids and fuel AGN
- AGN feedback cuts off star formation

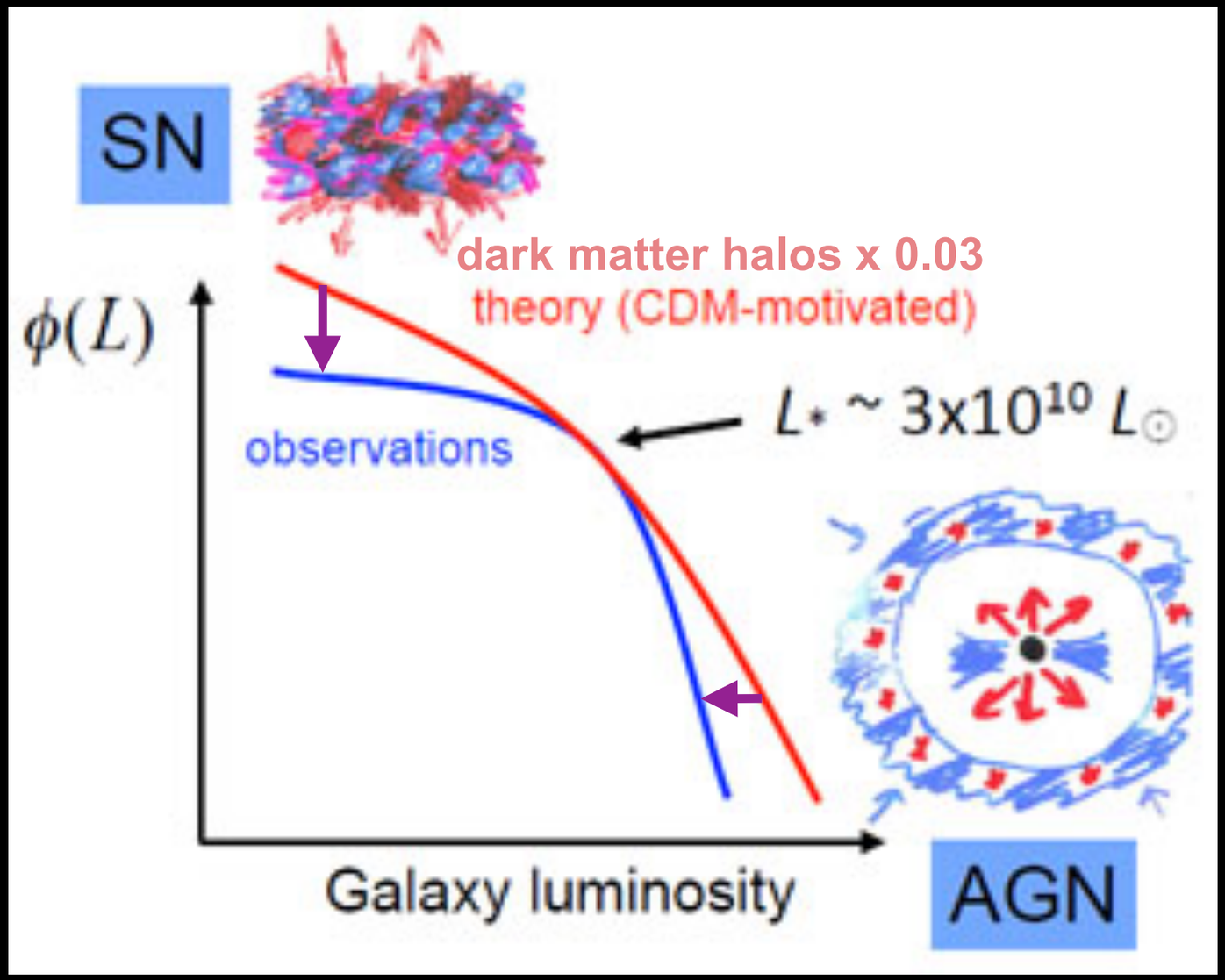

Galaxy Formation via SemiAnalytic Models

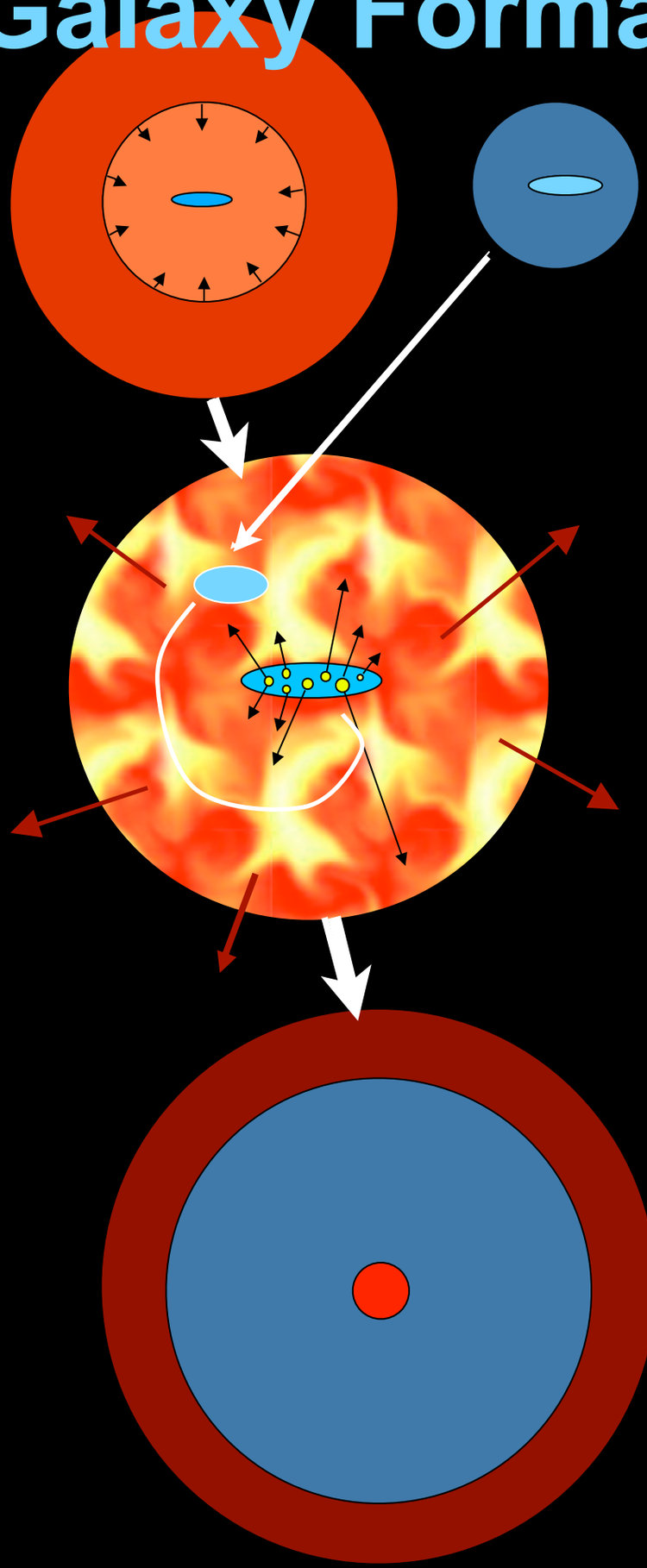

- cold gas forms stars, with efficiency a function of gas density (e.g. Schmidt-Kennicutt Law, metallicity effects?)
- massive stars and SNe reheat (and in small halos expel) cold gas and some metals
- AGN feedback cuts off star formation
- Illustration of galaxy bimodality. The contours are the density of SDSS galaxies in color-luminosity space, after correction for selection effects (Baldry et al. 2004).

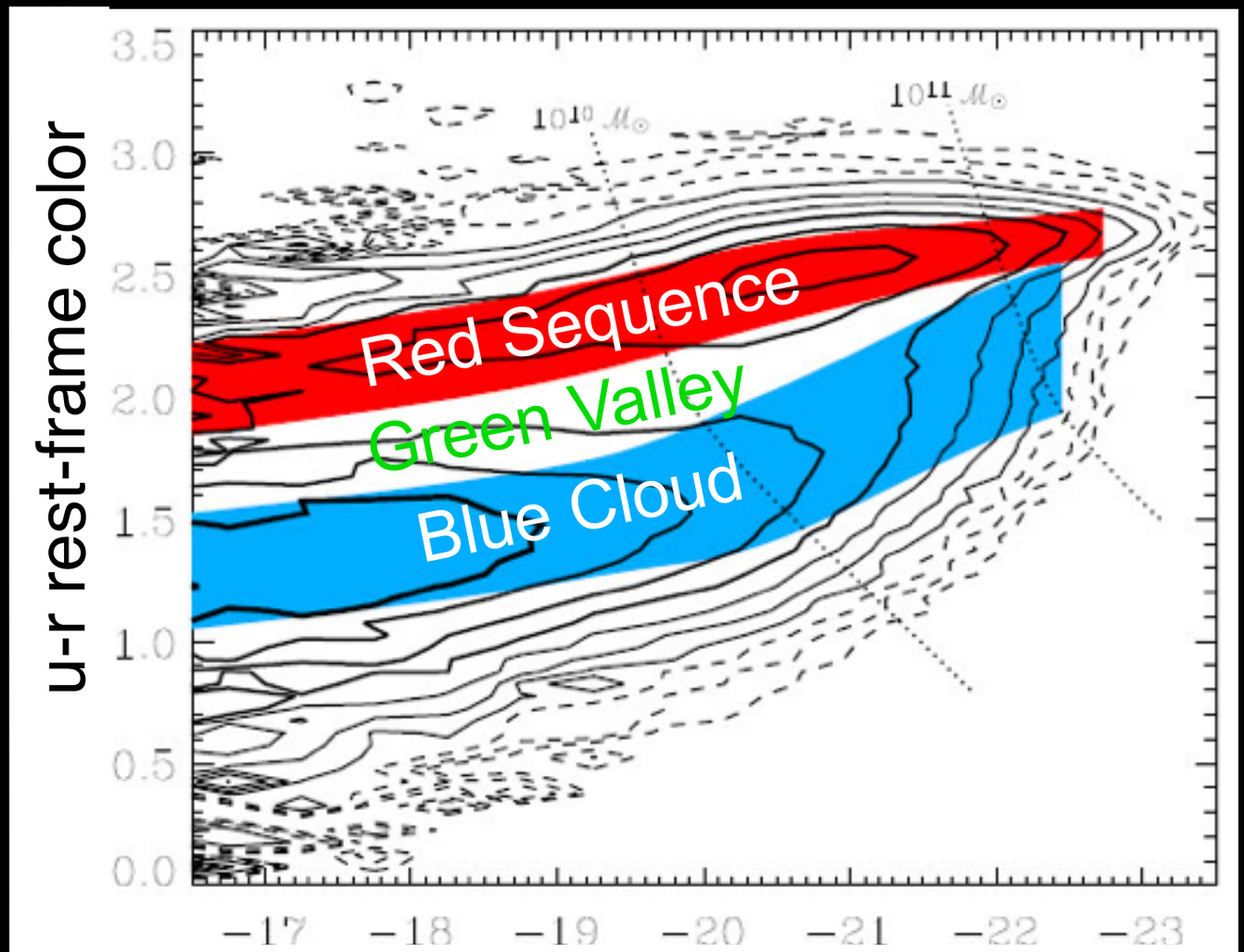

The “Fundamental Plane”

3D view of scaling relations of spheroidal systems from globular clusters (GC) to clusters of galaxies (CSph), via ultra-compact dwarfs (UCD), dwarf spheroidals (dSph), dwarf ellipticals (dE) and giant ellipticals (E), where the axes are half-luminosity, half-luminosity radius and total mass within half-luminosity radius. The red and blue planes respectively represent the Fundamental Plane and the "virial plane" of constant M / L.

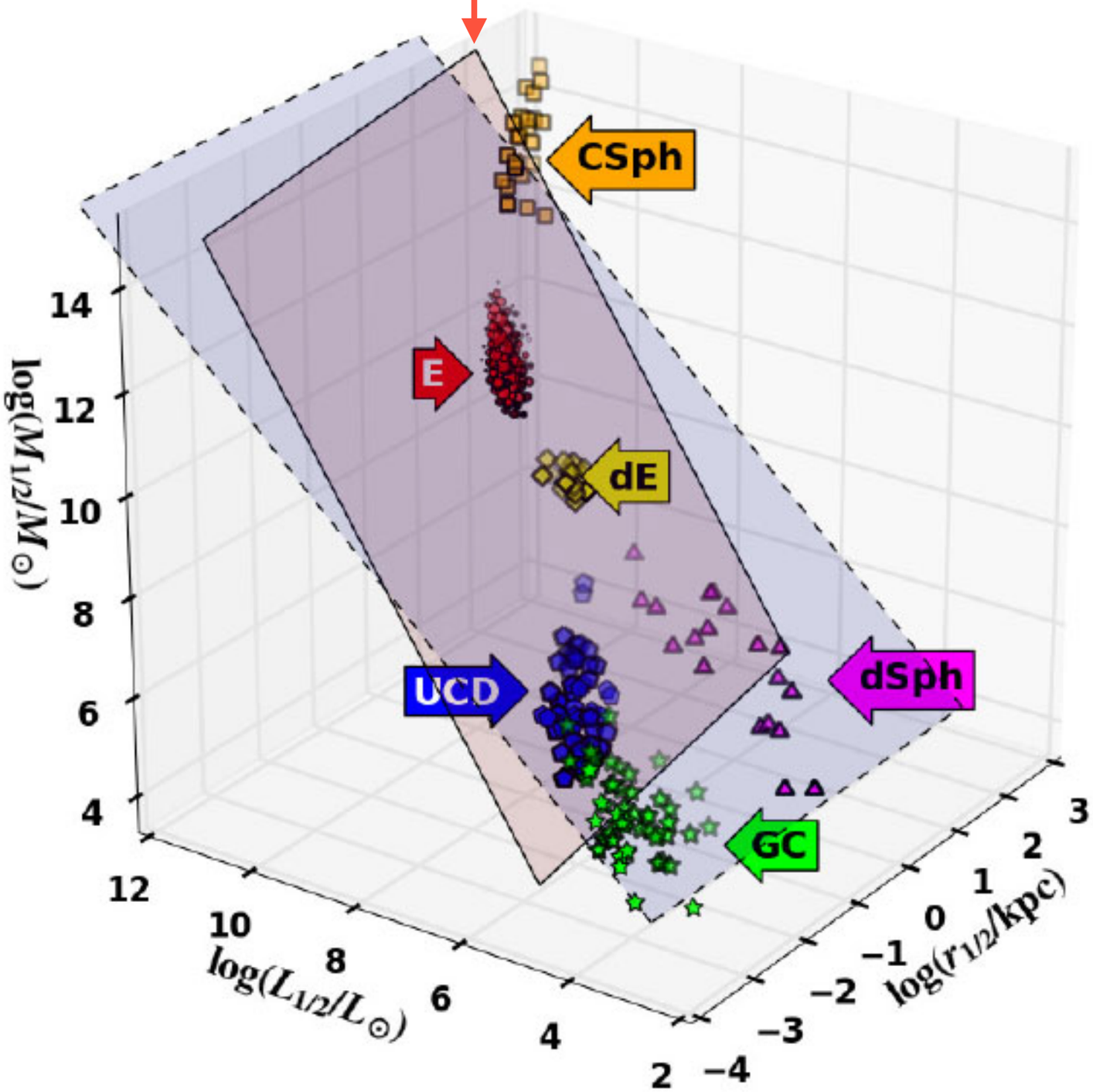

Tollerud et al. 2011

Black Hole mass

$M_{BH} \sim \sigma^4 \sim M^*$

(here σ = galaxy stellar spheroid velocity dispersion, M^* = galaxy stellar spheroid mass)

Luminosity-weighted, within one effective radius, from McConnell et al. (2011)

BCG = brightest cluster galaxy

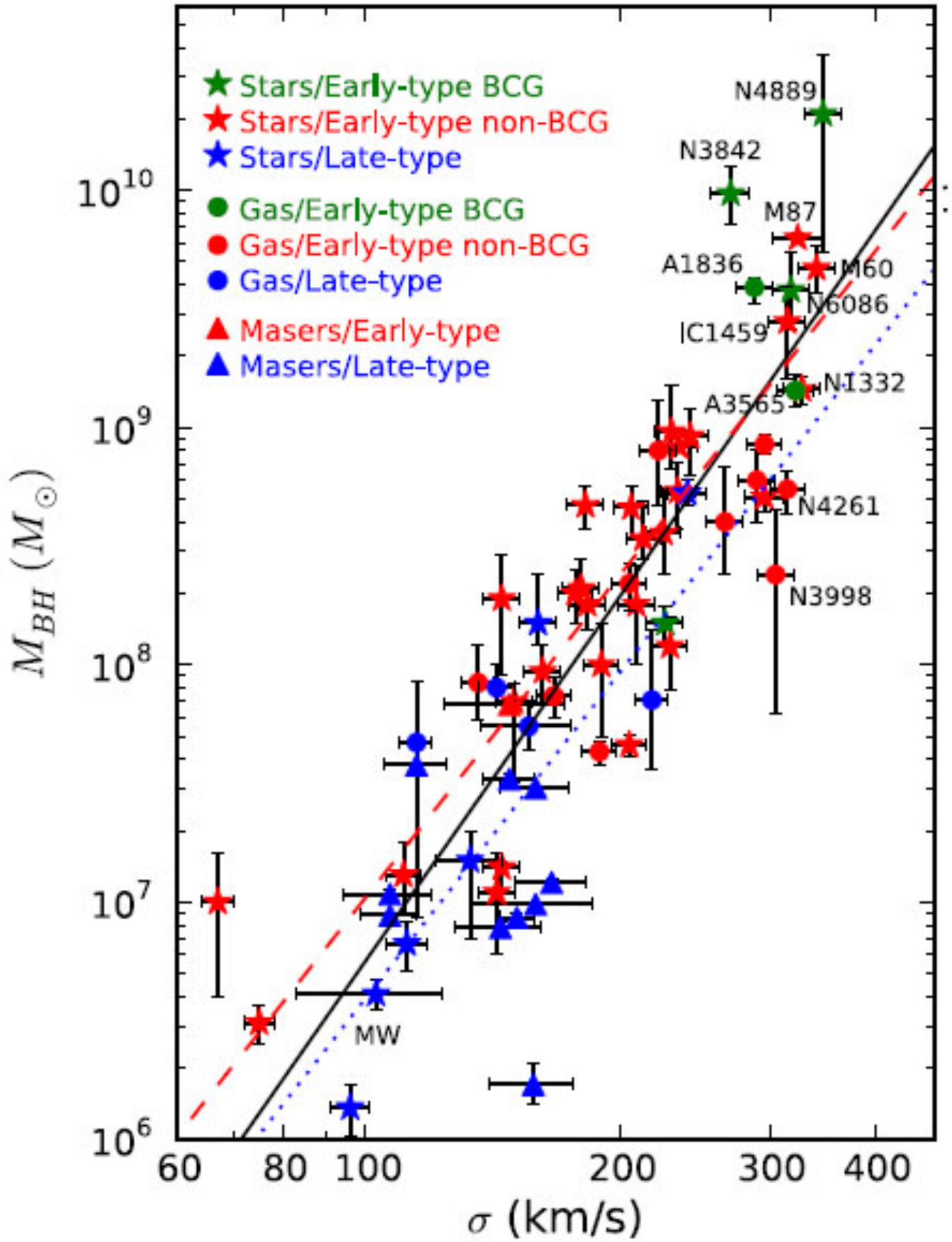

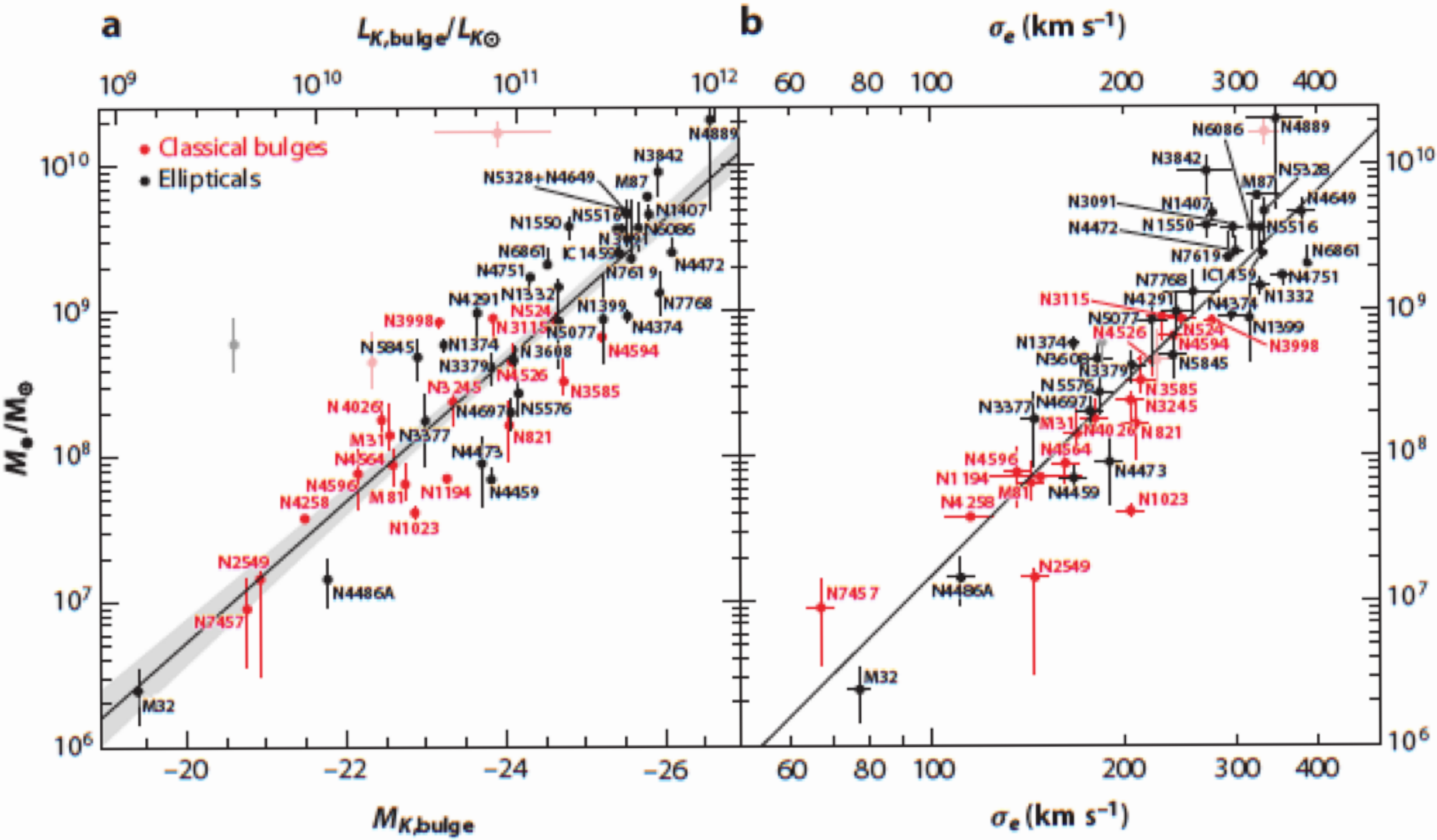

Correlation of dynamically measured black hole mass M• with (a) K-band absolute magnitude $M_{K,bulge}$ and luminosity $L_{K,bulge}$ and (b) velocity dispersion σ_e for (red) classical bulges and (black) elliptical galaxies. The lines are symmetric least-squares fits to all the points except the monsters (points in light colors), NGC 3842, and NGC 4889. (From Kormendy & Ho, Annual Review of Astronomy & Astrophysics 2013.)

The CANDELS Survey with new near-ir camera WFC3

GALAXIES ~10 BILLION YEARS AGO

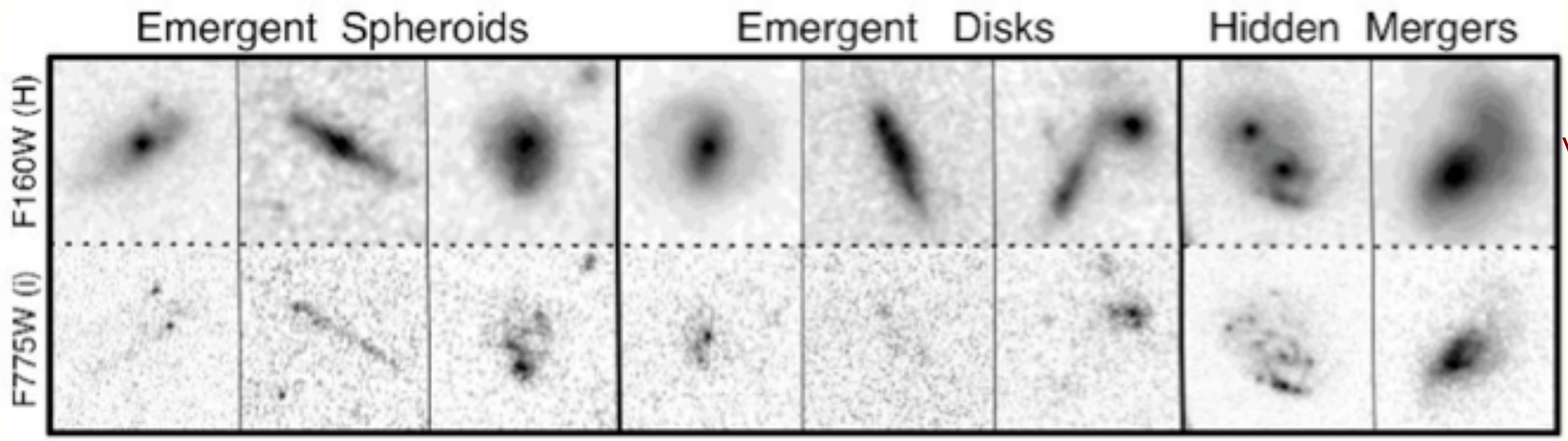

CANDELS makes use of the near-infrared WFC3 camera (top row) and the visible-light ACS camera (bottom row). Using these two cameras, CANDELS will reveal new details of the distant Universe and test the reality of cosmic dark energy.

Hubble Space Telescope

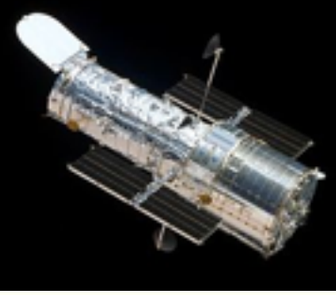

http://candels.ucolick.org

CANDELS is a powerful imaging survey of the distant Universe being carried out with two cameras on board the Hubble Space Telescope.

- CANDELS is the largest project in the history of Hubble, with 902 assigned orbits of observing time. This is the equivalent of four months of Hubble time if executed consecutively, but in practice CANDELS will take three years to complete (2010-2013).
- The core of CANDELS is the revolutionary near-infrared WFC3 camera, installed on Hubble in May 2009. WFC3 is sensitive to longer, redder wavelengths, which permits it to follow the stretching of lightwaves caused by the expanding Universe. This enables CANDELS to detect and measure objects much farther out in space and nearer to the Big Bang than before. CANDELS also uses the visible-light ACS camera, and together the two cameras give unprecedented panchromatic coverage of galaxies from optical wavelengths to the near-IR.

CANDELS: THE PROGENITORS OF COMPACT QUIESCENT GALAXIES AT $Z\sim2$

Guillermo Barro[1], S. M. Faber[1], Pablo G. Pérez-González[2,3], David C. Koo[1], Christina C. Williams[4], Dale D. Kocevski[1], Jonathan R. Trump[1], Mark Mozena[1], Elizabeth McGrath[1], Arjen van der Wel[5], Stijn Wuyts[6], Eric F. Bell[7], Darren J. Croton[8], Avishai Dekel[9], M. L. N. Ashby[10], Henry C. Ferguson[11], Adriano Fontana[12], Mauro Giavalisco[4], Norman A. Grogin[11], Yicheng Guo[4], Nimish P. Hathi[13], Philip F. Hopkins[14], Kuang-Han Huang[11], Anton M. Koekemoer[11], Jeyhan S. Kartaltepe[15], Kyoung-Soo Lee[16], Jeffrey A. Newman[17], Lauren A. Porter[1], Joel R. Primack[1], Russell E. Ryan[11], David Rosario[6], Rachel S. Somerville[18]

ABSTRACT We combine high-resolution HST/WFC3 images with multi-wavelength photometry to track the evolution of structure and activity of massive ($M\star > 10^{10}M_{\odot}$) galaxies at redshifts $z = 1.4 - 3$ in two fields of the Cosmic Assembly Near-infrared Deep Extragalactic Legacy Survey (CANDELS). We detect compact, star-forming galaxies (cSFGs) whose number densities, masses, sizes, and star formation rates qualify them as likely progenitors of compact, quiescent, massive galaxies (cQGs) at $z = 1.5 - 3$. At $z > 2$, most cSFGs have specific star-formation rates half that of typical massive SFGs, and host X-ray luminous AGNs 30 times more frequently. These properties suggest that cSFGs are formed by gas-rich processes (mergers or disk-instabilities) that induce a compact starburst and feed an AGN, which, in turn, quench the star formation on dynamical timescales (few 10^8yr). The cSFGs are continuously being formed at $z = 2 - 3$ and fade to cQGs down to $z \sim 1.5$. After this epoch, cSFGs are rare, thereby truncating the formation of new cQGs. In summary, we propose two evolutionary tracks of QG formation: an early ($z > 2$), fast-formation path of rapidly-quenched cSFGs fading into cQGs that later enlarge within the quiescent phase, and a slow, late-arrival ($z < 2$) path in which larger SFGs form extended QGs without passing through a compact state.

ApJ 2013

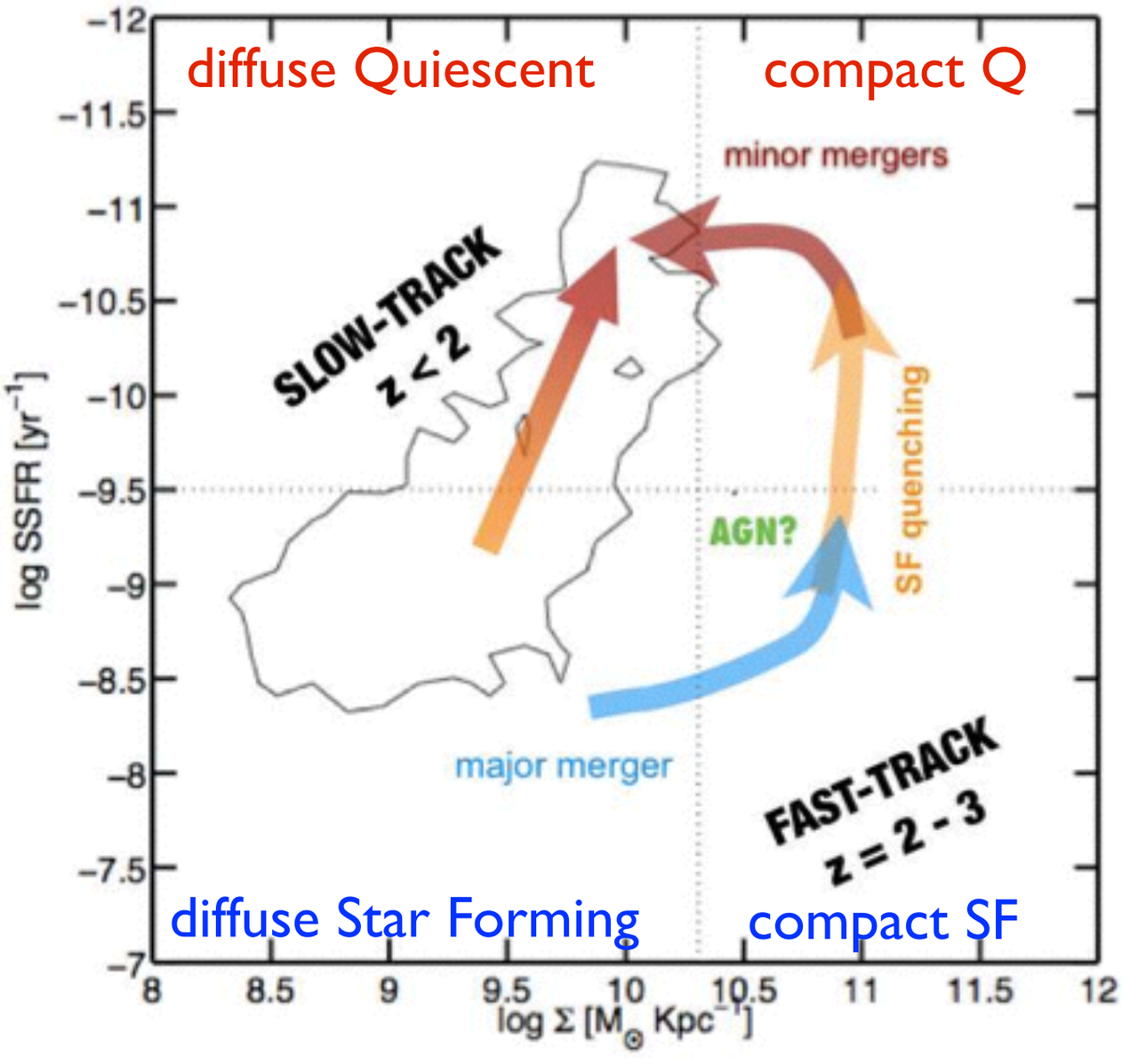

Barro et al. (CANDELS) 2013

Evolution of Galaxies: CANDELS Observations vs. Theory

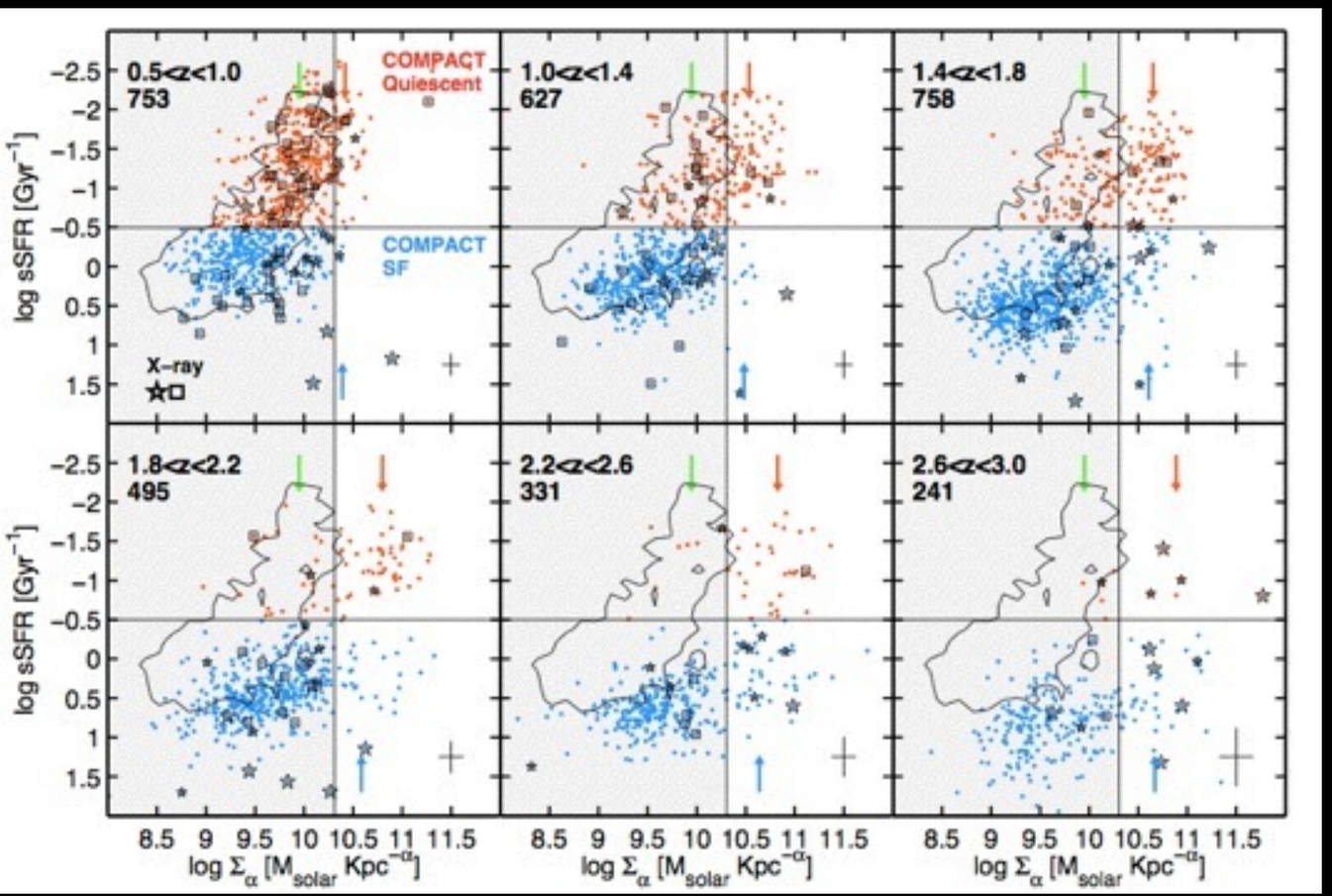

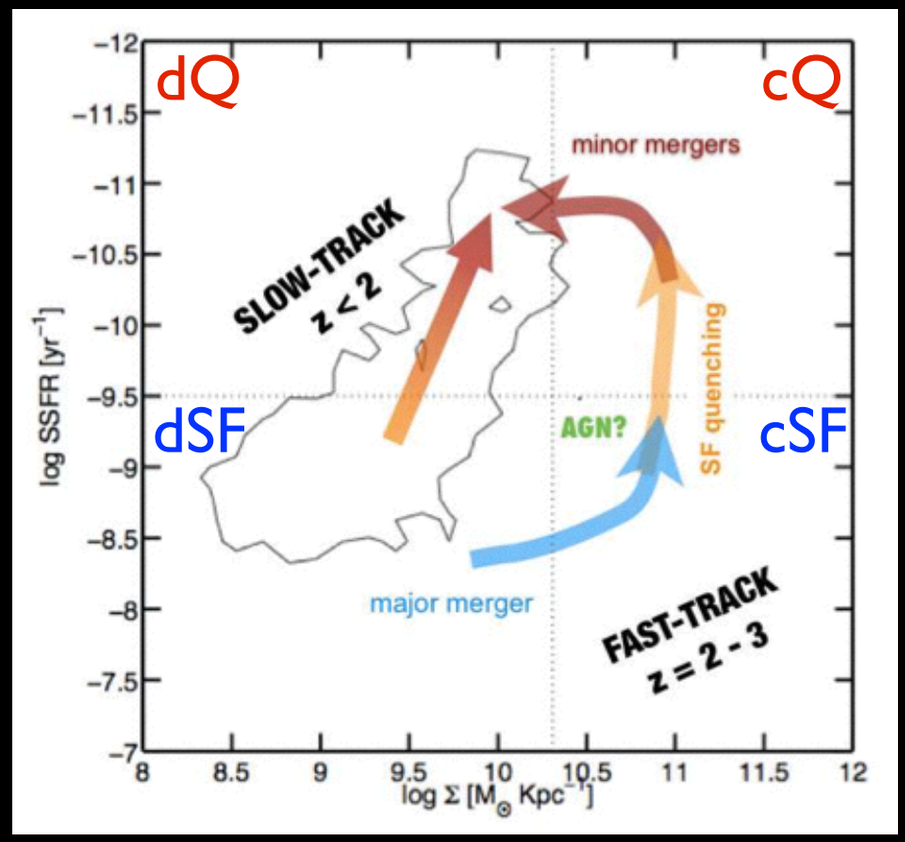

Barro et al. (2013 - Hubble Observations)

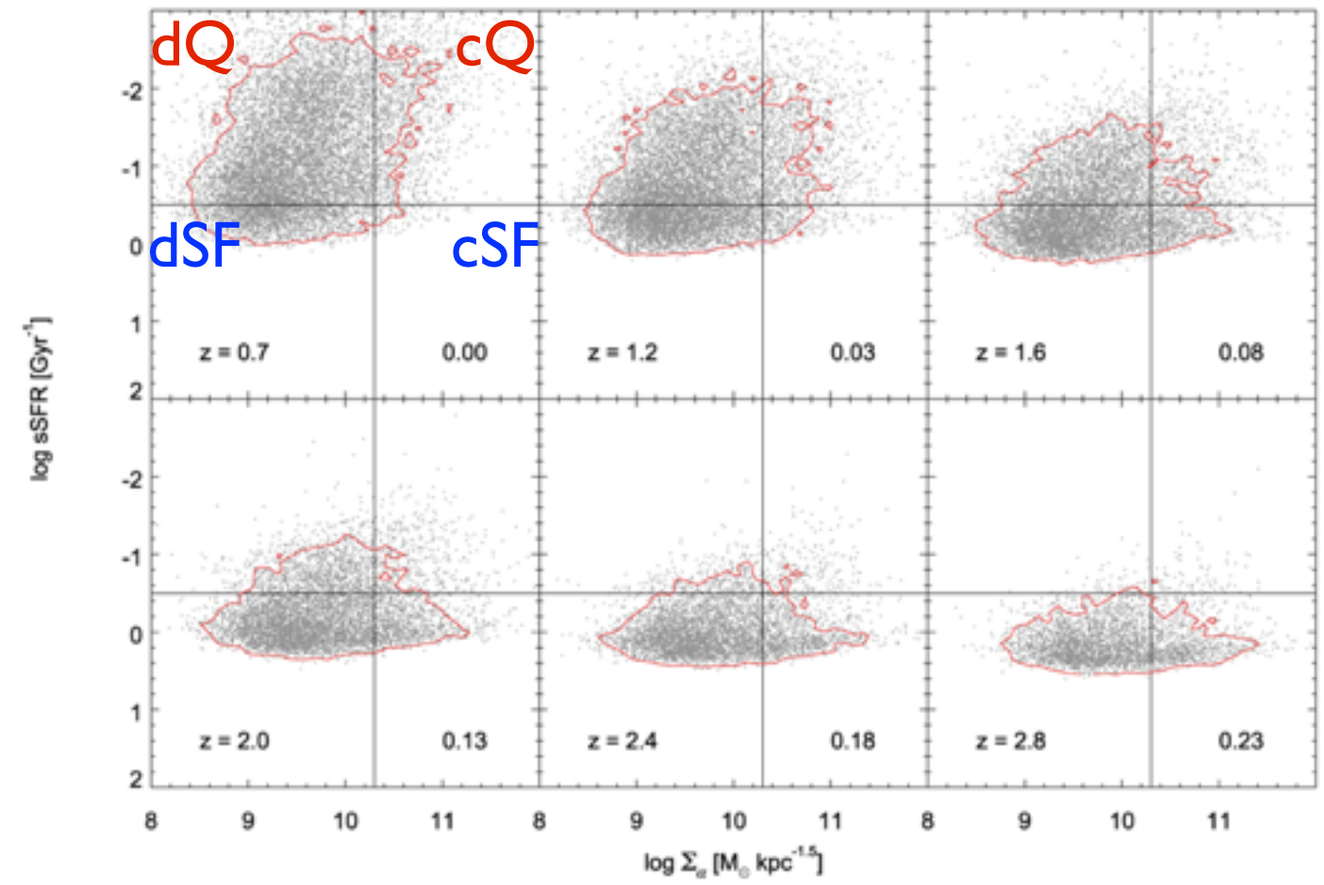

Bolshoi DM Halo Merger Tree

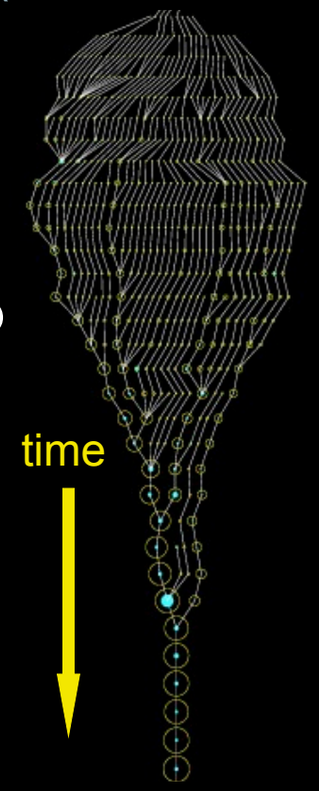

Astrophysical processes modeled:

- shock heating & radiative cooling
- photoionization squelching
- merging
- star formation (quiescent & burst)
- SN heating & SN-driven winds
- AGN accretion and feedback
- chemical evolution
- stellar populations & dust

Porter et al. 2013c - Bolshoi SAM

Fast-Track Evolution of Compact Star-Forming Galaxies According to Bolshoi-based Semi-Analytic Model

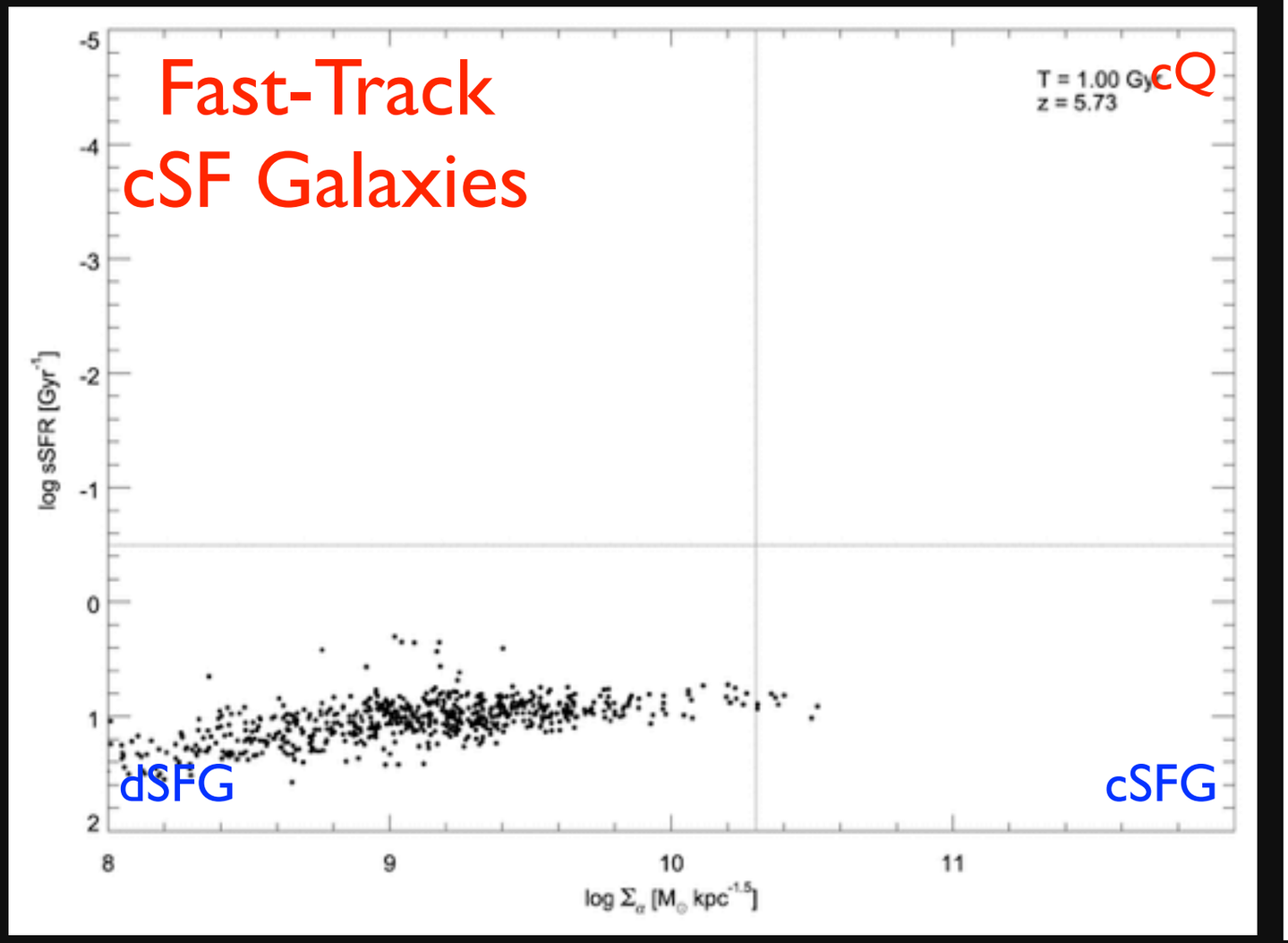

Gas-rich merger in past Gyr

Gas-poor merger in past Gyr

cSFG at z = 2.4

Observed Evolution of Galaxies from Latest Hubble Telescope Data

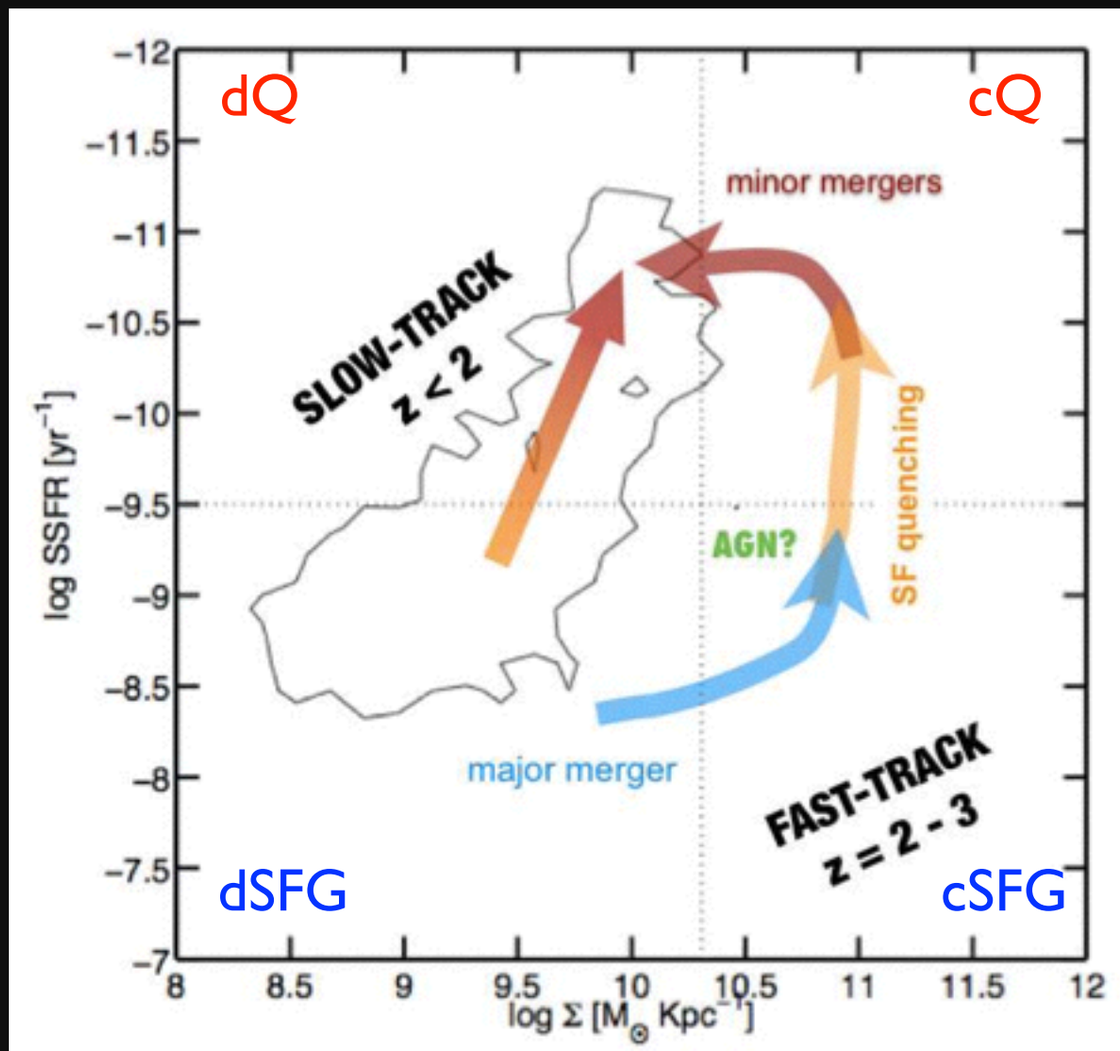

Barro et al. (2012 - Hubble Observations)

Porter et al. 2013c - Bolshoi SAM

Summary

SAM Predictions

- Galaxies move from dSFG to cSFG through disk instabilities, as well as gas-rich major and minor mergers. Major mergers may *not* be the dominant mechanism for creating compact galaxies.
- Minor mergers decrease the surface density of cSFG, but most remain compact down to redshift 0.
- High-resolution galaxy simulations appear consistent with this.

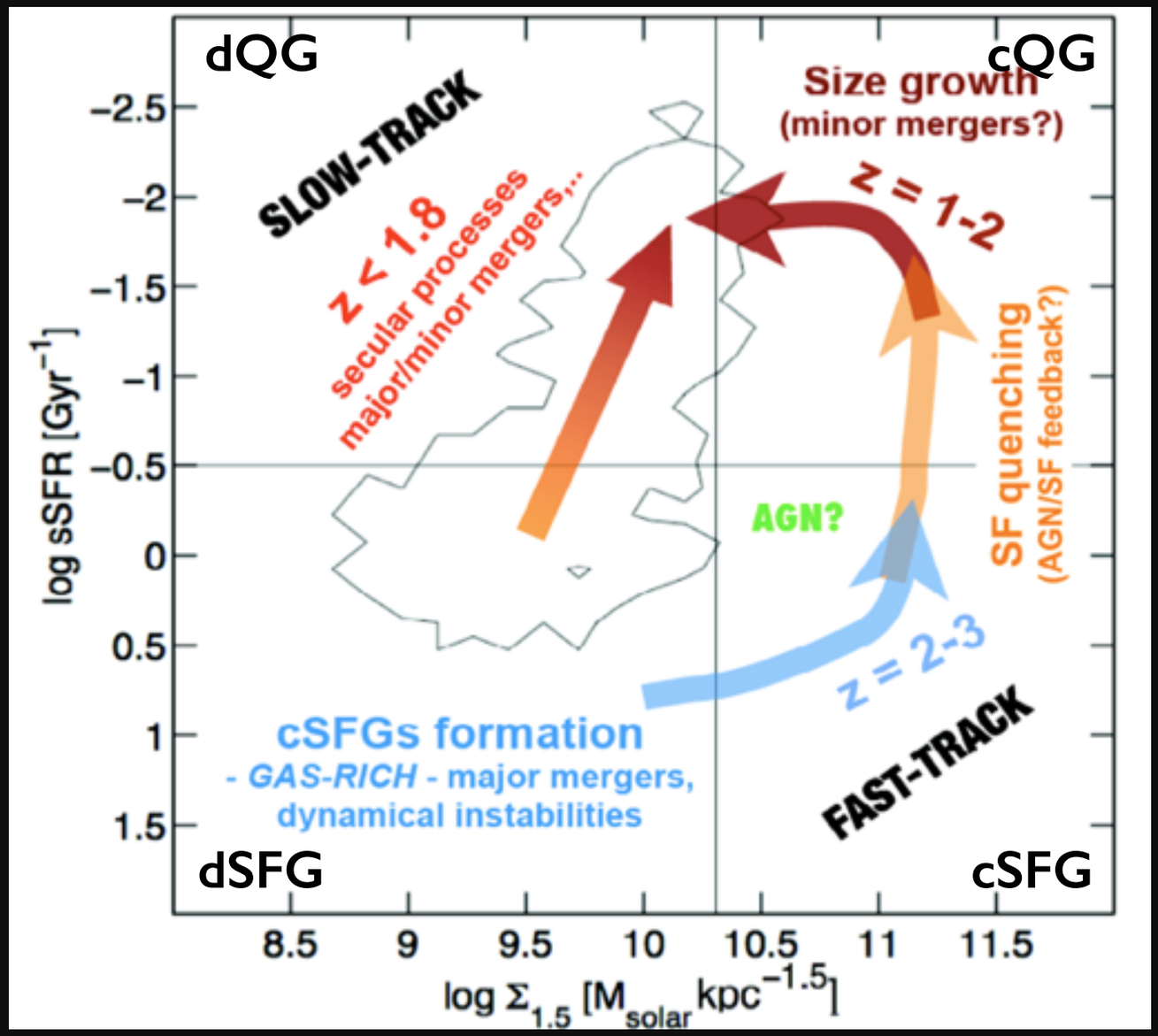

Barro et al. (2012)

Porter et al. 2013c - Bolshoi SAM

Cosmological Simulations

Astronomical observations represent snapshots of moments in time. It is the role of astrophysical theory to produce movies -- both metaphorical and actual -- that link these snapshots together into a coherent physical theory.

Cosmological dark matter simulations show large scale structure, growth of structure, and dark matter halo properties

Hydrodynamic galaxy formation simulations: evolution of galaxies, formation of galactic spheroids via mergers, galaxy images in all wavebands including stellar evolution and dust

The Angular Momentum Catastrophe

In practice it is not trivial to form galaxies with massive, extended disks and small spheroids. The angular momentum content of the disk determines its final structure.

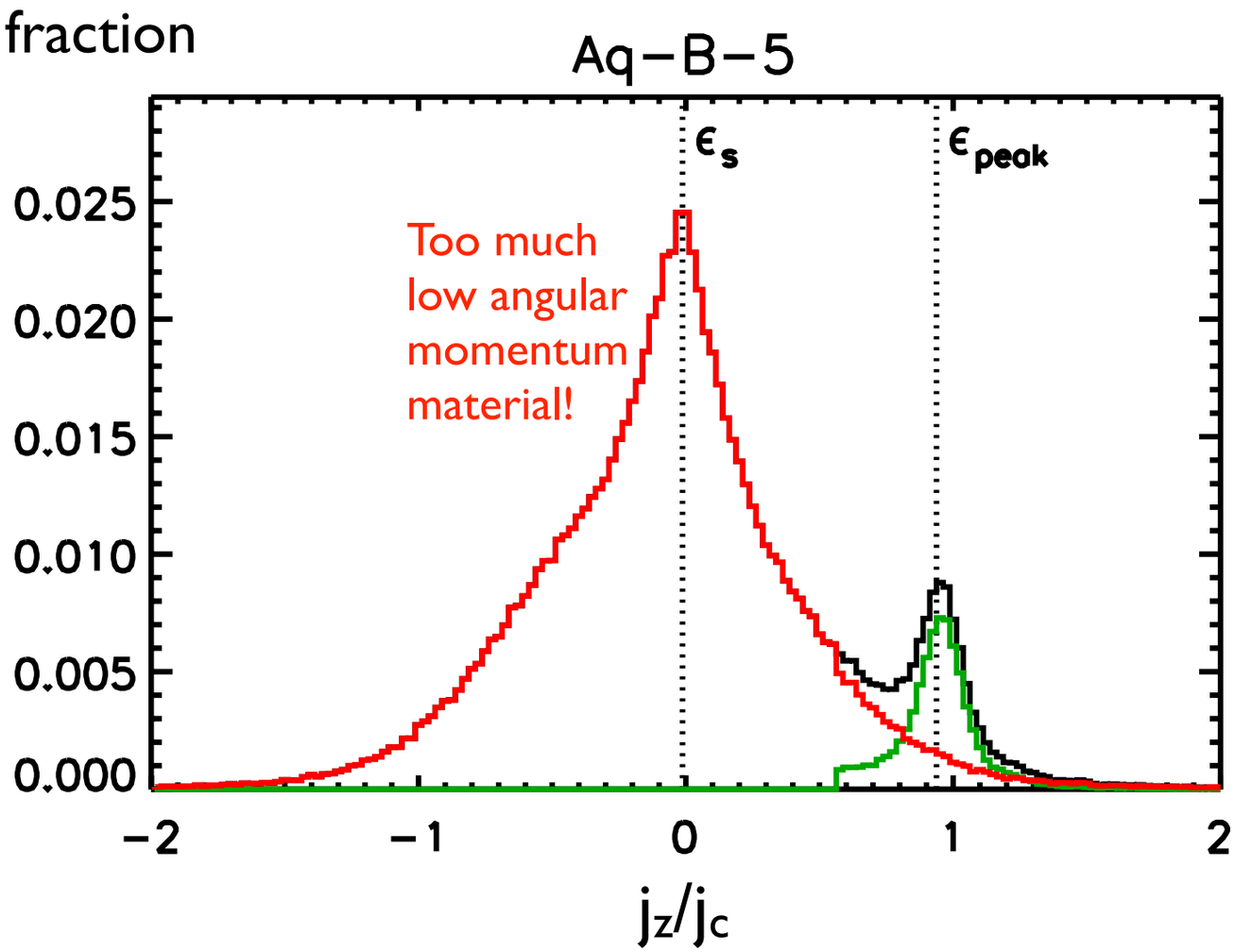

≠

Scannapieco et al. 2009

angular momentum / ang mom needed for rotational support

The Angular Momentum Catastrophe

In practice it is not trivial to form galaxies with massive, extended disks and small spheroids. The angular momentum content of the disk determines its final structure. None of the 2012 Aquila low-resolution galaxy simulations had realistic disks.

fraction

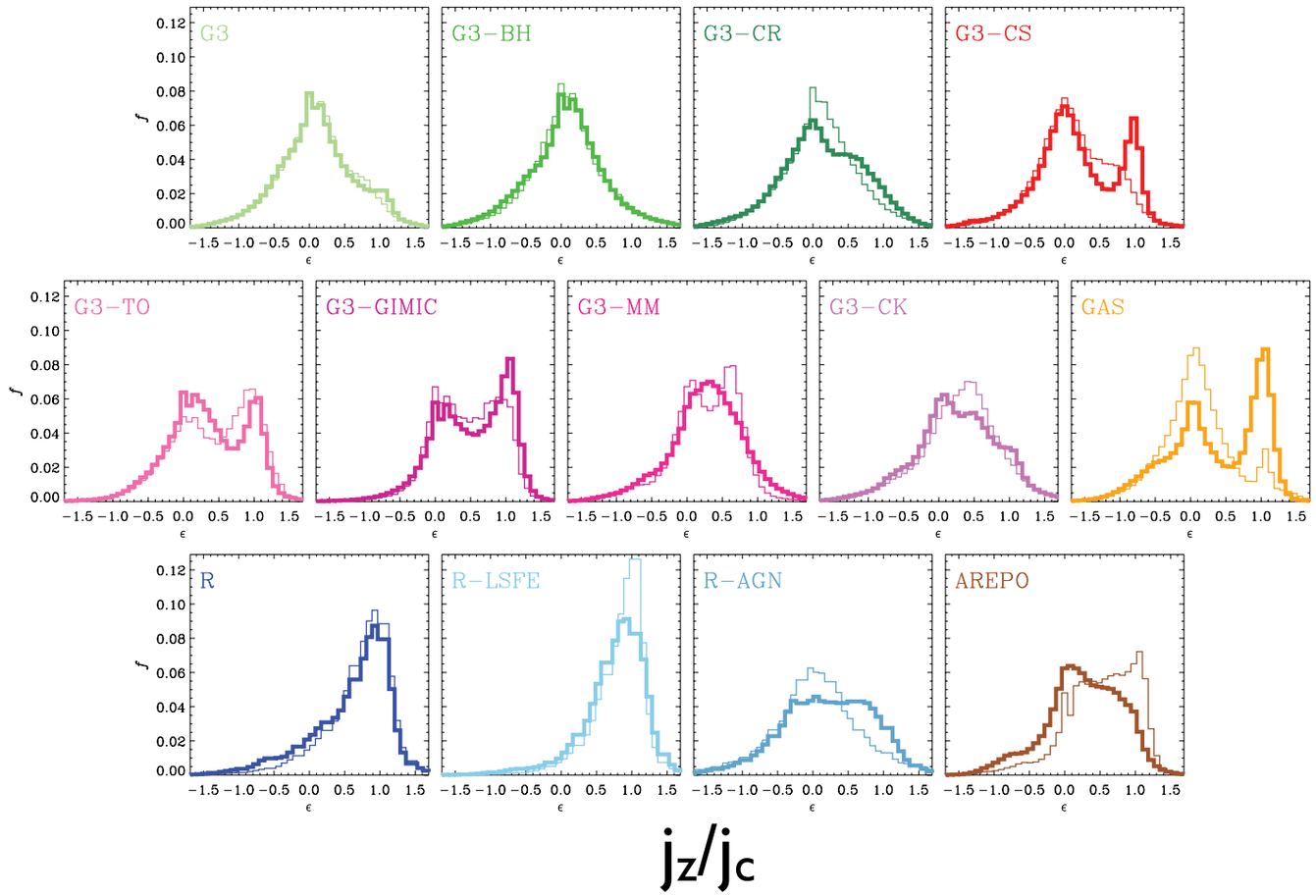

≠

Scannapieco et al., Aquila Galaxy Simulation Comparison, 2012

The Angular Momentum ~~Catastrophe~~

Eris, the first high-resolution simulation of a ~10^{12} $M_\odot$ halo, produced a realistic spiral galaxy. Adequate resolution and physically realistic feedback appear to be sufficient.

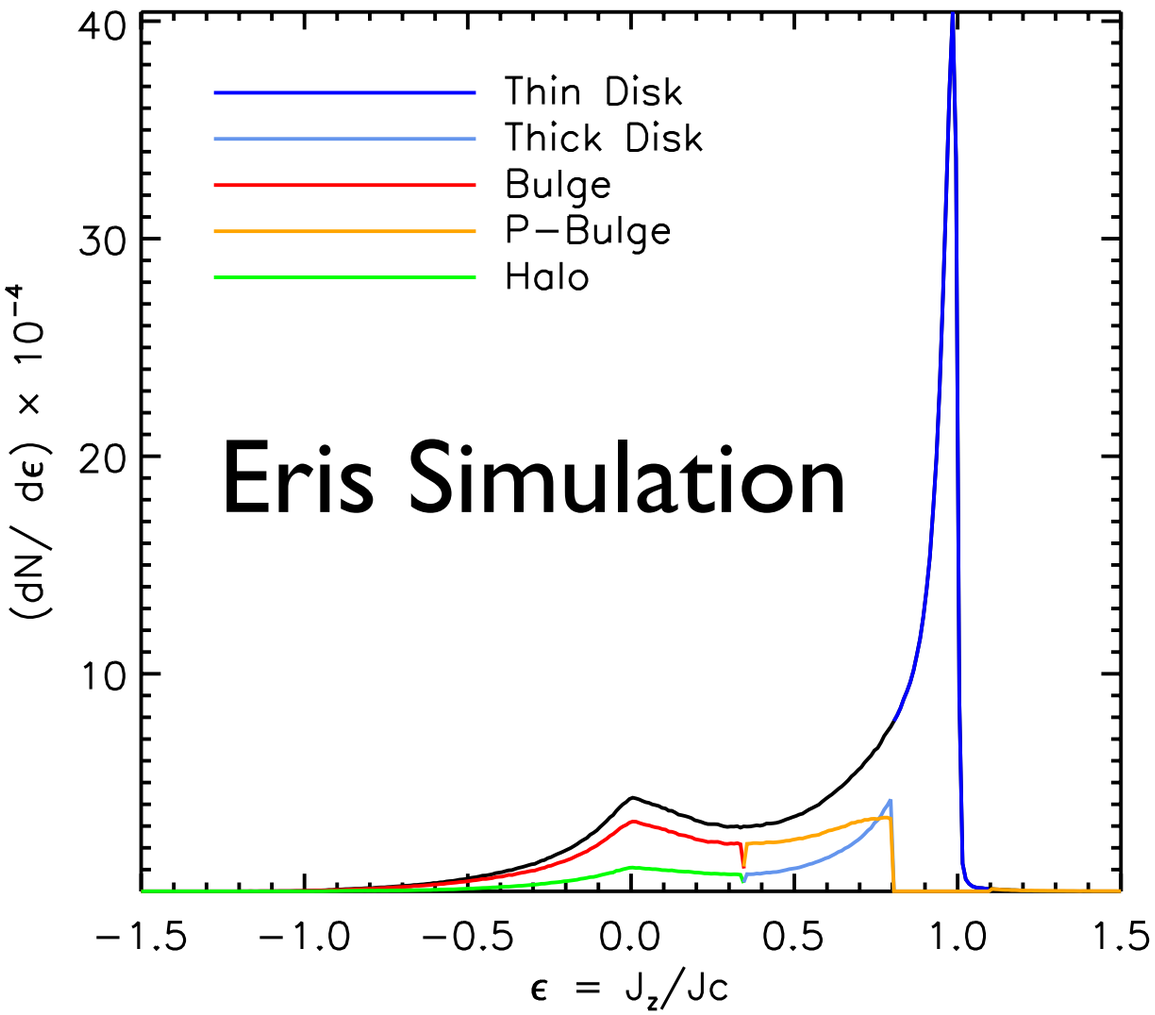

=

Guedes, Callegari, Madau, Mayer 2011 ApJ

The *Eris* N-body/SPH simulation of a massive late-type spiral galaxy in a *WMAP3* cosmology (Guedes, Callegari, Madau, & Mayer 2011). The simulation was performed with the *GASOLINE* code on NASA's *Pleiades* supercomputer and used 1.5 million cpu hours.

$M_{vir}=7.9 \times 10^{11}\ M_{\odot}$
$N_{DM}+N_{gas}+N_{star}$= 7M+3M+8.6M within final r_{vir}
force resolution=120 pc

RESEARCH FUNDED BY NASA, NSF, AND SNF

The CANDELS Survey with new near-ir camera WFC3

GALAXIES ~10 BILLION YEARS AGO

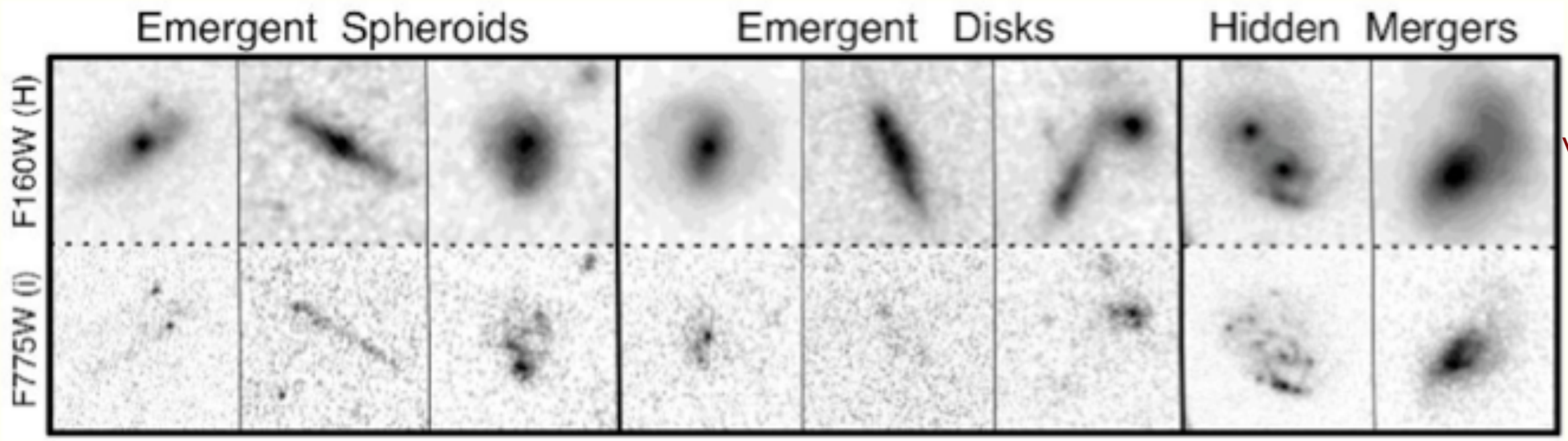

CANDELS makes use of the near-infrared WFC3 camera (top row) and the visible-light ACS camera (bottom row). Using these two cameras, CANDELS will reveal new details of the distant Universe and test the reality of cosmic dark energy.

Hubble Space Telescope

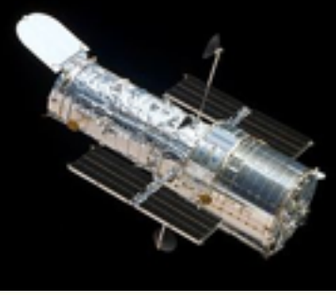

http://candels.ucolick.org

CANDELS is a powerful imaging survey of the distant Universe being carried out with two cameras on board the Hubble Space Telescope.

- CANDELS is the largest project in the history of Hubble, with 902 assigned orbits of observing time. This is the equivalent of four months of Hubble time if executed consecutively, but in practice CANDELS will take three years to complete (2010-2013).
- The core of CANDELS is the revolutionary near-infrared WFC3 camera, installed on Hubble in May 2009. WFC3 is sensitive to longer, redder wavelengths, which permits it to follow the stretching of lightwaves caused by the expanding Universe. This enables CANDELS to detect and measure objects much farther out in space and nearer to the Big Bang than before. CANDELS also uses the visible-light ACS camera, and together the two cameras give unprecedented panchromatic coverage of galaxies from optical wavelengths to the near-IR.

How Galaxies Form

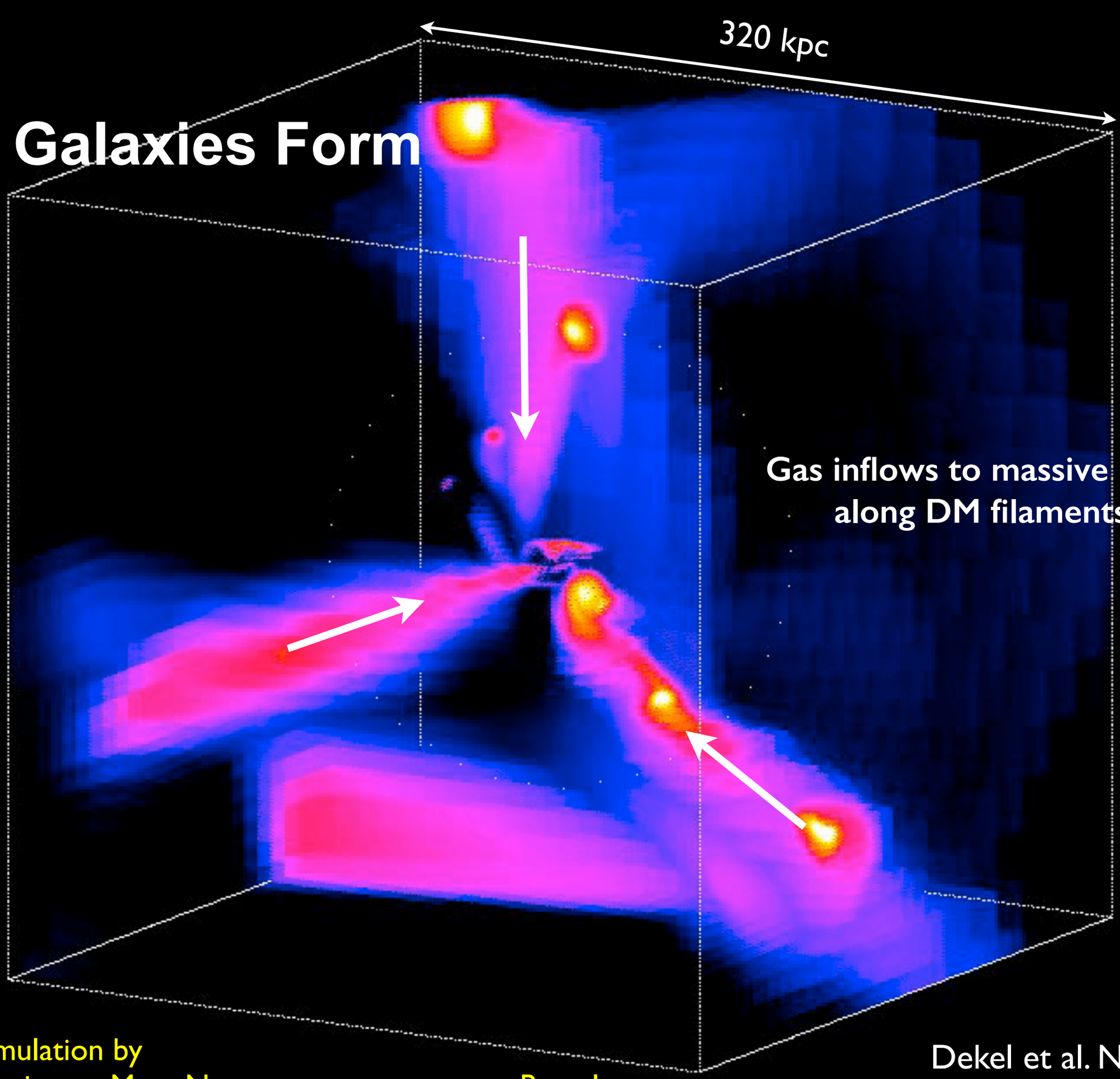

Gas inflows to massive halos
along DM filaments

RAMSES simulation by
Romain Teyssier on Mare Nostrum supercomputer, Barcelona

Dekel et al. Nature 2009

How Gas moves and Stars form according to galaxy simulations

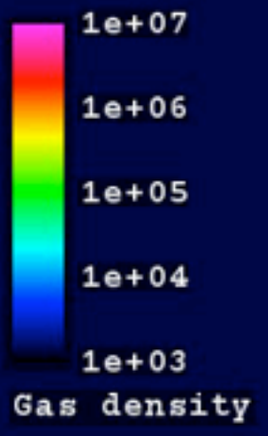

- Stars

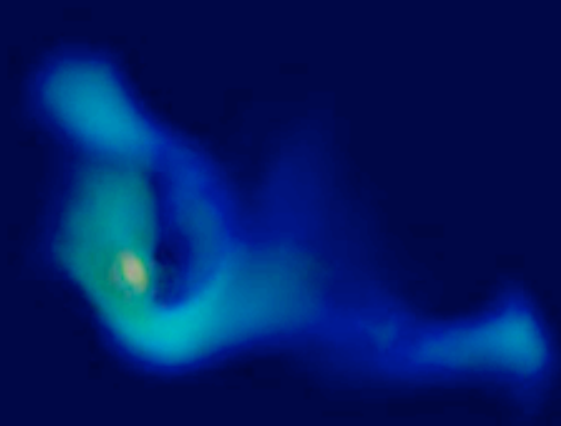

time=276

ART Simulation Daniel Ceverino;
Visualization: David Ellsworth

Sunrise Radiative Transfer Code

Patrik Jonsson
& Joel Primack

For every simulation snapshot:

- Evolving stellar spectra calculation
- Adaptive grid construction
- Monte Carlo radiative transfer
- “Polychromatic” rays save 100x CPU time
- Graphic Processor Units give 10x speedup

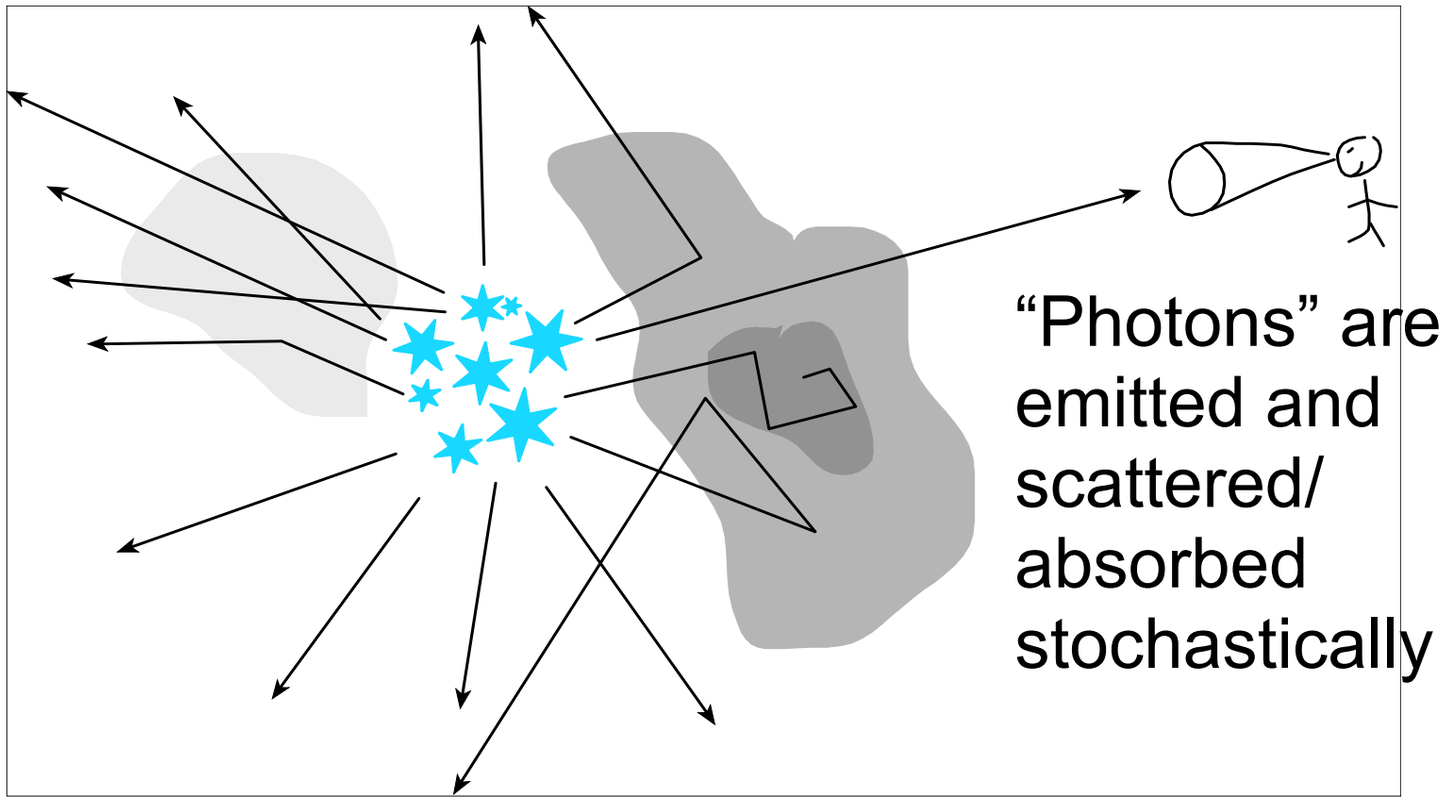

Spectral Energy Distribution

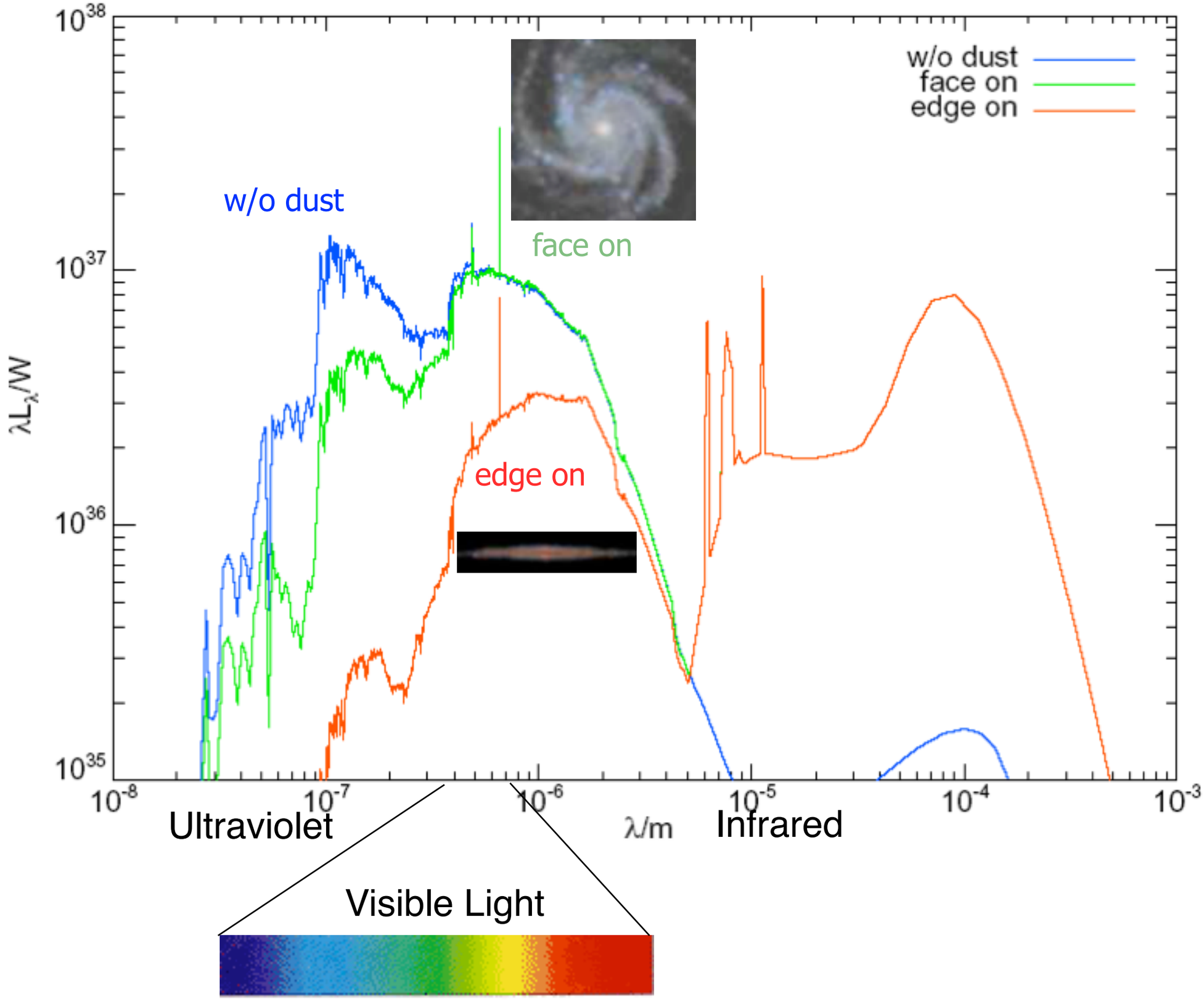

In about 5 billion years, our Milky Way Galaxy will collide and merge with our neighboring giant galaxy, Andromeda.

Spiral Galaxy Merger Simulation - Patrik Jønsson, Greg Novak, Joel Primack

Music: Nancy Abrams “All’s Well that Ends Well” from album *Alien Wisdom*

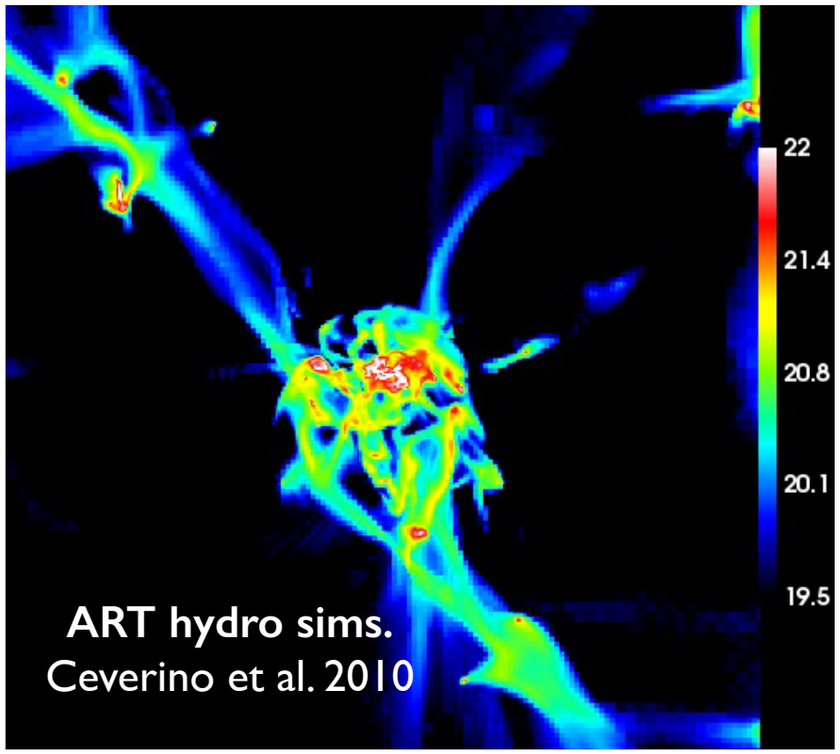

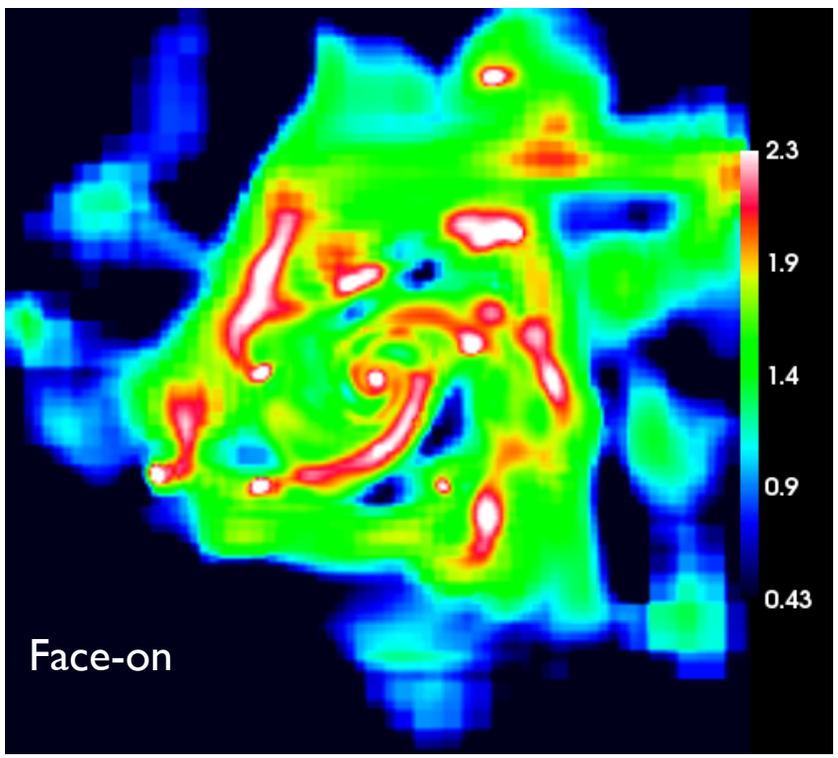

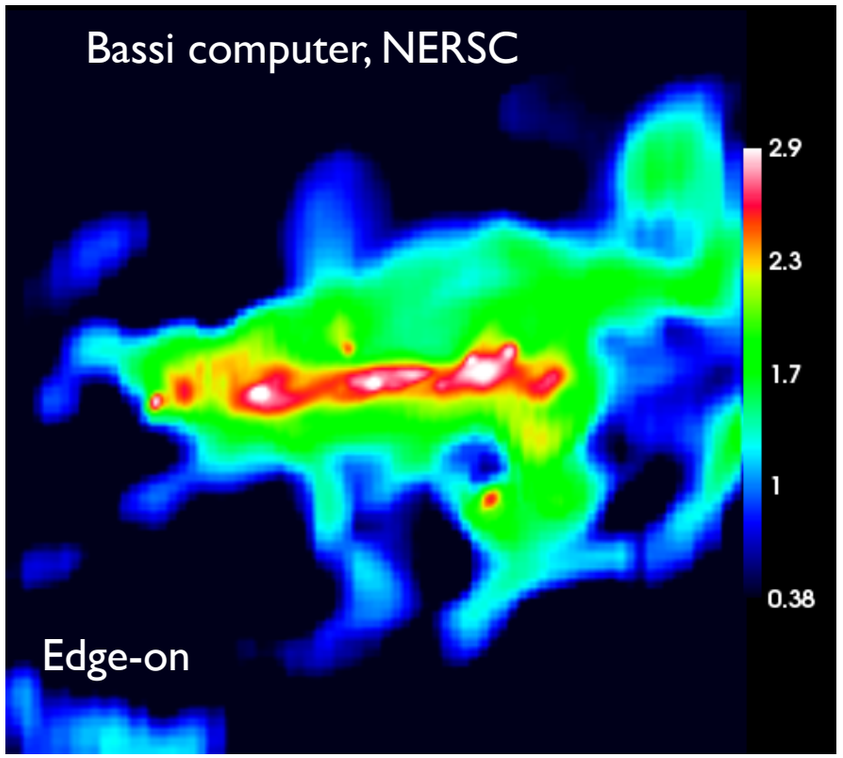

now running on NERSC Hopper-II
and NASA Ames Pleiades supercomputers

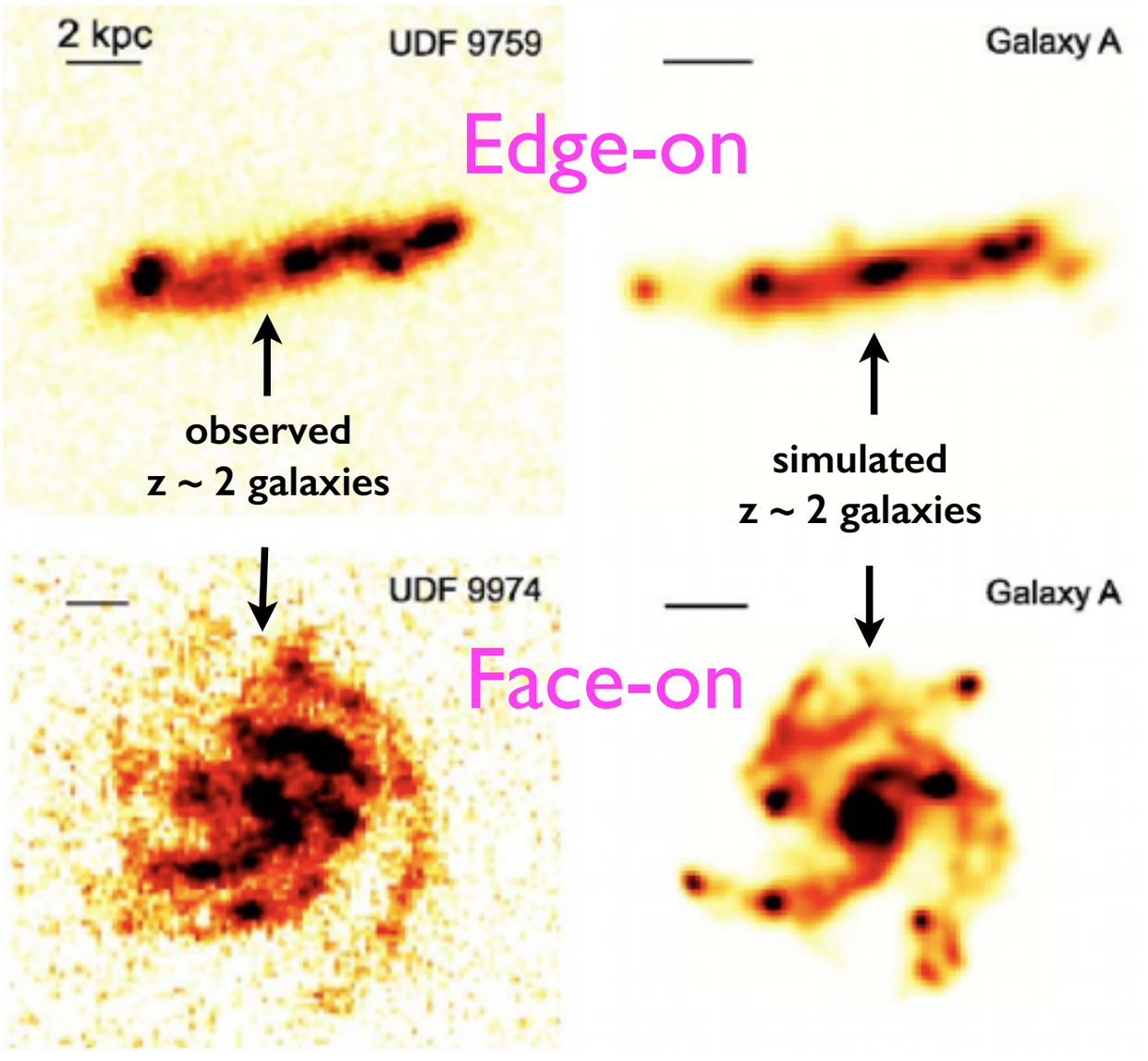

Ly alpha blobs from same simulation

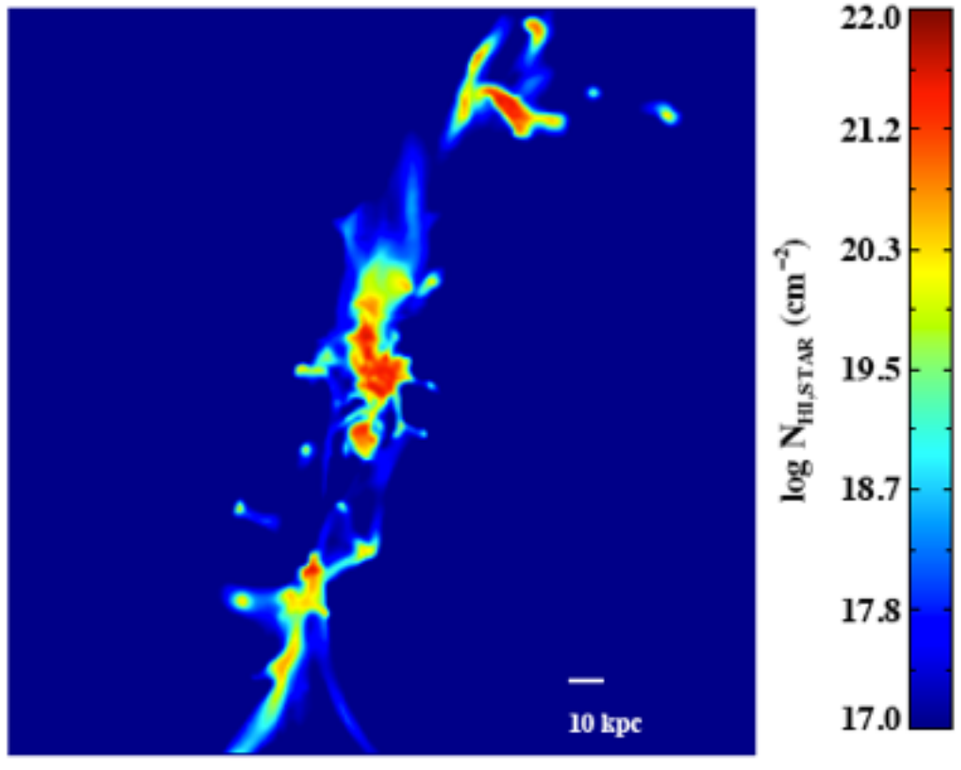

Fumagalli, Prochaska, Kasen, Dekel, Ceverino, & Primack 2011

What's the effect of including dust?

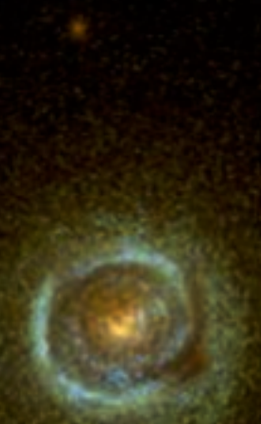

with
dust

Dramatic effects on
-Appearance
-Half-mass radii (bigger with dust)
-Sersic index (lower with dust)

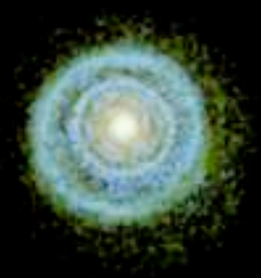

stars
only

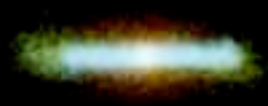

cemoody.imgur.com

Ceverino+ VL6 Cosmological Zoom-in Simulation

Face-On

Edge-On

VL06_a0.110_0000420_skipir_allrays7
z=8.1
NUV=-20.55
U=-20.95
V=-21.39
J=-21.49
z=-21.47

NUV=-20.42
U=-20.74
V=-21.14
J=-21.21
z=-21.19

$z = 8.1$

Chris Moody

Simulated Galaxy 10 billion years ago (z ~ 2) as it would appear nearby to our eyes

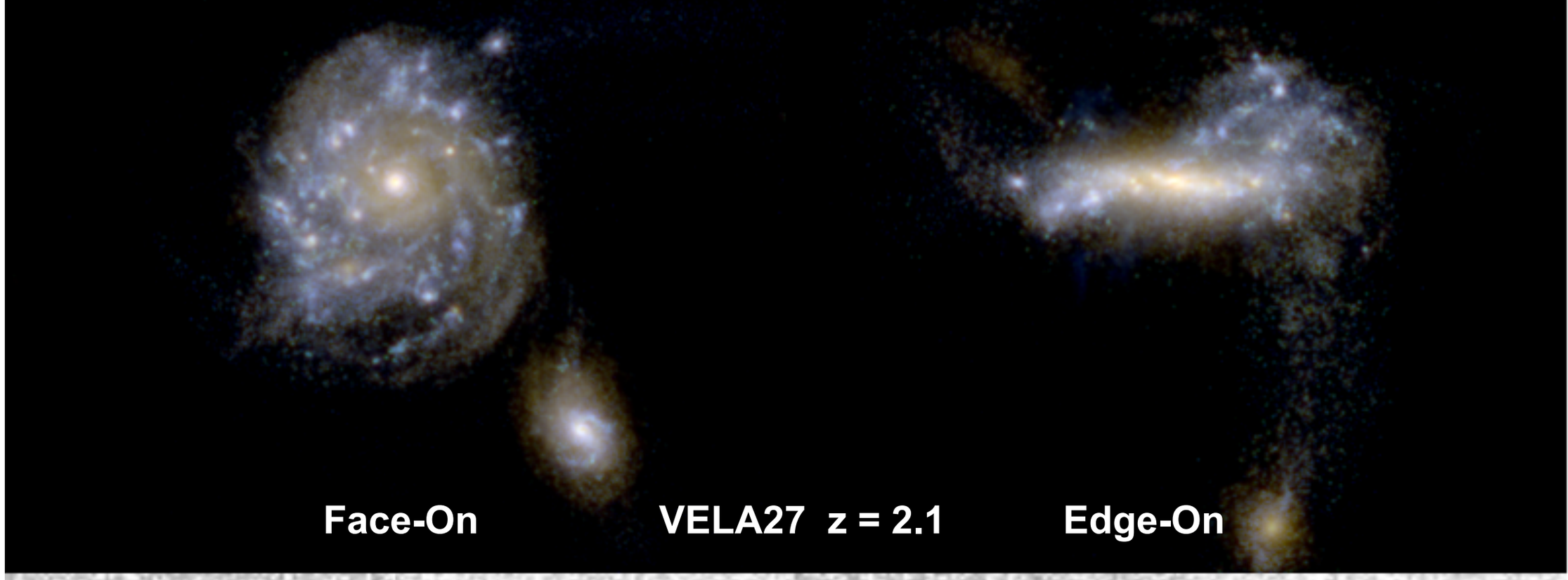

as it would appear to Hubble's ACS visual camera

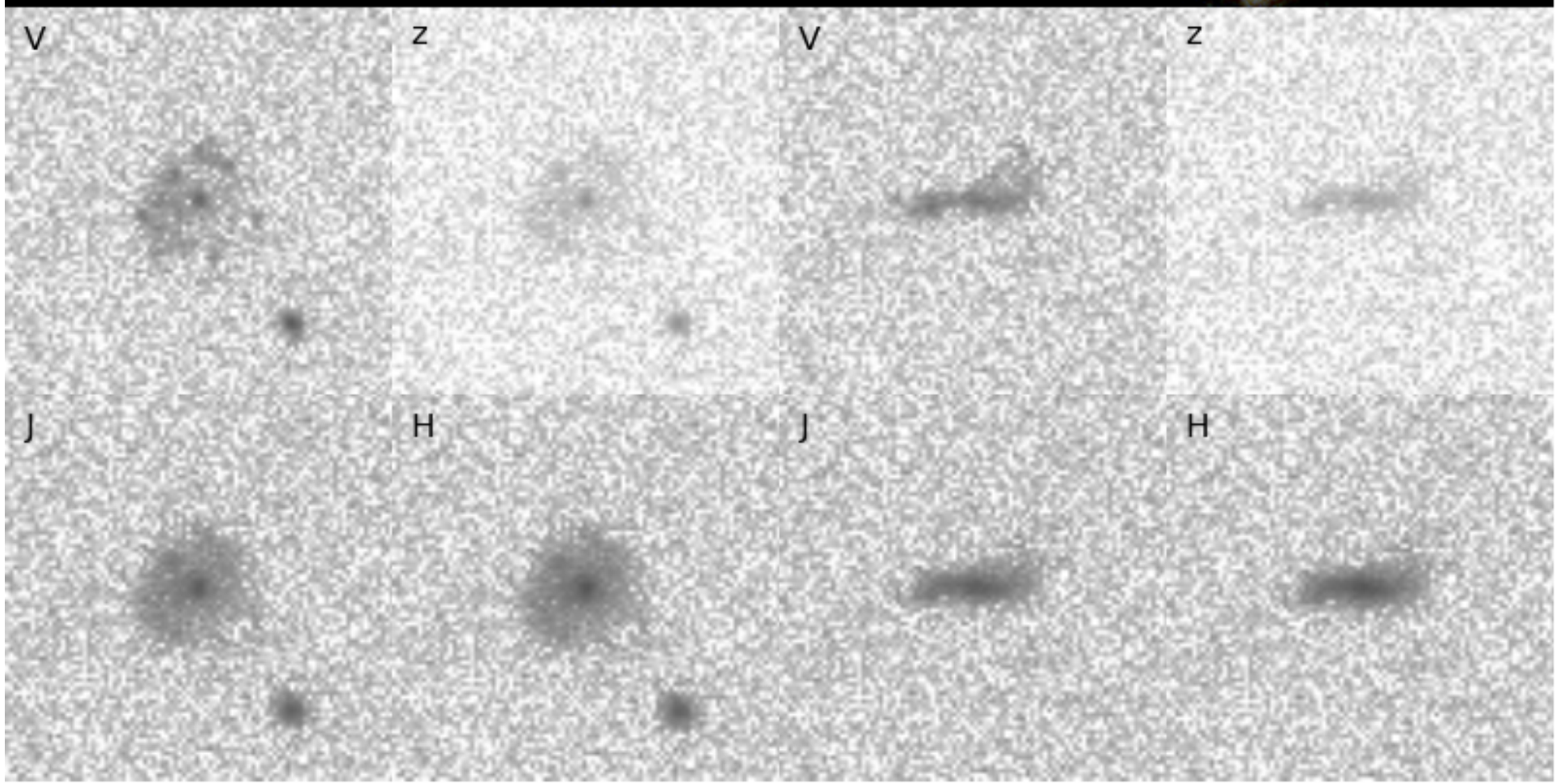

as it would appear to Hubble's WFC3 infrared camera

Our Simulations w/ Dust look a lot like galaxies from 10 billion years ago that we see with Hubble Space Telescope

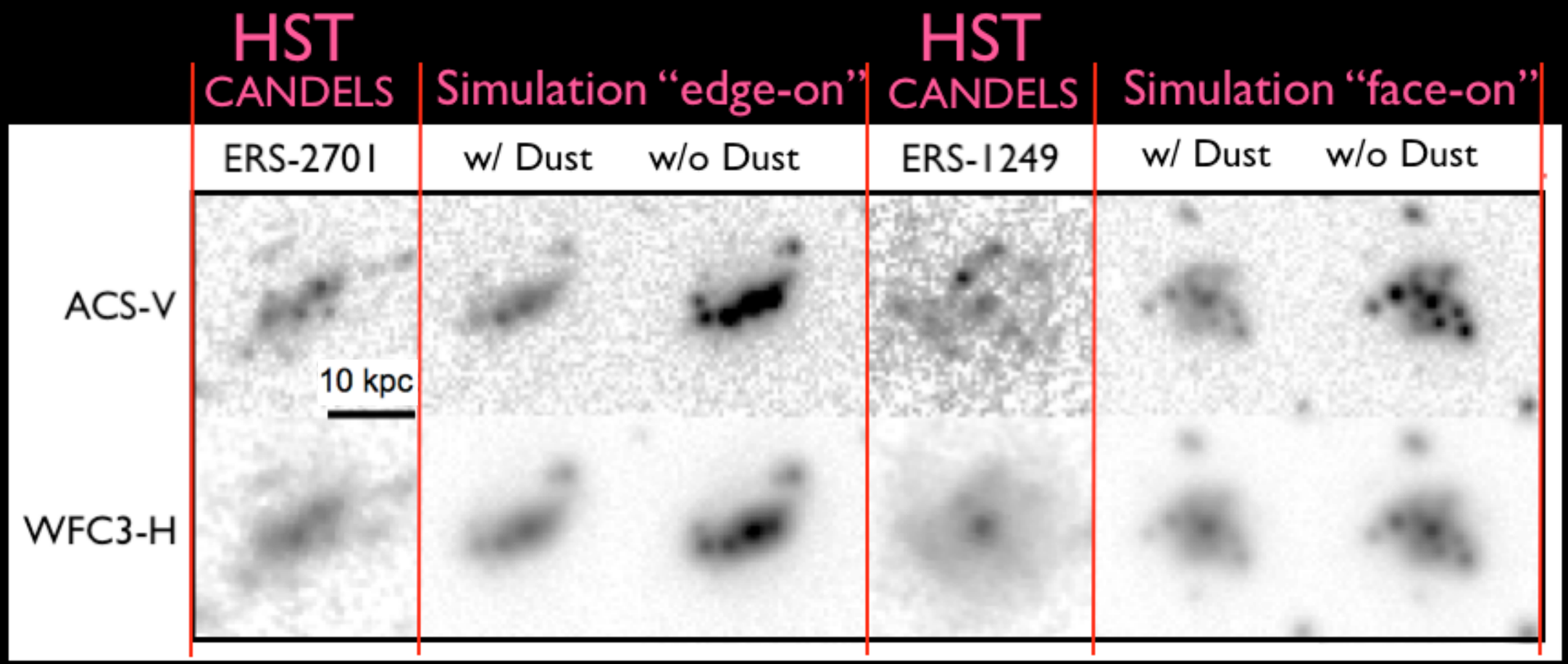

Our Simulations w/ Dust look a lot like galaxies from 10 billion years ago that we see with Hubble Space Telescope

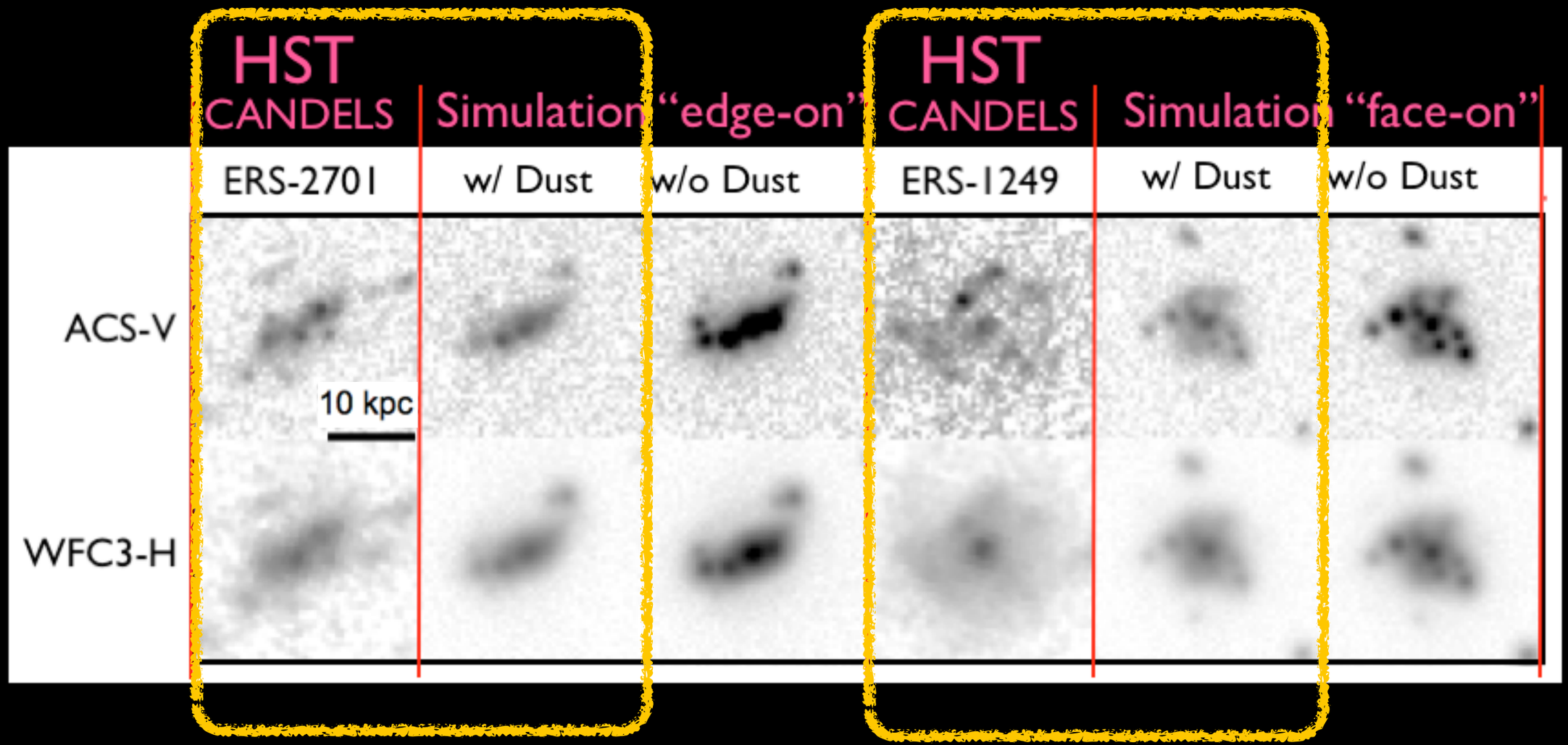

We are now systematically comparing simulated and observed galaxy images

CLUMPY GALAXIES

HST IMAGES

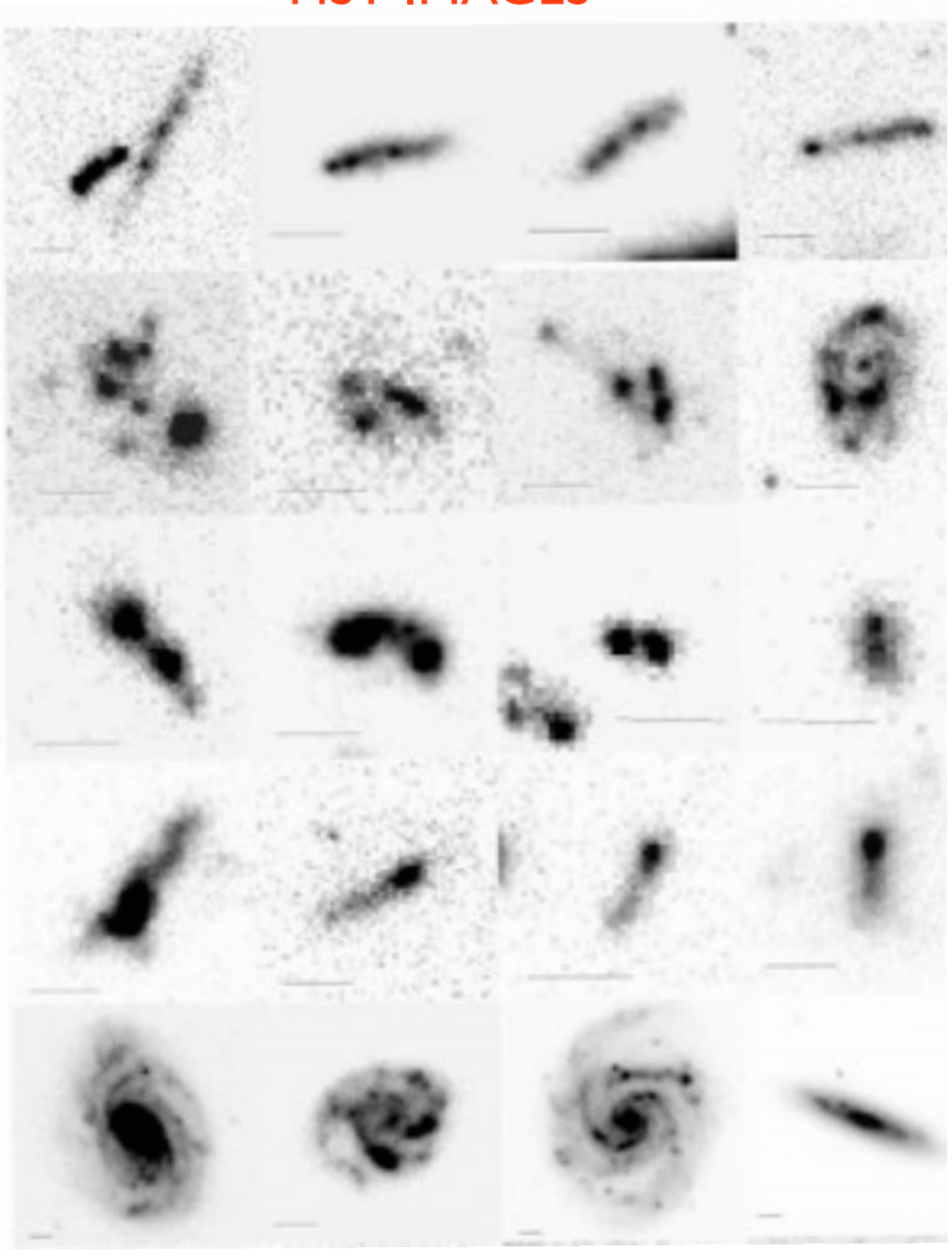

SIMULATED

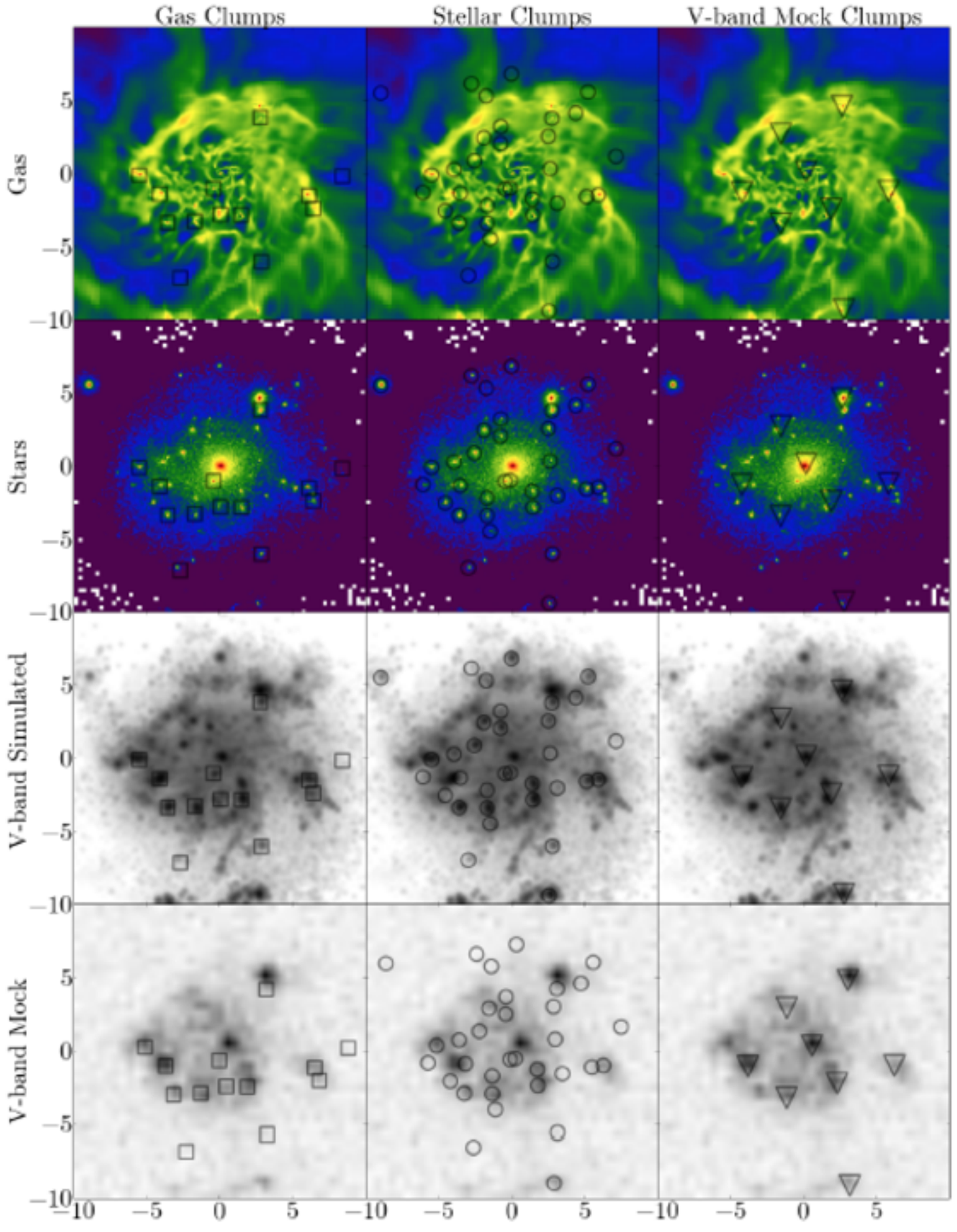

CANDELS Galaxies Compared with Generations 1 & 2 hydroART simulations using R_{eff}, Axis Ratio q, Sersic n, with clumpy vs. not clumpy from by-eye classification

Observations

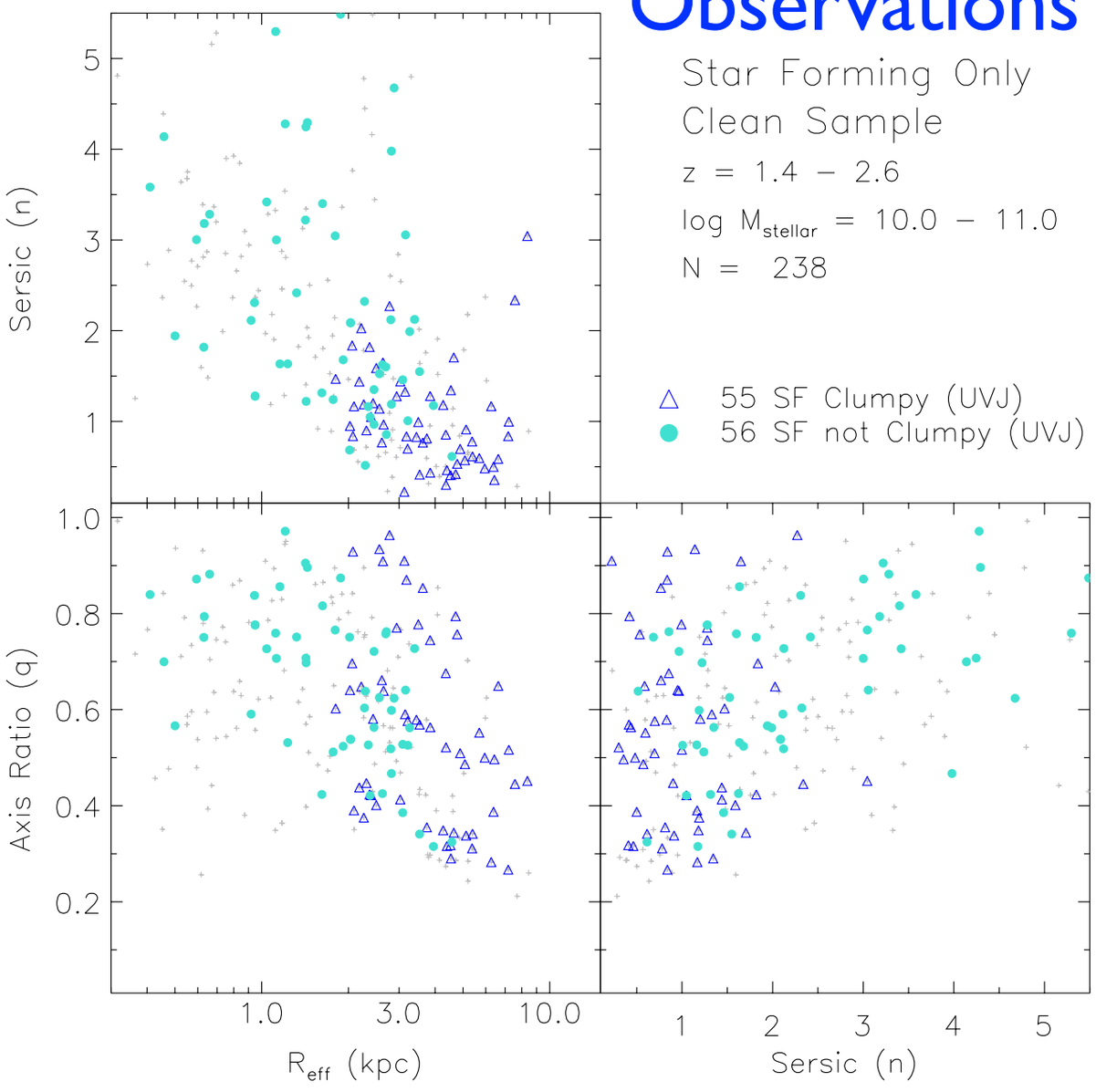

Simulations

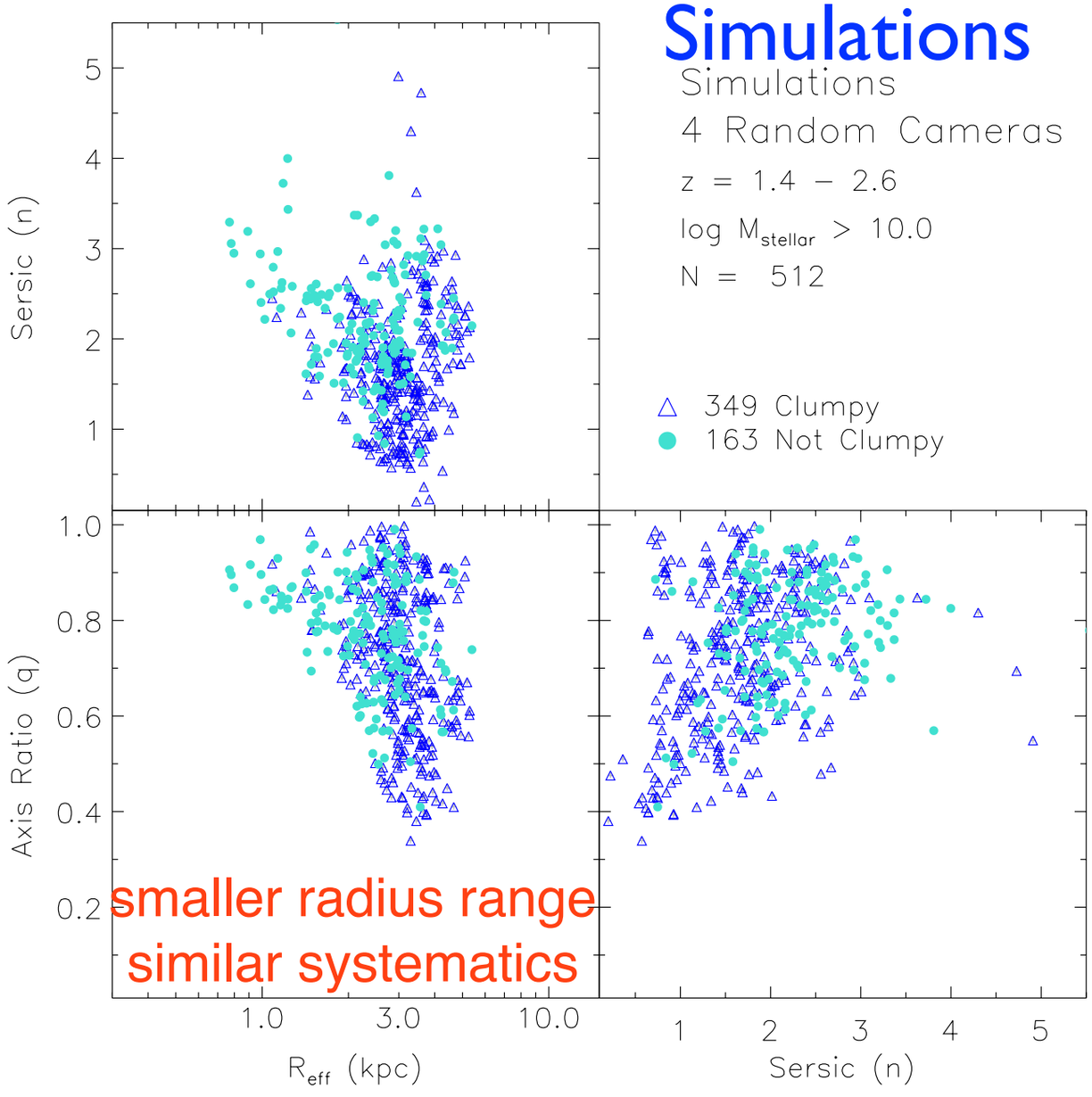

Mark Mozena (PhD thesis)

AGORA Assembling Galaxies of Resolved Anatomy

A High-resolution Galaxy Simulations Comparison Initiative To Tackle Longstanding Challenges in Galaxy Formation

High-res Galaxy Simulations

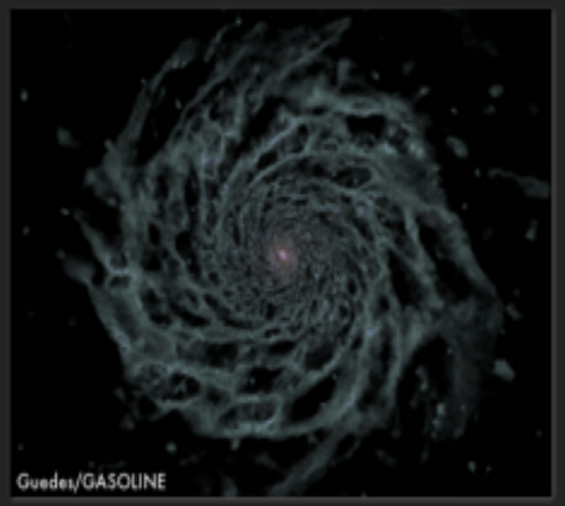

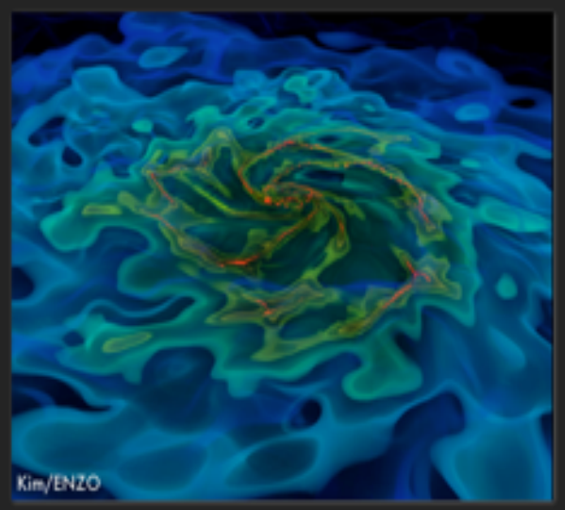

AGORA Comparison Infrastructure

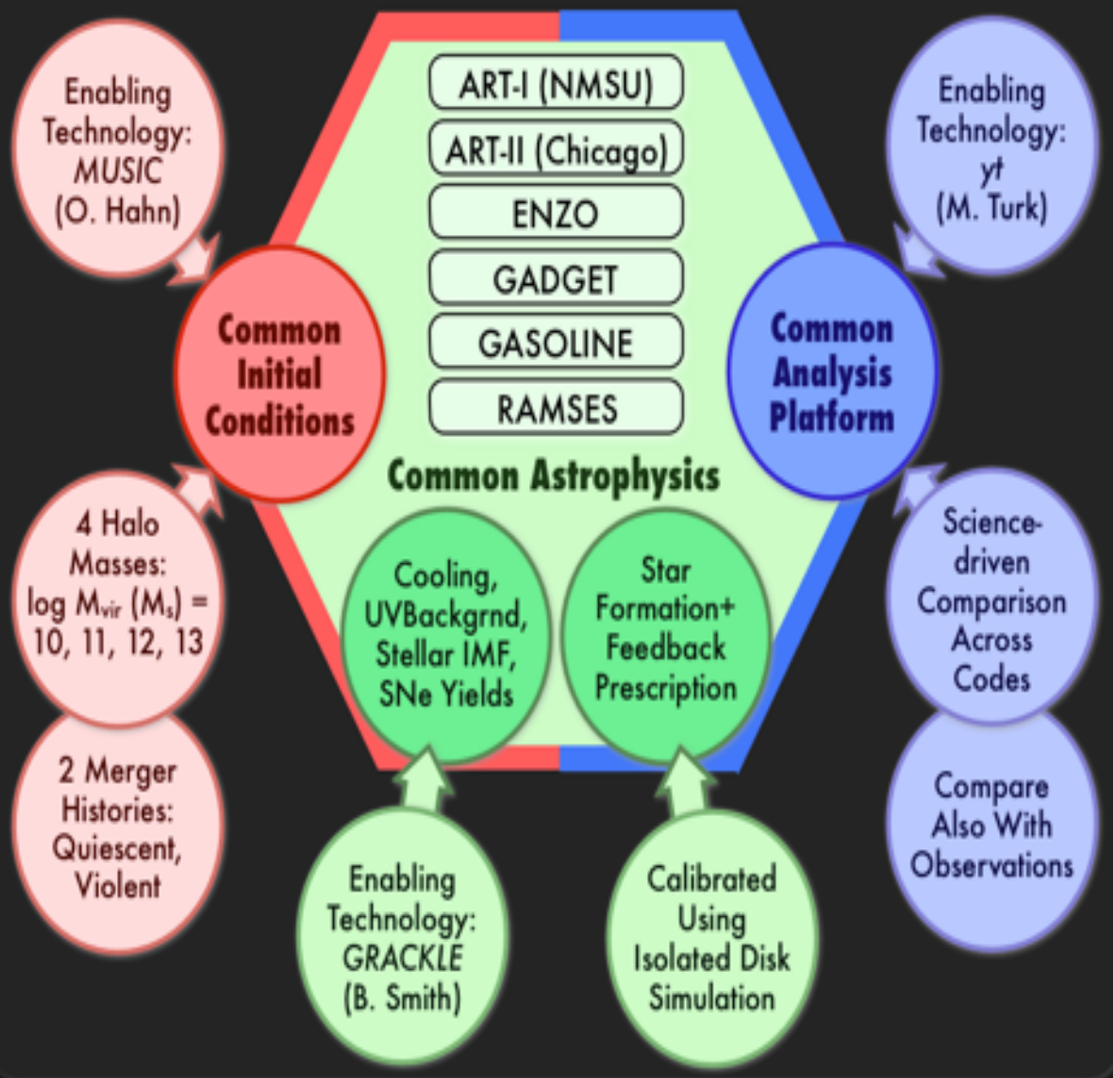

AGORA Goal & Team

- GOAL: A multi-platform study to raise the realism and predictive power of high-resolution (<100 pc) galaxy simulations collectively

- TEAM: 4 task working groups and 9+ science working groups, 94 participants from 47 institutions as of 2nd Workshop, Aug. 2013

- DATA SHARE: Simulation data will be radpily available to public

- AGORA First light: Flagship paper by Ji-hoon Kim et al. (arXiv:1308.2669; www.AGORAsimulations.org)

- Project funded in part by:

University of California
High-Performance
AstroComputing Center
(UC-HiPACC)
Joel Primack, Director

University of California
Santa Cruz
Next Telescope Science
Institute (NEXSI)
Piero Madau, Director

Assembling Galaxies of Resolved Anatomy

AGORA High-Resolution Galaxy Simulation Comparison Project Steering Committee

Piero Madau & Joel R. Primack, UCSC, Co-Chairs
Tom Abel, Stanford
Nick Gnedin, Chicago/Fermilab
Lucio Mayer, University of Zurich
Romain Teyssier, Saclay & Zurich
James Wadsley, McMaster
Ji-hoon Kim, UCSC (Coordinator)

94 astrophysicists using 10 codes have joined AGORA

www.AGORAsimulations.org

AGORA High-Resolution Simulation Comparison

Initial Conditions for Simulations

MUSIC galaxy masses at z~0: ~10^{10}, 10^{11}, 10^{12}, 10^{13} $M_\odot$
with both quiet and busy merging trees
isolation criteria agreed for Lagrangian regions

Isolated Spiral Galaxy at z~1: ~10^{12} $M_\odot$

Astrophysics that all groups will include

UV background (Haardt-Madau 2012)
cooling function (based on ENZO and Eris cooling)

Tools to compare simulations based on *yt*, to be available for all codes used in AGORA

Images and SEDs for all timesteps from *yt* ➠ *Sunrise*

www.AGORAsimulations.org

www.AGORAsimulations.org

AGORA Task-Oriented Working Groups

	Working Group	Objectives and Tasks
T1	Common Astrophysics	UV background, metal-dependent cooling, IMF, metal yields
T2	ICs: Isolated	common initial conditions for isolated low-z disk galaxies
T3	ICs: Cosmological	common initial conditions for cosmological zoom-in simulations
T4	Common Analysis	support `yt` and other analysis tools, define quantitative and physically meaningful comparisons across simulations

AGORA Science Working Groups

	Working Group	Science Questions (includes, but not limited to)
S1	Isolated Galaxies and Subgrid Physics	tune the subgrid physics across platforms to produce similar results for similar astrophysical assumptions
S2	Dwarf Galaxies	simulate $\sim 10^{10} M_{\odot}$ halos, compare results across all platforms
S3	Dark Matter	radial profile, shape, substructure, core-cusp problem
S4	Satellite Galaxies	effects of environment, UV background, tidal disruption
S5	Galactic Characteristics	surface brightness, stellar properties, metallicity, images, SEDs
S6	Outflows	outflows, circumgalactic medium, metal absorption systems
S7	High-redshift Galaxies	cold flows, clumpiness, kinematics, Lyman-limit systems
S8	Interstellar Medium	galactic interstellar medium, thermodynamics
S9	Massive Black Holes	black hole growth and feedback in galactic context
S10	Lyα Absorption and Emission	prediction of Lyα maps for simulated galaxies and their environments including effects of radiative transfer

THE *AGORA* HIGH-RESOLUTION GALAXY SIMULATIONS COMPARISON PROJECT

JI-HOON KIM[1], TOM ABEL[2], OSCAR AGERTZ[3,4], GREG L. BRYAN[5], DANIEL CEVERINO[6], CHARLOTTE CHRISTENSEN[7], CHARLIE CONROY[1], AVISHAI DEKEL[8], NICKOLAY Y. GNEDIN[3,9,10], NATHAN J. GOLDBAUM[1], JAVIERA GUEDES[11], OLIVER HAHN[11], ALEXANDER HOBBS[11], PHILIP F. HOPKINS[12,13], CAMERON B. HUMMELS[7], FRANCESCA IANNUZZI[14], DUŠAN KEREŠ[15], ANATOLY KLYPIN[16], ANDREY V. KRAVTSOV[3,10], MARK R. KRUMHOLZ[1], MICHAEL KUHLEN[1,13], SAMUEL N. LEITNER[17], PIERO MADAU[1], LUCIO MAYER[18], CHRISTOPHER E. MOODY[1], KENTARO NAGAMINE[19,20], MICHAEL L. NORMAN[15], JOSE OÑORBE[21], BRIAN W. O'SHEA[22], ANNALISA PILLEPICH[1], JOEL R. PRIMACK[23], THOMAS QUINN[24], JUSTIN I. READ[4], BRANT E. ROBERTSON[7], MIGUEL ROCHA[21], DOUGLAS H. RUDD[10, 25], SIJING SHEN[1], BRITTON D. SMITH[22], ALEXANDER S. SZALAY[26], ROMAIN TEYSSIER[18], ROBERT THOMPSON[7, 19], KEITA TODOROKI[19], MATTHEW J. TURK[5], JAMES W. WADSLEY[27], JOHN H. WISE[28], AND ADI ZOLOTOV[8] FOR THE *AGORA* COLLABORATION[29]

Draft version August 14, 2013

ABSTRACT

We introduce the *AGORA* project, a comprehensive numerical study of well-resolved galaxies within the ΛCDM cosmology. Cosmological hydrodynamic simulations with force resolutions of ~ 100 proper pc or better will be run with a variety of code platforms to follow the hierarchical growth, star formation history, morphological transformation, and the cycle of baryons in and out of 8 galaxies with halo masses $M_{\rm vir} \simeq 10^{10}$, 10^{11}, 10^{12}, and 10^{13} $M_\odot$ at $z = 0$ and two different ("violent" and "quiescent") assembly histories. The numerical techniques and implementations used in this project include the smoothed particle hydrodynamics codes GADGET and GASOLINE, and the adaptive mesh refinement codes ART, ENZO, and RAMSES. The codes will share common initial conditions and common astrophysics packages including UV background, metal-dependent radiative cooling, metal and energy yields of supernovae, and stellar initial mass function. These are described in detail in the present paper. Subgrid star formation and feedback prescriptions will be tuned to provide a realistic interstellar and circumgalactic medium using a non-cosmological disk galaxy simulation. Cosmological runs will be systematically compared with each other using a common analysis toolkit, and validated against observations to verify that the solutions are robust – i.e., that the astrophysical assumptions are responsible for any success, rather than artifacts of particular implementations. The goals of the *AGORA* project are, broadly speaking, to raise the realism and predictive power of galaxy simulations and the understanding of the feedback processes that regulate galaxy "metabolism." The initial conditions for the *AGORA* galaxies as well as simulation outputs at various epochs will be made publicly available to the community. The proof-of-concept dark matter-only test of the formation of a galactic halo with a $z = 0$ mass of $M_{\rm vir} \simeq 1.7 \times 10^{11}$ $M_\odot$ by 9 different versions of the participating codes is also presented to validate the infrastructure of the project.